Binary lipid model system of *Staphylococcus aureus:*

Characterization of biophysical parameters

Dipl. Ing. Florian Proßnigg

DISSERTATION

Zur Erlangung des akademischen Grades

Doktor der technischen Wissenschaften

Eingereicht an der

Technischen Universität Graz

Betreuer

Univ. Doz. Dipl. Ing. Dr. Karl Lohner

Institut für Molekulare Biowissenschaften

Karl Franzens Universität Graz

Eidesstattliche Erklärung

Ich erkläre an Eides statt, dass ich die vorliegende Arbeit selbstständig verfasst, andere als die angegebenen Quellen/Hilfsmittel nicht benutzt, und die den benutzten Quellen wörtlich und inhaltlich entnommenen Stellen als solche kenntlich gemacht habe.

Das in TUGRAZonline hochgeladene Textdokument ist mit der vorliegenden Dissertation identisch.

Datum	Unterschrift

Kurzfassung

In dieser Arbeit werden die Eigenschaften des binären Phasendiagramms der Phospholipide Dipalmitoylphosphatidylglycerol und Tetramyristoylcardiolipin beschrieben. Beide Lipide sind Hauptbestandteile der Zellmembran der Bakterienart *Staphylococcus aureus*, von welcher eine große Anzahl von Antibiotika-resistenten Stämmen dokumentiert ist. Anhand der Beschreibung des thermischen Phasenverhaltens der reinen Lipid-Mischungen mittels physikalischer Messmethoden wurde die Grundlage gelegt, sowohl weitere Modellsysteme zu beschreiben als auch die Reaktionen mit neuen potentiellen Medikamenten wie antimikrobieller Peptide zu untersuchen, um in weiterer Folge neue Medikamente zu designen, die die klassischen Antibiotika ersetzen können. Charakteristische Parameter wie Phasenübergangstemperaturen und -enthalpien, Membrandicke und strukturelle Ordnung der Fettsäureketten wurden mittels Mikro-Kalorimetrie und Röntgen-Streumethoden bestimmt.

Abstract

In this thesis, the binary phasediagram of the phospholipids dipalmitoylphosphatidylglycerol and Tetramyristoylcardiolipin are presented. Both lipids represent the main components of the cell membrane of *Staphylococcus aureus*, from which numerous antibiotic resistant strains are documented. The characterisation of the thermotropic phase behaviour of the pure lipid system serves as basis for more complex model systems and for the development of new antibiotics, respectively. The methods used to determine characteristic parameters such as phase transition temperatures and enthalpies, the membrane thickness, and the structural order of the hydro carbon chain lattice were Differential Scanning Calorimetry (DSC) and X-ray scattering techniques.

Danksagung

„Denke immer daran, dass es nur eine wichtige Zeit gibt: Heute. Hier. Jetzt.“
(Lew Nikolajewitsch Tolstoi)

Heute, hier, jetzt und ENDLICH ist es Zeit, DANKE zu sagen. Ein herzliches Dankeschön an alle, die geholfen haben, dass diese Arbeit fertig gestellt wurde. Allen voran gilt mein Dank Univ. Doz. Dr. Karl Lohner, der mit seinem grenzenlosen Wissen über die Membran-Mimetik, seiner steten Unterstützung und auch seiner Motivationsfähigkeit großen Anteil an dieser Arbeit hatte. Weiters gilt mein Dank auch Dr. Andrea Hickel, die mich in ihr Forschungs-Projektteam aufgenommen hat, um an dieser Doktorarbeit zu schreiben, sowie allen Kollegen in der Arbeitsgruppe und dem Institut.

Zu guter Letzt, Danke auch an Lydia, meiner Frau und großen Liebe, dass sie auch bei den „naturwissenschaftlichsten“ Diskussionen immer da war und ist.

Table of content

List of Figures

List of tables

1 General introduction

1.1 Novel strategies to fight antibiotic resistance

Mankind is facing an emerging medical problem as worldwide the number of antibiotic resistant bacterial strains is rapidly increasing, provoking fast and well-considered efforts in science. For a long time, antibiotics have been seen as the ultimate drug to defeat bacterial infections. In the 1940s, shortly after the introduction of penicillin as a potent drug against bacteria, first strains were already detected being resistant to it. At the end of the 1960s, over 80% of community and hospital-acquired *Staphylococcus aureus* isolates were resistant to penicillin [32].

In the following years, various microorganisms were screened for resistance towards other antibiotic drugs. Thereby, resistance towards cephalosporins, tetracyclines, macrolides and quinolones were discovered until the end of the 1960s. Beside the search for new classes, the semi-synthetic optimization of existing antibiotics led to some, even more potent drugs. In the following decade, the pharmaceutical industry maximized their profits with more than 270 antibiotics in the early 1970s.

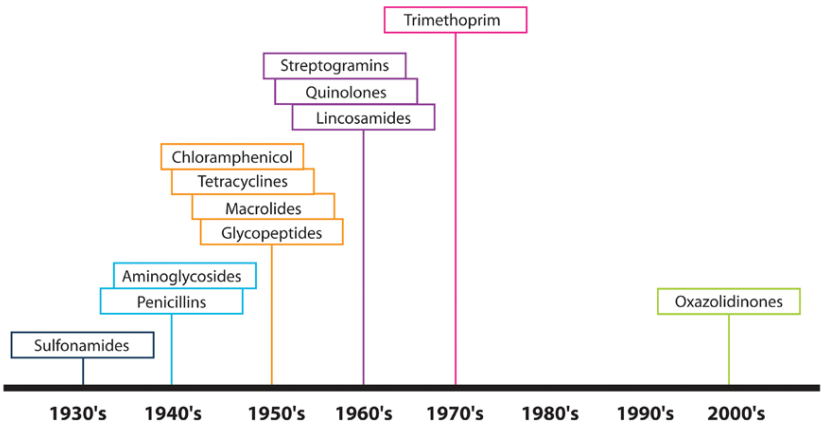

Figure 1: Time scale showing the approval of various antibiotics as presented by the FDA [46] (citation therein: Singh et al. [66])

During this period, the market for these types of drugs became sufficiently saturated, which made the companies to concentrate more in the development of new pharmaceuticals. Especially for chronic diseases, which were considered to be also more “profitable” [19]. Therefore, industry neglected the discovery and development of new antibiotics after the 1970s (Figure 1). With oxazolidinones and daptomycine, which were approved by the Food and Drug Administration (FDA) in 2005, only two new classes were introduced on the market in the last three decades [46]. Nevertheless, we find ourselves confronted with the increase in antibiotic resistances lacking novel drugs.

Bacterial resistances can evolve in many ways, whereby antibiotic drug misuse is a major issue. Furthermore, wrong dosage or too frequent and ill-conceived prevalent use of broad-spectrum antibiotics also facilitate the evolvement of defence mechanism by spontaneous mutations, resulting in a decreased susceptibility. In industrialized countries, about 80-90% of antibiotic treatment is done in the community but at least half of it is considered to be under- or misdiagnosed [46, 72]. One reason for this situation is the lack of easy and low cost laboratory analysis to differentiate fast enough between bacterial and viral infections and, consequently, between different bacterial species.

Additionally, the frequent application of antibiotics, in animal breeding at sub-inhibitory concentrations, promotes the formation of resistant bacteria found in this industry and in turn the distribution of ineffective dosages through the food chain. For example, penicillin is widely used preventively in cattle, swine and poultry to prevent infections. Incidences of persons with increased sensitivity to penicillin, suffering from allergic reactions after consumption of penicillin containing food, are documented. (see Doyle [11] and references therein). Further adverse health effects are chronic toxic effects caused by prolonged exposure or disruption of the intestinal flora [11].

Therefore, in 1998, the EU Commission established a Community Network for Epidemiological Surveillance and Control of Communicable Diseases, also covering the problem of antibiotic resistance. Since then, the "European Antimicrobial Resistance Surveillance System" (EARSS – later renamed to European Antimicrobial Resistance Surveillance Network, EARS-Net) is also supported by the EU [46]. One year later, the resolution "A Strategy Against the Microbial Threat" was adapted by the European Council followed by the "Community Strategy Against Antimicrobial Resistance" published by the Commission in 2001. The latter document proposed four main key areas to combat antibiotic resistance: surveillance, prevention, research and development as well as international cooperation (see Nordberg et al. [46] and references therein).

1.2 Staphylococcus aureus and its Methicillin resistant strains

Staphylococcus aureus was discovered in 1880 by Sir Alexander Ogston in pus from surgical abscesses (orig. publication: [47]). It occurs as a commensal on human skin and also frequently in the nose. About 20% of the population are always colonized with *Staphylococcus aureus*, 60% are intermittent carriers and 20% never carry this organism [15].

Staphylococcus aureus causes both superficial infections on the skin and other tissues as well as infections in lung (pneumonia), heart (endocarditis) or bones (osteomyelitis). The latter diseases show also risk of increased lethality. Additionally, *Staphylococcus aureus* is the source of several toxins causing food poisoning (Staphylococcal enterotoxins), toxic shock syndrome (pyrogenic toxin antigens) or staphylococcal scaled skin syndrome (exfoliative toxins). Furthermore, Staphylococcal endotoxins (alpha-toxin, beta-toxin, and delta-toxin) can lyse cell membranes.

Strains of methicillin resistant *Staphylococcus aureus* (MRSA) are resistant to a large group of antibiotics, called the β-lactams including penicillin derivatives. These antibiotics inhibit the growth of the peptidoglycan layer by binding to the active site of the penicillin binding proteins interfering with cell wall biosynthesis. However, the kinetics of this mechanism, i.e. bacterial killing, is slow compared to the generation time of the bacteria giving them ample opportunities to develop resistance, one of the problems in antibiotic treatment. One mechanism of resistance to β-lactam antibiotics is the hydrolysis of the β-lactam ring in the drug molecule by β-lactamase. An alternative way is an altered penicillin binding protein, preventing the effective binding of penicillin.

Shortly after the introduction of methicillin as the first semisynthetic penicillinase resistant penicillin antibiotic in 1961, first MRSA strains were already discovered in the UK [38]. First incidences were observed in intensive care units of hospitals. Since the 1980s, the number of MRSA strains increased from close to zero up to 70% in Japan and the Republic of Korea and up to 40% in the USA [67]. In European countries, the MRSA levels also increased till 2002 up to 40% in Ireland, United Kingdom, Italy, Greece, Malta, and Portugal [12]. Between the late 1990s and 2002, the proportion of MRSA reported in Germany and Austria was astonishingly doubled from 8 to 19% for Germany and from 5 to 11% for Austria as published in EARSS report 2002 [12] (Figure 2).

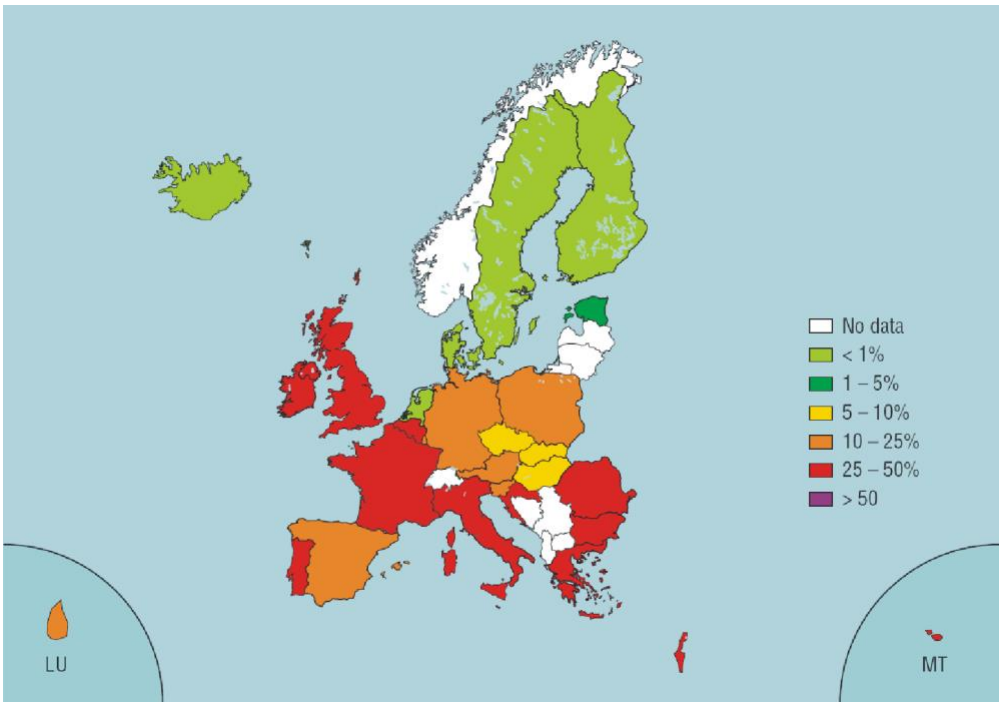

Figure 2: Registered MRSA strains as proportions of total *Staphylococcus aureus* reports (Figure taken from Annual Report of the EARSS, 2002 [12]).

In the 2006 report [13], decreased or stable MRSA proportions could be seen for some countries, such as France, Greece, Ireland or the central European countries. In northern European countries, MRSA rates were still lower than 4%, although in the Netherlands and Finland an increase could be detected (Figure 3). Only Malta, Portugal, and Spain showed significant increase in the *Staphylococcus aureus* resistance in the last few years.

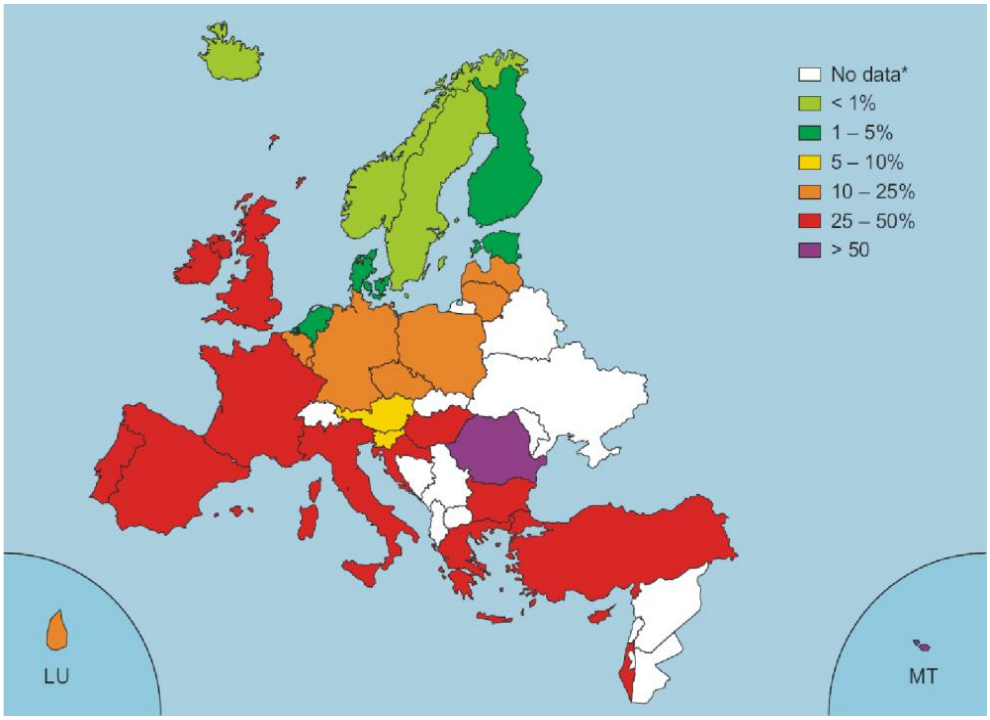

Figure 3: Registered MRSA strains as proportions of total *Staphylococcus aureus* reports (Figure taken from the Annual Report of the EARSS, 2006 [13]).

In the most recent report from 2013 [14], further stabilization and even a decrease of the resistance rate was observed in some countries (Figure 4). Nine out of 30 countries showed a decrease of percentage of invasive isolates. Especially UK, France, Ireland and Spain had now values below 25%. For instance, UK is, as best case, now rating at 13.7% compared to the 2006 value of around 42%. In contrast, seven of 30 countries, mainly in South Eastern Europe, still reported percentages above 25% and two of them even above 50%. Therefore, the mean percentage value over all EU/EEA countries remains at 18% although positive trends are observed.

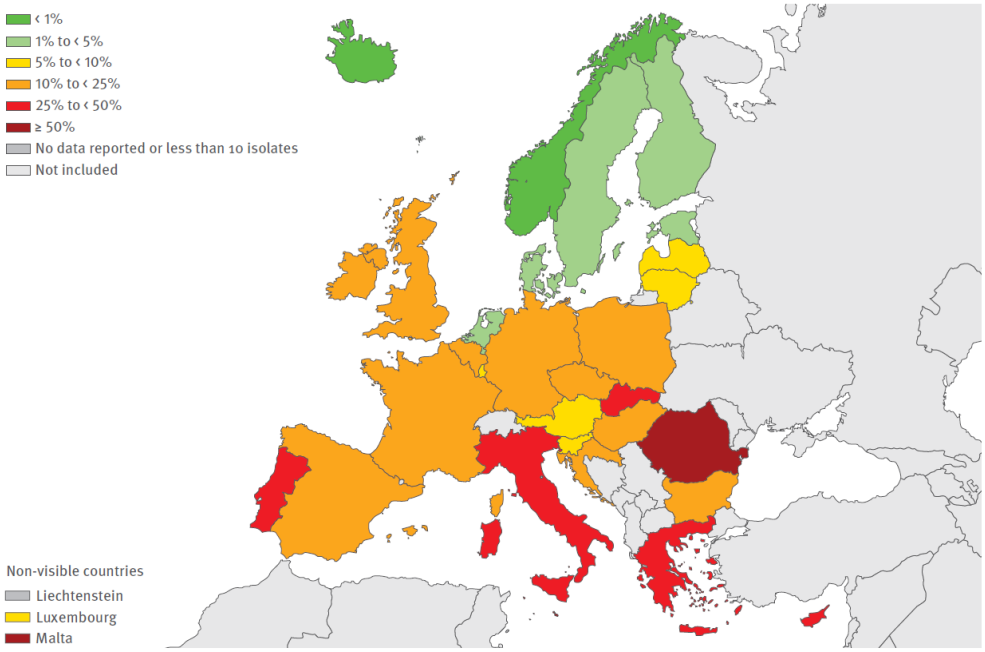

Figure 4: Registered MRSA strains as proportions of total *Staphylococcus aureus* reports (Figure taken from Annual Report of the EARS-Net, 2013 [14]).

One of the first observations of community acquired MRSA was made in USA in 1980 [4]. Surprisingly, some cases of methicillin resistance were reported in countries such as Poland and Turkey before methicillin was even introduced, which was explained to be due to either an earlier developed resistance to naturally occurring penicillin or a resistance, which evolved from exposure to a methicillin-like antimicrobial agent 0. Since the first resistant strains were detected, methicillin is only used in susceptibility tests for laboratory use. In some European countries, oxacillin is also used as a reference antibiotic instead of methicillin.

MRSA infections are generally treated with antibiotics of last resort, as drugs of the beta lactam family do not assure a successful result. Therefore, mostly therapeutics of the group of glycopeptides are used. Therein, Vancomycin, isolated in 1956 from the actinomycete *Streptomyces orientalis*, serves as the prototype for this group 0. However, the identification of the first Vancomycin resistant *Staphylococcus aureus* (VRSA) strain, in Japan in 1996, makes all efforts to handle this problem more and more difficult and emphasizes the urgent

development of novel antibiotics [1, 5]. A number of MRSA strains are still susceptible to vancomycin and other glycopeptides, but decreased vancomycin susceptibility has now emerged within all pandemic MRSA lineages [26]. In the EARSS report from 2006, nine Vancomycin intermediate resistant *Staphylococcus aureus* (VISA) strains were mentioned [46]. Such a strain was reported in Austria, Belgium, France, Ireland, and United Kingdom. Whereby the only one invasive *Staphylococcus aureus* isolate resistant to vancomycin was reported in Austria, although the tested MIC value was only slightly above the clinical CLSI breakpoint of 16 µg/ml [46]. Recent publications reported a decrease of bacterial susceptibility against biocides, too, but *Staphylococcus aureus* still shows a distinct susceptibility against antiseptics and disinfectants [59]. This suggests that the hygienic standards established in the healthcare systems of the industrialized countries enables the control of onset of MRSA infections.

Nevertheless, the efforts in treatment and therefore expanding costs caused by the rising number of nosocomial as well as community acquired MRSA infections also have a strong economic impact. In hospitals, the antibiotic costs account for 20-30% of the total budget [46]. There are estimates that adaptation of infection therapies would cause a twofold increase of the antibiotic treatment costs [46]. Additionally, one patient suffering from a MRSA infection needs a prolonged hospitalization under isolation conditions and special treatment. Goetghebeur et al. [18] mentioned in their report total costs of more than 12.000 CAN$ (about 8.000 €) for an average treatment of 26 days per patient. It is also estimated that infections due to antibiotic resistant bacteria will cause health care costs of 100 million € up to billion € per year worldwide [18, 46].

1.3 Antimicrobial Peptides – A Novel Class of Antibiotics

Antimicrobial peptides (AMPs) are a class of small peptide molecules composed of 10 to 50 amino acid residues found in various species. They are part of the innate immunity since the first single cell organisms and evolved also in higher vertebrates [20]. This system is simple, non-specific and it is not adaptive [20]. Innate immunity is rapid and multifunctional. Therein, AMPs play a relevant role as mediators active against Gram-positive and Gram-negative bacteria, fungi, parasites, and some viruses [20] including HIV (see Wang et al.[71] and references therein). A small fraction of the tremendous variety of natural AMPs is yet investigated and still topic of intensive scientific work. Actually, the Antimicrobial Peptide Database administrated by Wang and colleagues shows a total number of 2835 registered AMPs [70].

The amino acid sequences of AMPs show a high variability, but always include various residues with a positive charge giving these molecules a total positive net charge. Both the cytoplasmic membrane of all bacteria and the lipopolysaccharide layer of Gram-negative bacteria are negatively charged and show therefore a high affinity to cationic peptides. The second common characteristic is the amphipathicity giving AMPs potent abilities to interact with hydrophilic (lipid head groups) and hydrophobic (lipid hydrocarbon chains) parts of the lipid molecules. Depending on the amino acid sequence, AMPs fold into various structures including α-helices, β-sheets, extended helices and loops [23, 52].

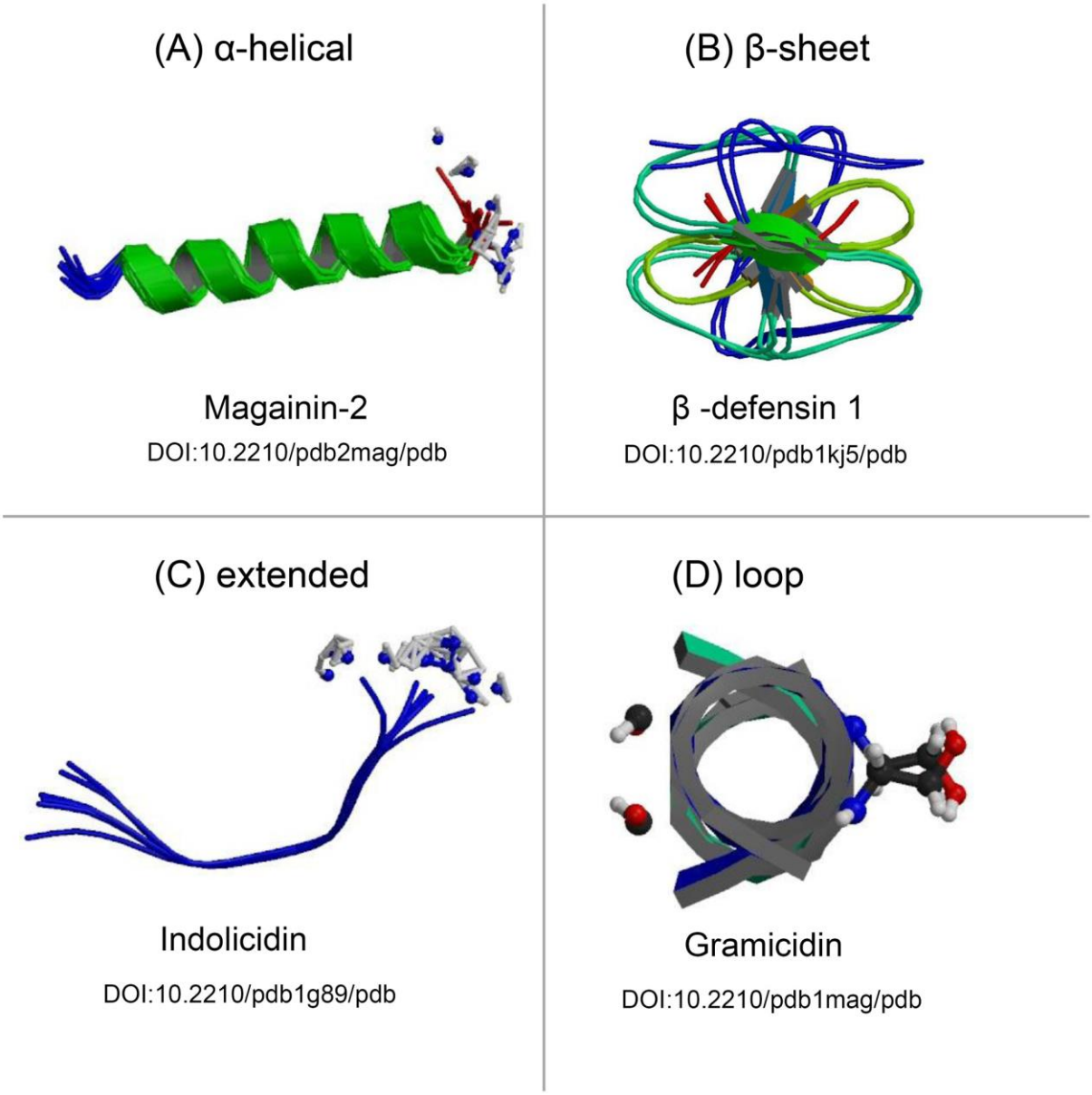

Figure 5: Presentation of the four main structures of antimicrobial peptides.
Figure taken from Peters et al 2010 [52]

The main mode of action of antimicrobial peptides is perturbation of the bilayer membrane, which at high concentrations can lead to destruction of cell envelope integrity. Various molecular mechanisms are described for the mode of action of AMPs to interact with cell membranes, whereby toroidal pore formation, the carpet model, interfacial activity, formation of voids, clustering of lipids and effects of membrane curvature are discussed (for review see Lohner 2017 [36]).

In brief, the torroidal pore formation was first time described by Matsuzaki [43] and Ludtke and Huang [39] for magainin 2. In this model, magainin and lipid molecules build a pore in the bilayer. The peptide molecules are thereby oriented perpendicular to the membrane surface. The polar surfaces of the alpha helices and lipid head groups constitute the pore lining. This allows free lipid diffusion between the inner and outer membrane leaflet caused by the continuous bilayer surface. Thereby, the pore causes two modes of cell killing, first destruction of the physiologically important asymmetry in the lipid composition of both membrane-layers and second the large openings in the membrane leading to lysis and instant death [43].

In contrast, the antibiotic peptide dermaseptin showed a different mode of membrane interaction leading to the carpet model [53, 64, 68]. The sequence of dermaseptin is rich in lysine residues and like maiginin also adopts an amphipathic α-helix. Especially the content of negatively charged lipids in the membrane promotes the carpet formation on the membrane surface by moderating the electrostatic repulsion forces between the positively charged peptides.

The interfacial activity model describes the accommodation of AMPs, which do not exhibit a perfect amphipathicity, into the hydrophilic and hydrophobic region of the bilayer. Thererby, local rearrangements and deformation of the lipid packing are driven by the imperfect separation of the polar and apolar amino acid residues and allow (at least partly) the perturbation of the hydrocarbon core.

In case the peptides exhibit ideal lateral amphipathicity, they get aligned in parallel orientation on the surface of the lipid membrane. Depending on the electrostatic nature of the lipid headgroups the peptide penetrates to different extent into the hydrophobic region being less deeply inserted in anionic bilayers. This would create free space or voids, which is

energetically unfavorable resulting in a quasi interdigitation by moving the inner leaflet towards the hydrophobic face of the peptide.

A further mode of action is the AMP induced separation of the phospholipids in neutral and in negatively charged lipid clusters (see Lohner 2017 [36] and references therein). Two domains can be distinguished, the peptide free bulk domain and the AMP enriched domain with cationic peptides bound to the anionic lipids.

Due to their truncated cone shaped geometry, PEs are known to induce non-lamellar phases such as inverted hexagonal (HII) or cubic phase [56, 62, 65]. Additionally, this molecular shape leads to a a curvature starin of the membrane. In bacterial cells, the balance between lipids inducing lamellar or non-lamellar structures is regulated within a small window. AMPs can disturb this balance facilitating the formation of non-lamellar structures leading to membrane disintegration. In any case, a distinct threshold is needed to lead to destabilization of the membrane integrity. It was also shown, that, at very low peptide concentrations, the peptide can fill up defects in the bilayer which leads to a homogenization and stabilization of the lipid matrix (see Bechinger et al. [2] and references therein).

Several steps are induced by AMPs and/or combinations of peptides: Loss of the membrane barrier function, dissipation of the trans-membrane electrochemical gradient, loss of cytoplasmic constituents and, additionally, interference with the energy metabolism in the cell [2]. It is worth mentioning that different types of peptides can interact cooperatively with other antibiotic molecules. For example, cell wall disintegration is induced by one peptide enabling the diffusion of smaller active molecules into the cell.

1.4 The Phospholipid Matrix as Target of Antimicrobial Peptides

Lipids are defined as a group of naturally occurring amphiphilic molecules. In biological systems, cell membranes are layers composed of such amphiphilic lipids having the main functionality to separate the interior cell system from the surrounding environment. Additionally, various proteins are embedded in the lipid matrix. Within these assemblies, lipids serve as structural matrix and assist in the protein function as well as in protein incorporation into the bilayer (Figure 6).

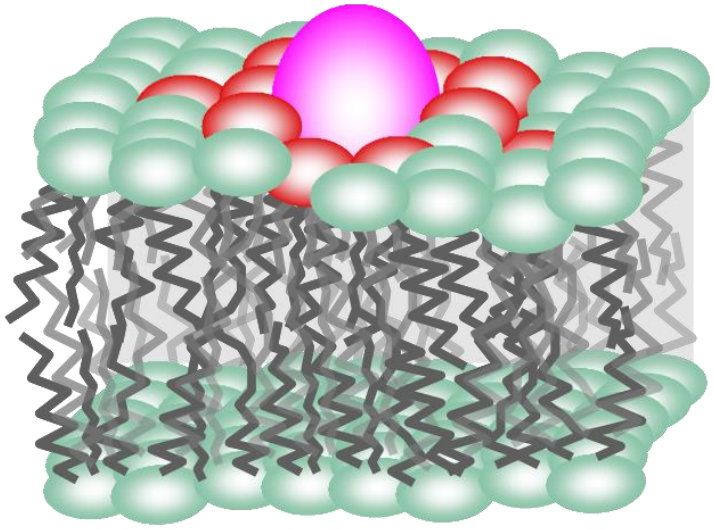

Figure 6: Schematic presentation of a protein embedded in a lipid bilayer.

The physical behaviour of lipid assemblies is a typical example of fluid crystalline phases, which was for the first time observed with cholesterol by Friedrich Reinitzer in 1888 [33]. The lipid molecules can be arranged in a variety of different two or three-dimensional lattices. Luzzati and Husson [40] proposed a nomenclature to classify all different phases, which is used in this work (Table 1).

Table 1: Overview of used letters classifying the various lipid phases

long range order		chain order		type of curved structured	
L	lamellar (one dimensional)	α	disordered (fluid phase)	I	normal (e.g. paraffin in water)
H	hexagonal (two-dimensional)	β	ordered untilted (gel phase)	II	inverted (e.g. water in paraffin)
P	oblique (two-dimensional)	β’	ordered tilted (gel phase)		
Q	cubic (three-dimensional)	c	crystalline		
C	crystalline (three-dimensional)				

Membrane architecture and lipid composition varies significantly between eukaryotic and prokaryotic cells. While the fatty acid chain length and degree of saturation vary depending on the environmental parameters to maintain the bilayer in the so-called fluid phase for optimal biological functionality, the variety of the different head groups seem to have more specific biological function. For example, human cell membranes as well as other mammalian membranes contain high contents of phosphatidylglycerol (PC) and sphingomyelin (SM) with a preferential location in the outer layer of the membrane. Additionally, phosphatidyethanolamine (PE) and phosphatidylserine (PS) are mainly found in the inner leaflet. Eukaryotic cells show a variety up to 500 different lipids they are composed of [44]. Besides, cholesterol is also found as a major component (up to 50%) in mammalian cell membranes, responsible for membrane permeability and fluidity [54]. Furthermore, Zheng et al. [75] showed for cholesterol a higher affinity to saturated lipid chains supposed to be involved in raft formation.

In the following, a brief description of the major phospholipids of eukaryotic and prokaryotic cytoplasmic membrane is given:

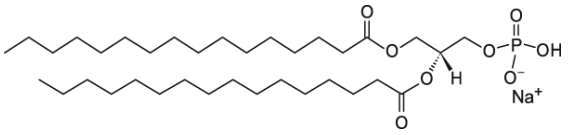

Phosphatidic acid (PA) is the smallest of the phospholipids. PA is involved as a precursor in lipid synthesis and serves also as a signalling lipid [9]. Additionally, its physical properties have a distinct influence on membrane curvature and in vesicle formation.

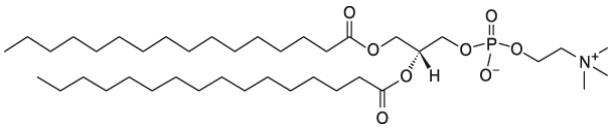

Phosphatidylcholine (PC, Lecithin) can be described as the main component found in human cell membranes. It forms a continuous membrane matrix and is responsible for precise fluidity, charge distribution and electronic character needed by enzymes and other molecules for functionality [29].

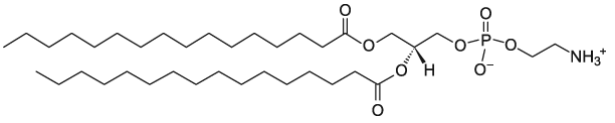

Phosphatidylethanolamine (PE, also: "Cephalin") is found to a large extent in eukaryotic cell membranes. Though it is also a major component of prokaryotic cell membranes, such as the Gram-negative bacteria *Escherichia coli*. As well as PC, PE is zwitterionic, i.e. has no net charge at physiological conditions.

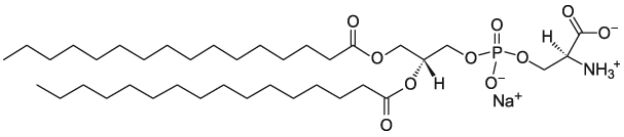

Phosphatidylserine (PS) is present in most biological membranes of animals and plants. For example, PS can be found at 15% of the lipid content in human brain. It is mainly located in the internal layer of the membrane bilayer and serves therein as a regulator for membrane fluidity and biological cell activities [29].

Phosphatidylinositol (PI) is 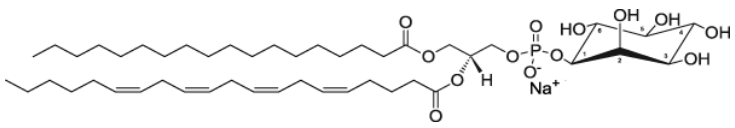 especially found in brain tissue at a content of about 10%, but it is present in all tissues and cell types. The characteristic head residue is inositol (cyclohexane-1,2,3,4,5,6-hexanol). It serves as a key membrane constituent and participates in essential metabolic processes in all plants and animals.

Besides above presented lipids, the negatively charged phosphatidylglycerol (PG) and diphosphatidylglycerol (DPG, Cardiolipin, CL) can be found in both the mitochondrial inner membranes of mammalian cells and typically to a high amount in bacterial or prokaryotic cell membranes [42], such as *Bacillus megaterium*, *Bacillus subtilis*, *Micrococcus luteus* and *Staphylococcus aureus* (see Table 2).

Table 2: Membrane phospholipid composition as percentages of the total of Gram-positive bacteria species.

		Phospholipid				
Bacteria species	**Cell Membrane**	**PE**	**PG**	**CL**	**Lysyl-PG**	**Others**
Staphylococcus aureus	CM	0	57	5	38	Trace
Bacillus megaterium	CM	40	40	5	15	0
Bacillus subtilis	CM	10	29	47	7	6 [a)]
Micrococcus luteus	CM	0	26	67	0	7 [b)]

Abbreviations: PE, phosphatidylethanolamine; PG, phosphatidylglycerol; CL, diphosphatidylglycerol; CM, cytoplasmic membrane or inner membrane for Gram-negative bacteria;
a) including phosphatidic acid and glycolipids; b) almost exclusively phosphatidylinositol.

In contrast, phosphatidylethanolamine (PE) is with 82% of the lipid content the main lipid found in the membrane of *Escherichia coli* [35]. Other bacterial species showing PE as main

lipid component are, for instance, *Salmonella typhimurium* and *Pseudomonas cepacia* (see Table 3).

Table 3: Membrane phospholipid composition as percentages of the total of representative Gram-negative bacteria species.

		Phospholipid		
Bacteria species	**Cell Membrane**	**PE**	**PG**	**CL**
Escherichia coli	OM	91	3	6
	CM	82	6	12
Salmonella typhimurium	OM	81	17	2
	CM	60	33	7
Pseudomonas cepacia	OM	87	13	0
	CM	82	18	0

Abbreviations: PE, phosphatidylethanolamine; PG, phosphatidylglycerol; CL, diphosphatidylglycerol, cardiolipin; OM, outer membrane; CM, cytoplasmic membrane or inner membrane for Gram-negative bacteria.

Anionic phospholipids are essential for insertion and translocation of proteins in the inner membrane. It is also known that anionic lipids interact or bind coordinatively to cationic charged residues of proteins [8].

Generally, cardiolipin is often investigated in its role as a lipid interacting with several membrane proteins. Examples, such as β2-glycoprotein [31] or the dnaA protein [63], are summarised by Schlame et al. [61]. Due to its unique conformation (Figure 6), CL is able to pack tightly forming micro-domains [22].

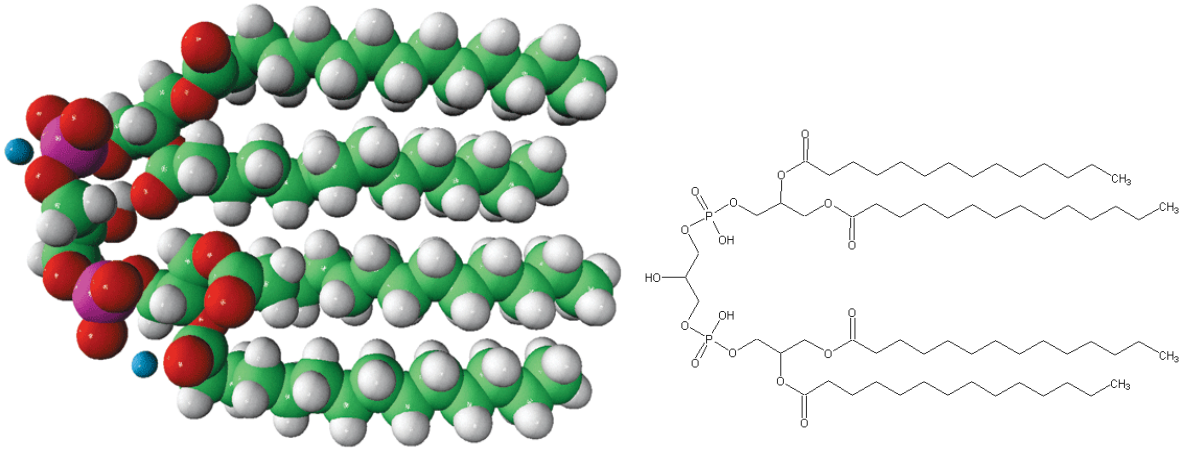

Figure 7: Space-filling model and structural formula of tetramyristoyl-cardiolipin

Interestingly, these domains are also used both to stabilize the protein structure and to support actively their functions. The intrinsic curvature of self assembled CL-aggregates makes them prone to be localised in the polar or septal regions of bacterial cell membrane (see Schlame [60] and ref. therein [27]). Another main function of CL is suggested by Haines and Dencher [22], due to its high pK_{a2} (>8), it traps protons at the H^+ uptake pathway of the energy transducing membrane (for details see Palsdottir and Hunte 2004 [51]).

In contrast, PG (Figure 8) does not show such a variety of specific functions. One role of PG is to be the precursor molecule for the synthesis of CL or other molecules [28]. Another reported specific function is the restoration of the activity of the resolved cytochrome bc1 complex (see Cruciat et al. [7] or for review Zhang et al. [74]).

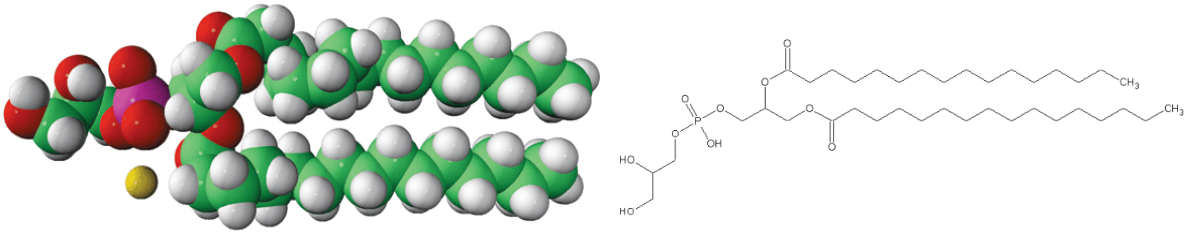

Figure 8: Space-filling model and structural formula of dipalmitoylphosphatidylglycerol

Beside PG and CL, other unusual lipids are found in Gram-positive bacteria. One of them is the positively charged lysyl-phosphatidylglycerol (Lysyl-PG), which is synthesized from PG and can be found to high content especially in *Staphylococcus aureus*.

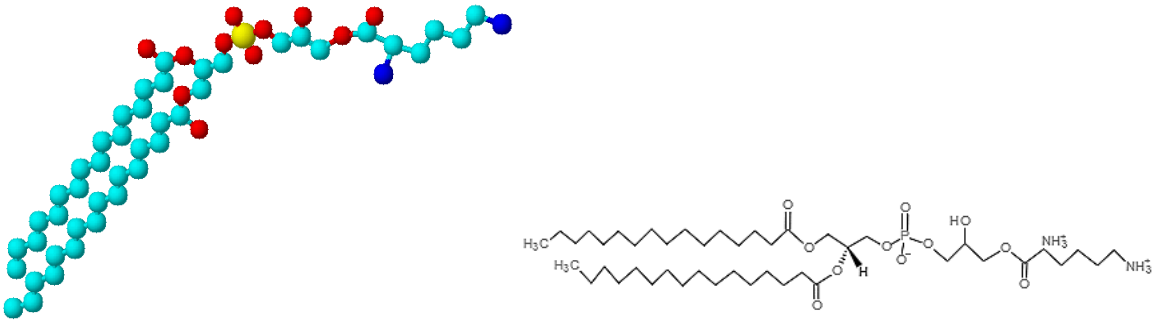

Figure 9: Structural formula of lysyl-dipalmitoylphosphatidylglycerol

Lysine with its two amino groups changes the net charge of the lipid headgroup from negative to positive (Figure 9). Various bacteria species have developed mechanisms to survive in inhospitable environments, e.g. on human epithelia (for review see Hornef et al. 2005 [24]). In detail, *Staphylococcus aureus* exhibits under mild acidic environment (pH 5.5), as found on human epidermis, an increase of the lysyl-PG content in its lipidome [10, 45]. The overall lysyl-PG quantity in *Staphylococcus aureus*' lipid mixture was found to a ratio of more than 30% and even reaches with up to 55% a parity level to the anionic lipids [58]. In consequence, this neutralizes the net charge of the lipid membrane and, additionally, leads to a more closed packing of lipids [6]. Cox et al. presented that this lysylation of PG leads to a reduction of the activity of AMPs such as cecropin A and mastoparan X [6].

1.5 Experimental approach for bacterial model systems

1.5.1 Differential Scanning Calorimetry (DSC)

Calorimetry is used to gain information about the thermotropic behaviour of lipids. Thereby information on transition temperatures, enthalpy, entropy and cooperativity can be calculated from the heat capacity curves.

In a DSC experiment, a sample and a reference cell are heated simultaneously. During a phase transition, different amounts of power are supplied to maintain both cells at the same temperature. This additional heat flow is determined by measuring the consumed electric current. As a DSC-measurement is performed at constant pressure, the first law of thermodynamics can be applied:

$$dH = \partial Q + Vdp \tag{1}$$

To be continued with the following conditional equation

$$dH = \left(\frac{\partial H}{\partial T}\right)_p dT + \left(\frac{\partial H}{\partial p}\right)_T dp \tag{2}$$

and its first partial derivative, the heat capacity, can be defined as:

$$\left(\frac{\partial H}{\partial T}\right)_p = C_p \tag{3}$$

While the temperature of the system changes from T_0 to T, the enthalpy change ($\Delta H = H(T) - H(T_0)$) follows equation (4):

$$\Delta H = \int_{T_0}^{T} C_p dT \tag{4}$$

At the transition temperature, both phases are in equilibrium and, consequently by definition, any transfer of heat is reversible. The entropy can then be calculated using equation (5):

$$\Delta S = \frac{\Delta H_{cal}}{T_m} \tag{5}$$

Additional to the calorimetric enthalpy, ΔH_{cal}, the van't Hoff enthalpy, ΔH_{vH}, can be calculated using equation (**6**) below [16, 41]:

$$\Delta H_{vH} = \frac{4 \cdot R \cdot (T_m + 273.15)^2 \cdot \Delta C_{p\max}}{\Delta H_{cal}} \tag{6}$$

where R is the ideal gas constant (R= 1,9859 cal·mol^{-1}·K^{-1}), T_m the transition temperature at the peak maximum (°C) and ΔC_{pmax} the peak maximum of the heat capacity. The cooperativity (N) of a transition can be calculated from the ratio between van't Hoff and calorimetric enthalpy:

$$N = \frac{\Delta H_{vH}}{\Delta H_{cal}} \tag{7}$$

and represents the average number of lipid molecules per cluster. A ratio of 1 indicates a two-state transition without any intermediates, while a ratio larger than 1 as seen with phospholipids shows that the molecules are arranged in clusters [16].

For quantitative data determination, recorded DSC thermograms are normalized to the lipid concentration and scan-rate. After baseline subtraction, the calorimetric enthalpies can be determined by integrating the peak areas under the obtained heat capacity curves. For each peak, the temperature of the maximum heat capacity (ΔC_{pmax}) was taken as the phase transition temperature, T_m. Values for onset (T_{on}) and completion (T_{off}) temperatures were determined by the tangent method as the intersection of the peak slopes with the baseline following the procedure described by Garidel et al. [17]. In the case of pure lipids the

differences of these values to the main transition temperatures (ΔT) were calculated and used in equation 8 and 9.

In theory, ideal phase transitions assume infinite cooperativity [16, 30]. Therefore, in calorimetric measurements one should expect transition peaks with a high C_{pmax} and an infinite small width at half maximum. In reality, a broadening caused by finite cooperativity is detected for pure lipids and mixtures, as well. To correct this non-ideality, the broadening of the pure lipids is set as a standard. Therefore, the measured onset and offset values, $T_{on/off,meas}$, of all lipid samples were corrected by the ΔT-values of the pure components weighted by their mole fractions (X_{DPPG} and X_{TMCL}) [30, 41].

$$T_{on,korr} = T_{on,meas.} + X_{DPPG} \cdot \Delta T_{DPPG,on} + X_{TMCL} \cdot \Delta T_{TMCL,on} \quad (8)$$

$$T_{off,korr} = T_{off,meas.} - X_{DPPG} \cdot \Delta T_{DPPG,off} - X_{TMCL} \cdot \Delta T_{TMCL,off} \quad (9)$$

1.5.2 X-ray Scattering

X-ray scattering measurements base on the interaction of electromagnetic waves with matter. Depending on the absorption and scattering power of the investigated material the energy can be chosen such that the scattering power is maximized. For biological material as investigated in this work usually a photon energy of 8 keV is ideal, since it results in optimal sample thicknesses of about 1 millimeter.

X-ray scattering experiments can be carried out both on lab sources as well as at a synchrotron. The first are composed of an electron-emitting cathode and an anode made of or covered by metal e.g. copper or molybdenum. Emitted electrons are accelerated to the

anode by a high voltage source. Depending on both anode material and applied voltage, three types of radiation are emitted after the electrons hit the anode material: Characteristic x-ray radiation, Bremsstrahlung and Lilienfeld radiation. In practice, normally only one of the characteristic x-ray wavelengths is used, while all other radiation is filtered. At a synchrotron site electrons are accelerated in storage rings up to almost speed of light. Magnets are used to keep the electrons on a circular path causing thereby the emission of the synchrotron radiation. To generate stronger radiation (used in synchrotrons of the third generation), insertion devices are applied. These devices are straight sections composed of many permanent magnets having a special repeating row of N and S poles. Electrons are forced into a sinusoidal trajectory, when they pass such an insertion device. There are two types of insertion devices, wiggler and undulators. Depending on their design, they produce beams with a broad energy spectrum (wiggler) or a narrow energy spectrum with high brilliance (undulator).

In any case - lab or synchrotron - the emitted radiation is guided through a collimation system, passes through the sample and finally the scattered X-rays are recorded in the focal/detector plan. Small and wide-angle x-ray scattering (SWAXS) are used to investigate structures in the nanometer scale range. The wavelength of the emitted beam is not changed, while the direction is. Scattered waves undergo constructive interference under distinct angles following the Braggs law:

$$n\lambda = 2d\sin(\theta) \tag{10}$$

For scattering measurements lipid samples can be prepared as mono- and multi layers, respectively, oriented on a solid surface or as a dispersion of non-planar particles (e.g. vesicles or bicelles). Scattering patterns of a bilayer with a perfect crystalline order show Bragg peaks that are independent of their order and of equal width and intensity. However,

lattice defects, thermal disorder, stacking disorder and bending fluctuation disorder of the lipid bilayer stacks can change size and shape of the Bragg peaks.

Scattering patterns are recorded with linear or also two-dimensional detectors. In practise using a SWAX camera with Kratky collimation system (Hecus X-ray Systems, Graz, Austria) [34], patterns are divided into two regimes of 10^{-3} Å^{-1} < q < 1 Å^{-1} (SAXS) and 1.2 Å^{-1} < q < 2.7 Å^{-1} (WAXS), wherein $q = 4\pi \sin(\theta)/\lambda$ is the modulus of the scattering vector. The intensity of a stack of layers scattered in the SAXS regime can be described as:

$$I(q) = \frac{S(q)|F(q)|^2}{q^2} \tag{11}$$

Therein, *S(q)* is the structure factor and *F(q)* is the form factor, respectively. The latter describes the electron density distribution of the bilayer cross section. This electron density is adequately simulated by two Gaussians [50], one representing the head group the other the fatty acid chains of the lipid molecules (Figure 10). The main parameters determined by SAXS data evaluation are the lamellar repeat distance (d), the distance between head group and end of the fatty acids chains (z_H), the electron density relation of the head group to hydrocarbon chains (ρ_C /ρ_H), the thickness of the bilayer (d_B) and the water layer (d_W), respectively (Figure 10).

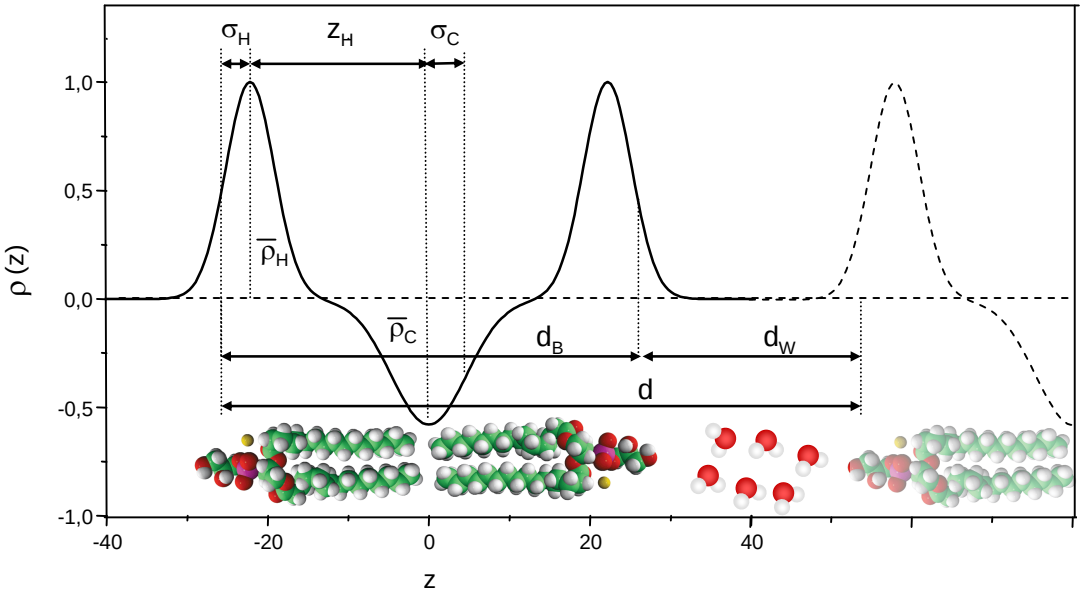

Figure 10: Electron density profile. ρ(z), as a function of distance, z, from the bilayer center.

S(q) is the intraparticle structure factor showing how bilayers are positionally correlated with each other. To model the structure factor, some theories were established. First the paracrystalline theory [21, 25] and second the Caillé theory [3]. Both theories in common is the assumption of deficiencies in the long range order. The main difference is the description of stochastic fluctuations of single, ideally flat layers described by the paracrystalline theory and bilayer undulations considered by the Caillé theory (for reviews see Pabst [48] and Rappolt et al. [55]). All above-mentioned parameters are determined by a fitting procedure based on the models described above. Data treatment generally follows the rules and steps described in detail by Pabst et al. [49, 50].

The hydrocarbon chain lattice can be determined by the peak positions in a WAXS pattern. In the case of an ideal hexagonal chain lattice, the area per lipid chain, A_c, can be deduced from the first order peak only. If the chains are tilted relatively to the surface plane like in the L_{β}' lamellar gel phase, the hexagonal chain lattice is not preserved any more, but slightly distorted and thus described by an orthorhombic lattice instead, i.e. a sharp peak (d_{20})

flanked by a second broad peak shifted to higher angle (d_{11}). In this case A_c can be calculated with data obtained from WAXS patterns according to Tristram-Nagle et al. [69]:

$$A_c = \frac{d_{20} d_{11}}{\sqrt{1 - \left(\frac{d_{11}}{2d_{20}}\right)^2}} \tag{3}$$

which compares to an ideal hexagonal chain packing (d_{20}= d_{11}= d) as follows

$$A_c = \frac{2d^2}{\sqrt{3}} \tag{4}$$

In lamellar (two-dimensional) composition, the fatty acid chains are arranged in a hexagonal or orthorhombic structure (Figure 11). In the former the hydrocarbon chains stand perpendicularly to the surface plane. In the latter case, they are tilted and the angle between the chains and the plane is unequal to 90°. The therefore caused stretching of the hexagonal arrangement leads to the orthorhombic structure (Figure 11).

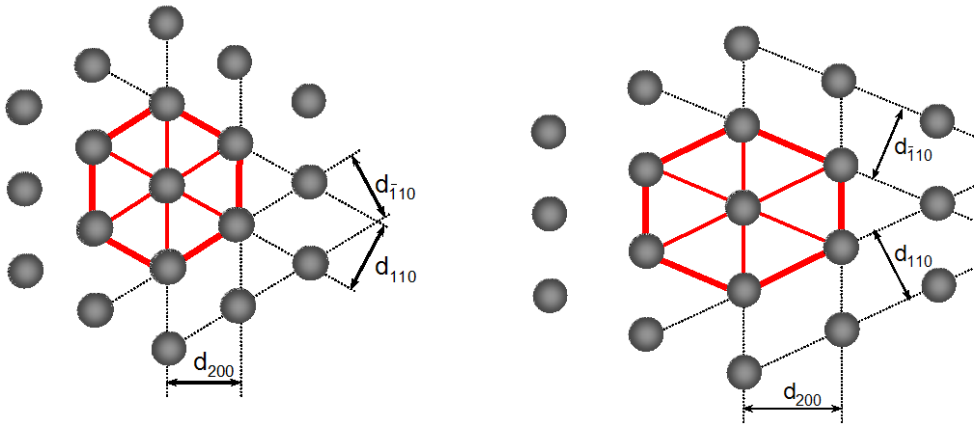

Figure 11: Top-view presentation of chain packing in hexagonal (left) and orthorhombic lattice (right).

Reference list:

[1] A.C. Fluit and F.J. Schmitz., 2003, MRSA: Current Perspectives, Caister Academic Press, Wymondham, Norfolk, England, ISBN: 0-9542464-5-4

[2] B. Bechinger and K. Lohner, 2006, Detergent-like actions of linear amphipathic cationic antimicrobial peptides, Biochim.Biophys.Acta, 1758, 1529-1539

[3] A. Caillé, 1972, C R Hebd Seances Acad Sci, Ser. B, 891-

[4] CDC, 1-5-1981, Community-acquired methicillin-resistant Staphylococcus aureus infections--Michigan, MMWR Morb.Mortal.Wkly.Rep., 30, 185-187

[5] S. Chang, D.M. Sievert, J.C. Hageman, M.L. Boulton, F.C. Tenover, F.P. Downes, S. Shah, J.T. Rudrik, G.R. Pupp, W.J. Brown, D. Cardo and S.K. Fridkin, 3-4-2003, Infection with vancomycin-resistant Staphylococcus aureus containing the vanA resistance gene, N.Engl.J.Med., 348, 1342-1347

[6] E. Cox, A. Michalak, S. Pagentine, P. Seaton and A. Pokorny, 2014, Lysylated Phospholipids Stabilize Models of Bacterial Lipid Bilayers and Protect Against Antimicrobial Peptides, Biochim Biophys Acta., 2014 Sep; 1838(9): 2198–2204.

[7] C.M. Cruciat, S. Brunner, F. Baumann, W. Neupert and R.A. Stuart, 16-6-2000, The cytochrome bc1 and cytochrome c oxidase complexes associate to form a single supracomplex in yeast mitochondria, J.Biol.Chem., 275, 18093-18098

[8] B. de Kruijff, 6-6-1994, Anionic phospholipids and protein translocation, FEBS Lett., 346, 78-82

[9] C. Delon, M. Manifava, E. Wood, D. Thompson, S. Krugmann, S. Pyne and N.T. Ktistakis, 22-10-2004, Sphingosine kinase 1 is an intracellular effector of phosphatidic acid, J.Biol.Chem., 279, 44763-44774

[10] T.J. Denich, L.A. Beaudette, H. Lee, J.T. Trevors, 2003, Effect of selected environmental and physico-chemical factors on bacterial cytoplasmic membranes, J. Microbiol. Methods, 52, 149–182

[11] M.E. Doyle, 2006, Veterinary Drug Residues in Processed Meats — Potential Health Risk, Food Research Institute

[12] EARSS, 2002, Annual Report 2002, The European Antimicrobial Resistance Surveillance System (EARSS)

[13] EARSS, 2006, Annual Report 2006, The European Antimicrobial Resistance Surveillance System (EARSS)

[14] European Centre for Disease Prevention and Control. Antimicrobial resistance surveillance in Europe 2013. Annual Report of the European Antimicrobial Resistance Surveillance Network (EARS-Net). Stockholm: ECDC; 2014.

[15] T.J. Foster, 2004, The Staphylococcus aureus "superbug", J.Clin.Invest, 114, 1693-1696

[16] P. Garidel, C. Johann, and A. Blume, 1997, Nonideal mixing and phase separation in phosphatidylcholine-phosphatidic acid mixtures as a function of acyl chain length and pH, Biophys.J., 72, 2196-2210

[17] P. Garidel, C. Johann, and A. Blume, 2005, The calculation of heat capacity curves and phase diagrams based on regular solution theory, Journal of Thermal Analysis and Calorimetry, 82, 447-455

[18] M. Goetghebeur, P.A. Landry, D. Han and C. Vicente, 2007, Methicillin-resistant Staphylococcus aureus: A public health issue with economic consequences, Can.J.Infect.Dis.Med.Microbiol., 18, 27-34

[19] M. Goozner, 2005, Cost of new drugs, Health Aff.(Millwood.), 24, 883-884

[20] Y.J. Gordon, E.G. Romanowski and A.M. McDermott, 2005, A review of antimicrobial peptides and their therapeutic potential as anti-infective drugs, Cur r.Eye Res., 30, 505-515

[21] A. Guinier, 1963, X-Ray Diffraction, W.H. Freeman

[22] T.H. Haines and N.A. Dencher, 25-9-2002, Cardiolipin: a proton trap for oxidative phosphorylation, FEBS Lett., 528, 35-39

[23] R.E. Hancock, 8-2-1997, Peptide antibiotics, Lancet, 349, 418-422

[24] M.W. Hornef, S. Normark, B. Henriques-Normark and M. Rhen, 2005, Bacterial evasion of innate defense at epithelial linings, Chemical Immunology and Allergy, Volume 86, 72-98

[25] R. Hosemann and S.N. Bagchi, 1962, Direct Analysis of Diffraction by Matter, North-Holland publishing Co., Amsterdam

[26] R.A. Howe, A. Monk, M. Wootton, T.R. Walsh and M.C. Enright, 2004, Vancomycin susceptibility within methicillin-resistant Staphylococcus aureus lineages, Emerg.Infect.Dis., 10, 855-857

[27] K.C. Huang, R. Mukhopadhyay and N.S. Wingreen, 10-11-2006, A curvature-mediated mechanism for localization of lipids to bacterial poles, PLoS.Comput.Biol., 2, e151-

[28] R.P. Huijbregts, A.I. de Kroon and B. de Kruijff, 10-3-2000, Topology and transport of membrane lipids in bacteria, Biochim.Biophys.Acta, 1469, 43-61

[29] R. Jager, M. Purpura and M. Kingsley, 2007, Phospholipids and sports performance, J.Int.Soc.Sports Nutr., 4, 5-

[30] C. Johann, P. Garidel, L. Mennicke and A. Blume, 1996, New approaches to the simulation of heat-capacity curves and phase diagrams of pseudobinary phospholipid mixtures, Biophys.J., 71, 3215-3228

[31] Z. Kertesz, B.B. Yu, A. Steinkasserer, H. Haupt, A. Benham and R.B. Sim, 15-8-1995, Characterization of binding of human beta 2-glycoprotein I to cardiolipin, Biochem.J., 310 (Pt 1), 315-321

[32] E. Klein, D.L. Smith and R. Laxminarayan, 2007, Hospitalizations and deaths caused by methicillin-resistant Staphylococcus aureus, United States, 1999-2005, Emerg.Infect.Dis., 13, 1840-1846

[33] P. Laggner, 2007, Friedrich Reinitzer (1857-1927): vom Entdecker der Flüssigkristalle zum Kämpfer gegen den "Cognac-Wahn" , Karl Acham, Böhlau Verlag GmbH, 319-326

[34] P. Laggner and H. Mio, 1992, SWAX - A dual-detector camera for simultaneous small- and wide-angle X-ray diffraction in polymer and liquid crystall research., Nucl.Instr.and Meth.Phys.Res., A, 86-90

[35] K. Lohner, A. Latal, G. Degovics and P. Garidel, 2001, Packing characteristics of a model system mimicking cytoplasmic bacterial membranes, Chem.Phys.Lipids, 111, 177-192

[36] K. Lohner, 2017, Membrane-active Antimicrobial Peptides as Template Structures for Novel Antibiotic Agents, Current Topics in Medicinal Chemistry, Volume 17, Number 5, 508-519(12)

[37] K. Lohner; A. Latal; R.I. Lehrer and T. Ganz, 1997, Differential scanning microcalorimetry indicates that human defensin, HNP-2, interacts specifically with biomembrane mimetic systems. Biochemistry, 36, 1525-1531.

[38] F.D. Lowy, 2003, Antimicrobial resistance: the example of Staphylococcus aureus, J.Clin.Invest, 111, 1265-1273

[39] S.J. Ludtke; K. He; W.T. Heller; T.A. Harroun; L. Yang; H.W. Huang, 1996, Membrane pores induced by magainin. Biochemistry, 35, 13723-13728.

[40] V. Luzzati and F. Husson; 1962; THE STRUCTURE OF THE LIQUID-CRYSTALLINE PHASES OF LIPID-WATER SYSTEMS. The Journal of Cell Biology, 12(2), 207–219.

[41] S. Mabrey and J.M. Sturtevant, 1976, Investigation of phase transitions of lipids and lipid mixtures by sensitivity differential scanning calorimetry, Proc.Natl.Acad.Sci.U.S.A, 73, 3862-3866

[42] K. Matsumoto, 2001, Dispensable nature of phosphatidylglycerol in Escherichia coli: dual roles of anionic phospholipids, Mol.Microbiol., 39, 1427-1433

[43] K. Matsuzaki, O. Murase, N. Fujii and K. Miyajima, 3-9-1996, An antimicrobial peptide, magainin 2, induced rapid flip-flop of phospholipids coupled with pore formation and peptide translocation, Biochemistry, 35, 11361-11368

[44] S. Mayor and M. Rao, 2004, Rafts: scale-dependent, active lipid organization at the cell surface, Traffic., 5, 231-240

[45] J.A. Nesbitt, W.J. Lennarz, 1968, Participation of aminoacyl transfer ribonucleic acid in aminoacyl phosphatidylglycerol synthesis. I. Specificity of lysyl phosphatidylglycerol synthetase, J. Biol. Chem., 243, 3088

[46] P. Nordberg, D.L. Monnet and O. Cars, 2005, Antibacterial drug resistance: Options for concerned action, WHO, Department of Medicines Policy and Standards

[47] A. Ogston, 1884, "On Abscesses" Classics in Infectious Diseases, Reviews of infectious diseases., 6, 122-128

[48] G. Pabst, 2006, Global properties of biomimetic membranes: perspectives on molecular features, Biophysical Reviews and Letters, 57-84

[49] G. Pabst, R. Koschuch, B. Pozo-Navas, M. Rappolt, K. Lohner, and P. Laggner, 2003, Structural analysis of weakly ordered membrane stacks, Journal of Applied Crystallography, 36, 1378-1388

[50] G. Pabst, M. Rappolt, H. Amenitsch, and P. Laggner, 2000, Structural information from multilamellar liposomes at full hydration: full q-range fitting with high quality x-ray data, Phys.Rev.E.Stat.Phys.Plasmas.Fluids Relat Interdiscip.Topics., 62, 4000-4009

[51] H. Palsdottir and C. Hunte, 3-11-2004, Lipids in membrane protein structures, Biochim.Biophys.Acta, 1666, 2-18

[52] B.M. Peters, M.E. Shirtliff and M.A. Jabra-Rizk, 2010, Antimicrobial Peptides: Primeval Molecules or Future Drugs?, PLoS Pathogens, Volume 6, Issue 10

[53] Y. Pouny, D. Rapaport, A. Mor, P. Nicolas and Y. Shai, Y., 15-12-1992, Interaction of antimicrobial dermaseptin and its fluorescently labeled analogues with phospholipid membranes, Biochemistry, 31, 12416-12423

[54] F. T. Presti and S.I. Chan, 3-8-1982, Cholesterol-phospholipid interaction in membranes. 1. Cholestane spin-label studies of phase behavior of cholesterol-phospholipid liposomes, Biochemistry, 21, 3821-3830

[55] M. Rappolt and G. Pabst, 2008, Flexibility and Structure of Fluid Bilayer Interfaces, John Wiley & Sons, Hoboken (NJ)3, 45-81

[56] M. Rappolt; A. Hickel; F. Bringezu and K. Lohner, 2003, Mechanism of the lamellar/inverse hexagonal phase transition examined by high resolution x-ray diffraction. Biophys. J., 84, 3111-3122.

[57] A. Raudino; M.G. Sarpietro and M. Pannuzzo, 2011 The thermodynamics of simple biomembrane mimetic systems. J. Pharm. Bioallied. Sci., 3, 15-38.

[58] R.P. Rehal, H. Marbach, A.T.M. Hubbard, A.A. Sacranie, F. Sebastiani, G. Fragneto and R.D. Harvey, 2017, The influence of mild acidity on lysyl-phosphatidylglycerol biosynthesis and lipid membrane physico-chemical properties in methicillin-resistant Staphylococcus aureus, Chem Phys Lipids., 206, 60-70

[59] A.D. Russell, 1999, Bacterial resistance to disinfectants: present knowledge and future problems, J.Hosp.Infect., 43 Suppl, S57-S68

[60] M. Schlame, 12-12-2007, Cardiolipin synthesis for the assembly of bacterial and mitochondrial membranes, J.Lipid Res.,

[61] M. Schlame, D. Rua and M.L. Greenberg, 2000, The biosynthesis and functional role of cardiolipin, Prog.Lipid Res., 39, 257-288

[62] J.M. Seddon, 1990, Structure of the inverted hexagonal (HII) phase, and non-lamellar phase transitions of lipids. Biochim. Biophys. Acta, 1031, 1-69.

[63] K. Sekimizu and A. Kornberg, 25-5-1988, Cardiolipin activation of dnaA protein, the initiation protein of replication in Escherichia coli, J.Biol.Chem., 263, 7131-7135

[64] Y. Shai, 15-12-1999, Mechanism of the binding, insertion and destabilization of phospholipid bilayer membranes by alpha-helical antimicrobial and cell non-selective membrane-lytic peptides, Biochim.Biophys.Acta, 1462, 55-70

[65] D.P. Siegel and J. Banschbach, 1990 Lamellar/inverted cubic (L alpha/QII) phase transition in N-methylated dioleoylphosphatidylethanolamine. Biochemistry, 29, 5975-5981.

[66] M.P. Singh and M. Greenstein, 2000, Antibacterial leads from microbial natural products discovery. Curr Opin Drug Discov Dev, 3:167-76

[67] R.D. Smith and J. Coast, 2002, Antimicrobial resistance: a global response, Bull.World Health Organ, 80, 126-133

[68] H. Steiner, D. Hultmark, A. Engstrom, H. Bennich and H.G. Boman, 16-7-1981, Sequence and specificity of two antibacterial proteins involved in insect immunity, Nature, 292, 246-248

[69] S. Tristram-Nagle, R. Zhang, R.M. Suter, C.R. Worthington, W.J. Sun and J.F. Nagle, 1993, Measurement of chain tilt angle in fully hydrated bilayers of gel phase lecithins, Biophys.J., 64, 1097-1109

[70] G. Wang [Online] Antimicrobial Peptide Database., 02 10 2017, http://aps.unmc.edu/AP/main.php

[71] G. Wang, K.M. Watson and R.W. Buckheit Jr., 2008, Anti-human immunodeficiency virus type 1 activities of antimicrobial peptides derived from human and bovine cathelicidins, Antimicrob.Agents Chemother., 52, 3438-3440

[72] R. Wise, T. Hart, O. Cars, M. Streulens, R. Helmuth, P. Huovinen and M. Sprenger, 5-9-1998, Antimicrobial resistance. Is a major threat to public health, BMJ, 317, 609-610

[73] World Economic Forum, Global Risks 2013, Editor in Chief: Lee Howell

[74] M. Zhang, E. Mileykovskaya and W. Dowhan, 15-11-2002, Gluing the respiratory chain together. Cardiolipin is required for supercomplex formation in the inner mitochondrial membrane, J.Biol.Chem., 277, 43553-43556

[75] L. Zheng, C.M. McQuaw, M.J. Baker, N.P. Lockyer, J.C. Vickerman, A.G. Ewing and N. Winograd, 2008, Investigating Lipid-Lipid and Lipid-Protein Interactions in Model Membranes by TOF-SIMS, Applied Surface Science,

2 Aim of this work

This doctoral thesis was performed within the framework of a research project of the FWF, dedicated to the description of the lipidome of *Staphylococcus aureus* strains showing different susceptibility to cationic antimicrobial peptides. A few instances of bacterial resistance to cationic AMPs have been reported earlier [5], whereby a role of surface charge in protection of bacteria against such peptides was suggested from experiments with staphylococcal mutants, that were characterized by a different degree of D-alanine esterified teichoic acids [4]. These mutants, characterized by an increased net negative surface charge as compared to the wild-type, were more sensitive than the wild-type to a number of AMPs, such as defensins, protegrins or magainin 2. Furthermore, modifying the negatively charged phosphatidylglycerol with charged L-lysine reverses the lipid charge presumably resulting in repulsion of cationic peptides [6]. Hence, the resistance of *S. aureus* to AMPs could also be explained by an increased content of lysyl-phosphatidylglycerol. This may imply that the AMPs of the innate immune system are rather ineffective against *S. aureus* infections. Recently, Mukhopadhyay et al. [3] indeed showed that the susceptibility of different mutant strains of *Staphylococcus aureus* to thrombin-induced platelet microbicidial proteins (tPMP) may correlate with the fraction of cationic lipids in the outer layer of their cytoplasmic membrane (tPMP-resistant strain 27.3±11.0% lysyl-PG as compared to 18.6±7.0% in the susceptible strain) [1]. A detailed understanding of this observation will be a key to implement new treatment strategies and will form the basis for the specific design of antimicrobial peptides. This requires, however, the analysis of the entire lipid spectrum (= lipidome) of the cytoplasmic membrane of *S. aureus*, which also implements the thermodynamic and structural characterization of these lipids. The three major lipids found

in the plasma membrane of *S. aureus* strains are phosphatidylglycerol (PG), cardiolipin (CL) and lysyl-phosphatidylglycerol (lysyl-PG).

Within this FWF project, the phase behavior of lysyl-PG was described by Danner et al. [2] for the first time. The aim of this doctoral thesis focussed on the characterization of the two other main membrane phospholipids constituents, the negatively charged lipids PG and CL. This includes the establishment of the binary phase diagram of the lipid mixtures serving as a first mimetic system not only for *S. aureus* but for a variety of Gram-positive bacteria, which contain these lipids in their cytoplasmic cell membrane. It also forms the basis for further systematic studies: (i) the elucidation of the more complex ternary lipid mixture including lysyl-PG, and (ii) interaction with antimicrobial peptides such as the frog skin peptide PGLa. The latter kind of consecutive investigations shall elucidate the mode of interaction of the cationic peptide PGLa with a lipid model system exhibiting with lysyl-PG an adjustable ratio of positively charged headgroups. The methods used to investigate the thermotropic phase behavior of the model system were DSC and X-ray scattering techniques.

Reference list:

[1] B. Bechinger and K. Lohner, 2006, Detergent-like actions of linear amphipathic cationic antimicrobial peptides; Biochim. Biophys. Acta; 9; Vols. 1758, 1529-1539.

[2] S. Danner, G. Pabst, K. Lohner and A. Hickel, 2008, Structure and Thermotropic Behavior of the Staphylococcus aureus Lipid Lysyl-Dipalmitoylphosphatidylglycerol, Biophysical Journal, Bd. 94, 2150 - 2159.

[3] K. Mukhopadhyay, W. Whitmire, Y.Q. Xiong, J. Molden, T. Jones, A. Peschel, P. Staubitz, J. Adler-Moore, P.J. McNamara, R.A. Proctor, M.R. Yeaman and A.S. Bayer, 2007, In vitro susceptibility of Staphylococcus aureus to thrombin-induced platelet microbicidal protein-1 (tPMP-1) is influenced by cell membrane phospholipid composition and asymmetry, Microbiology, Bd. 153, 1187 - 1197.

[4] A. Peschel, M. Otto, R.W. Jack, H. Kalbacher, G. Jung and F. Götz, 1999, Inactivation of the dlt Operon in Staphylococcus aureus Confers Sensitivity to Defensins, Protegrins, and Other Antimicrobial Peptides, The Journal of Biological Chemistry, Bde. Vol. 274, No. 13, 8405–8410.

[5] A. Peschel, 2002, How do bacteria resist human antimicrobial peptides? Trends in Microbiology, Vol. 10.; 179-86.

[6] P. Staubitz, H. Neumann, T. Schneider, I. Wiedemann and A. Peschel, 2004, MprF-mediated biosynthesis of lysylphosphatidylglycerol, an important determinant in staphylococcal defensin resistance, FEMS Microbiology Letters, Bd. 231, 67-71.

3 Packing behaviour of two predominant anionic phospholipids of bacterial cytoplasmic membranes

Florian Prossnigg, Andrea Hickel, Georg Pabst and Karl Lohner

Published in:

Biophysical Chemistry, 2010 August; 150(1-3): 129–135.

Dedicated to Prof. Dr. Alfred Blume on the occasion of his 65th birthday.

Content from original publication and fit to the format of this thesis

3.1 Abstract

Phosphatidylglycerol and cardiolipin represent the most abundant anionic phospholipid components of cytoplasmic bacterial membranes and thus are used as constituents for membrane mimetic systems. In this study, we have characterized the temperature dependent phase behaviour of the binary system dipalmitoyl-phosphatidylglycerol (DPPG) and tetramyristoyl-cardiolipin (TMCL) using microcalorimetry and x-ray scattering techniques. Both lipids exhibited a very similar main transition temperature (~ 41°C), showing a minimum (39.4°C) for the binary mixtures at X_{DPPG} = 0.8, and exhibited low temperature phase transitions, which were abolished by incorporation of small amounts (≤ 10 mol%) of the other lipid component. Therefore, over a wide temperature and composition range a lamellar L_β gel phase is the predominant structure below the chain melting transition, characterized by a relatively broad wide-angle peak for $X_{DPPG} \leq 0.8$. This observation suggests the existence of packing inconsistencies of the TMCL/DPPG hydrocarbon lattices in the gel phase, supported by the small average size of lipid clusters (~50 lipids) within this composition range. The bilayer thickness for the lamellar gel phase showed a monotonic increase (56 Å for TMCL to about 58 Å for X_{DPPG} = 0.8 at 30°C), which may be explained by different degrees of partial interdigitation of the acyl chains to compensate for the differences in the hydrocarbon lengths of DPPG and TMCL in the L_β phase.

Keywords:

Phase diagram; liposomes, membrane mimics, *S. aureus*, X-ray diffraction; differential scanning calorimetry

Abbreviations

CL.....diphosphatidylglycerol (cardiolipin)
TMCL.....tetramyristoyl-cardiolipin
(DP)PG...(dipalmitoyl-)phosphatidylglycerol
PE .....phosphatidylethanolamine
$L_{c'}$ .....subgel phase
SGII .....subsubgel phase with tilted hydrocarbons
L_{R1} .....subsubgel phase with untilted hydrocarbons
L_{β} .....lamellar-gel phase with untilted hydrocarbon chains
$L_{\beta'}$ .....lamellar-gel phase with tilted hydrocarbon chains
$P_{\beta'}$ .....ripple-gel phase
L_{α}.....fluid phase with melted hydrocarbon chains
DSC .....differential scanning calorimetry
$T_{(m)}$.....(main) transition temperature
T_{pre} .....pre-transition temperature
$\Delta H_{(m)}$.....(main) transition enthalpy
ΔH_{pre}.....pre-transition enthalpy
SWAXS..small and wide angle x-ray scattering
z_H .....distance between head group and center of the bilayer
d_B .....thickness of the bilayer
OLV.....oligolamellar vesicles
X_{DPPG} .....mol fraction of DPPG

3.2 Introduction

We face a worldwide increase in pathogenic bacteria that are (multi-)resistant to commercially available antibiotics, while the number of novel antibiotics on the market declines. Several strategies to retrieve control on bacterial infections have been developed in the last decade (e.g. Lohner [1]). One promising approach is based on antimicrobial peptides. They mostly perturb and destroy the structural integrity of the lipid membrane, although some of these peptides seem to pass the membrane barrier and to act on cytosolic targets [2, 3]. Of particular interest is in any case the cell specificity of antimicrobial peptides, i.e. to discriminate between the host and bacterial cell membrane. While the outer leaflet of mammalian plasma membranes almost exclusively consists of neutral phospholipids, the bacterial one has a high content of negatively charged phospholipids, which is supposed to be a predominant factor for the affinity of the positively charged peptides to bacterial membranes. However, recently we showed that in respect of membrane-perturbing mechanism lipid net charge is not the decisive factor, but lipid packing density, the ability to form intermolecular H-bonds and lipid molecular shape have to be also taken into account [4]. Therefore, it is of interest to study the properties of membrane mimetic systems such as structure or packing properties.

As indicated above bacterial cell membranes have high contents of negatively charged lipids like phosphatidylglycerol (PG) or diphosphatidylglycerol (DPG or cardiolipin, CL), which are the most abundant anionic phospholipids of cytoplasmic bacterial membranes. These phospholipids are particularly prominent in a number of Gram-positive bacteria (Table 4). Interestingly, the level of cardiolipin may substantially be increased under certain environmental (e.g. high salt) or stress conditions as reported for *S. aureus* [5-8]. The increased amount of cardiolipin may reflect a requirement for enhancement of the structural

integrity of the bacterial cell membrane or for the support of stress-related increases in energy transduction, or both [5, 9].

Table 4: Membrane phospholipid composition of representative Gram-positive bacteria (see K. Lohner [38] and references therein).

Bacteria Species	Phospholipid as percentages of the total				
	PG [1)]	Cardiolipin	Lysyl-PG	PE	Others
Staphylococcus aureus	57	5	38	0	Trace
Bacillus subtilis	29	47	7	10	6 [2)]
Micrococcus luteus	26	67	0	0	7 [3)]

[1)] PG, phosphatidylglycerol; PE, phosphatidylethanolamine;
[2)] including phosphatidic acid and glycolipids;
[3)] almost exclusively phosphatidylinositol.

Cardiolipin with its quadruple hydrocarbon chains is a unique lipid also found to a significant amount in the inner mitochondrial membrane of eukaryotic cells being essential for e.g. insertion and translocation of proteins in the inner mitochondrial membrane [10]. While it seems that a major biological role of cardiolipin is related to the function of membrane proteins [9], Haines and Dencher [11] suggested another important function for cardiolipin due to its high pK_{a2} value (>8), which enables cardiolipin to trap protons at the H^+-uptake pathway of the energy transducing membrane [for details see [12]]. PG does not show such a variety of specific functions, but serves as precursor molecule for the biosynthesis of cardiolipin and other phospholipid molecules [13].

Regarding bacteria, cardiolipin was described to be concentrated in polar and septal regions as visualized by nonyl acridine orange (see Mileyovskaya [14], Schlame [15], and references therein). The ability to form non-lamellar structures is supposed to be required for membrane curvature in the septal region of cytoplasmic membranes, which is related to the cell division

process. The propensity to form non-lamellar structures is referred to the small polar head group of cardiolipin (see Matsumoto [16] and references therein). Because of this unique conformation, this lipid is also able to pack tightly forming micro domains [11] and in stack like arrays, which are also stabilized by membrane proteins [16]. Haines et al. [11] described the head group as a bicyclic formation of the two phosphate groups linked to the centred glycerol residue. Thereby, the H-bonding to the hydroxyl residue alters the pKa to > 8 and creates - by trapping a proton – an acid-anion. Therefore, at physiological conditions, cardiolipin has a single negative charge on the head group [11]. PG also carries one net negative charge at physiological pH (pK_a value of ~ 3 [17, 18]), but unlike cardiolipin the cross section of the headgroup is comparable to the cross section of its hydrocarbon chains. This gives the lipid a cylindrical molecular shape and thus PG will prefer to form flat bilayers.

Although there is a wealth of knowledge on the individual lipids, to our knowledge no study has been reported so far on binary mixtures of PG and cardiolipin, which represents an interesting model system for some Gram-positive cytoplasmic membranes. As lipids we have chosen the saturated species dipalmitoyl-PG (DPPG) and tetramyristoyl-cardiolipin (TMCL). The thermotropic phase behaviour of both lipids has been characterized showing very similar chain melting transition (around 41°C) under comparable buffer conditions [19, 20]. Moreover, both lipids are characterized by a similar membrane hydrophobic core in the lamellar gel-phase, which can be explained by the chain tilt of DPPG that compensates for its longer chain length (C16 vs. C14) as shown in this study. The experiments were performed at physiologically relevant buffer conditions using differential scanning calorimetry (DSC) and small and wide angle x-ray scattering (SWAXS) techniques to yield thermodynamic and structural parameters of the DPPG/TMCL mixture.

3.3 Materials and Methods

Preparation of liposomes

1,2-dipalmitoylphosphatidylglycerol (DPPG) and tetramyristoyl-cardiolipin (TMCL) were obtained from Avanti Polar Lipids Inc. (Alabaster, AL, USA) as Na-salt powders and used without further purification. Stock solutions were prepared by dissolving the required amounts of DPPG or TMCL in chloroform/methanol, 2/1 (vol/vol). For film preparation, mixtures of calculated stock solution quantities were evaporated under a nitrogen gas stream and at a temperature of 40 °C until a thin lipid film remained. The films were kept under vacuum over night for total solvent evaporation. The hydration procedure comprised an incubation time of 90 minutes at 65 °C, interrupted by thorough vortex mixing. The hydration buffer consisted of 20 mM NaPi, pH 7.4, 130 mM NaCl prepared from highly purifed water (Milli-Q water purification system).

Differential scanning calorimetry

Differential scanning calorimetry (DSC) measurements were performed with a VP-DSC high-sensitivity calorimeter from MicroCal, LLC (Northampton, MA, USA). The lipid concentration was 1 mg/ml. At least two sample preparations were performed for each mixture to check on repeatability. Prior to experiments, all samples were degassed for 5 minutes at room temperature. The scanning temperature range was set between 1 – 60°C and the scan rate was adjusted at 30°C/h. The equilibration time before each scan was 15 minutes. For each measurement the scan program included three heating/cooling cycles showing identical thermograms for the second and third scan, which were used for data evaluation. This was performed with Origin 7 SR4 including a calorimetric modelling package. Recorded DSC thermograms were normalized with respect to the lipid concentration and scan rate. After baseline correction, the calorimetric enthalpies (ΔH) were

determined by integrating the peak areas. The calorimetric enthalpy, the maximum heat capacity and the phase transition temperature were used for calculation of the van't Hoff enthalpy [21, 22] in order to calculate the cooperativity of the main transition given by the ratio between van't Hoff and calorimetric enthalpy.

X-ray scattering

Small and wide angle X-ray scattering (SWAXS) patterns were recorded on a SWAX camera (System 3, Hecus X-ray Systems, Graz, Austria) using a sealed X-ray tube generator from Seifert (Ahrensburg, Germany) working at 50 kV and 40 mA. The X-ray beam was filtered for CuKα radiation (λ = 1.542 Å) using a Ni foil and a pulse height discriminator. The SWAXS patterns were recorded in the wave vector ($q = 4\pi\sin\theta/\lambda$, where θ is half the scattering angle) regimes of 10^{-3} Å^{-1} < q < 1 Å^{-1} (SAXS) and 1.2 Å^{-1} < q < 2.7 Å^{-1} (WAXS) using two linear, one-dimensional, position-sensitive detectors (PSD 50, Hecus X-ray Systems, Graz, Austria). Silver stearate and p-bromo-benzoic acid were used for detector calibration of the small and the wide-angle range, respectively. Temperature was controlled with a Peltier heating unit.

Lipid samples (concentration 50 mg/ml) were filled into thin walled 1 mm capillaries (Hilgenberg GmbH, Malsfeld, Germany) and sealed with a two-component adhesive. To prevent sedimentation, the capillaries were rotated at constant speed along their axis within the sample stage. Data sets of pure buffer solution were recorded at 25 °C and used for baseline subtraction. Background corrected SAXS data were evaluated in terms of the Global Analysing Program developed by Pabst et al. [23, 24]. In the applied model, the bilayer electron-density profile is given by the summation of three Gaussian distributions, two describing the electron-density of the head group region and one at the center of the

bilayer accounting for the minimum density at the methyl terminus of the hydrocarbon chains.

The main parameters determined by SAXS data evaluation are the distance between head group and center of the bilayer (z_H), the hydrocarbon chain length and the thickness of the bilayer (d_B), respectively, which were determined as detailed previously [25]. Peak positions in recorded WAXS patterns are fitted by Gaussians to determine the hydrocarbon chain lattice.

3.4 Results and Discussion

The thermotropic phase behaviour of both lipids, DPPG and TMCL, has been well documented previously [19, 20, 26, 27]. In accordance with published data the endotherm of pure DPPG liposomes showed two clearly discernable transitions (Figure 12, Table 5), which can be attributed to the pre-transition from the lamellar-gel (L_{β}') to the ripple-phase (P_{β}') at 33.2°C and the main or chain melting transition from the P_{β}' to the fluid (L_{α}) phase at 40.7°C. In addition, two overlapping weak enthalpic transitions were observed with transition temperatures of 9.2 and 14.4°C, respectively.

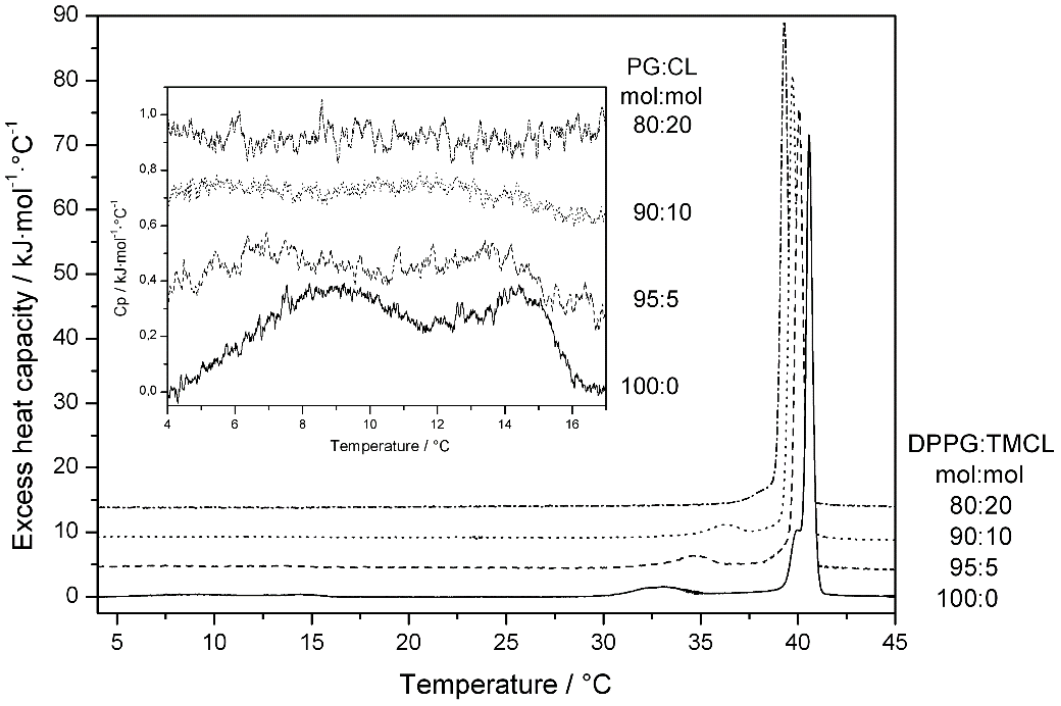

Figure 12: Selected thermograms of the DPPG enriched region of binary mixtures of DPPG/TMCL at a scan-rate of 30°C/h. Insert shows the subsubgel to lamellar gel phase transition region. Molar ratios of the binary mixtures are indicated in the panel.

These transitions can be attributed to the subsubgel SGII to $L_{\beta 1'}$ transition, also known as the Y-transition [28] and the headgroup tilt transition from $L_{\beta 1'}$ to $L_{\beta 2'}$ [27]. The SGII phase has been described as a highly compact metastable gel phase with the tilted hydrocarbon chains, packed on a orthorhombic lattice of two-nearest-neighbour type [28]. The $L_{\beta 1'} \rightarrow L_{\beta 2'}$

transition, in turn, is due to tilt of the PG headgroup away from the nearly horizontal position, because of lateral hydrocarbon chain pressure [27]. For TMCL it was shown that upon long-term incubation at low temperatures (-20°C overnight) this lipid adopts a stable subgel $L_{c`}$-phase, which transforms into a L_{β} phase upon heating between 25 to 29°C depending on the buffer used [20]. This phase transition exhibits a pronounced cooling hysteresis and is not completed during a simple cooling scan and therefore upon immediate reheating two low-temperature endothermal peaks between 14-18°C and 25°-30°C were reported [20]. This is the situation applied in our experiments and thus, in excellent agreement with these earlier findings using a similar phosphate buffer containing EDTA, we also observed two endothermic low temperature transitions at 17.9°C and 27.7°C, respectively, as well as the main transition at 40.9 °C (Figure 13, Table 5)

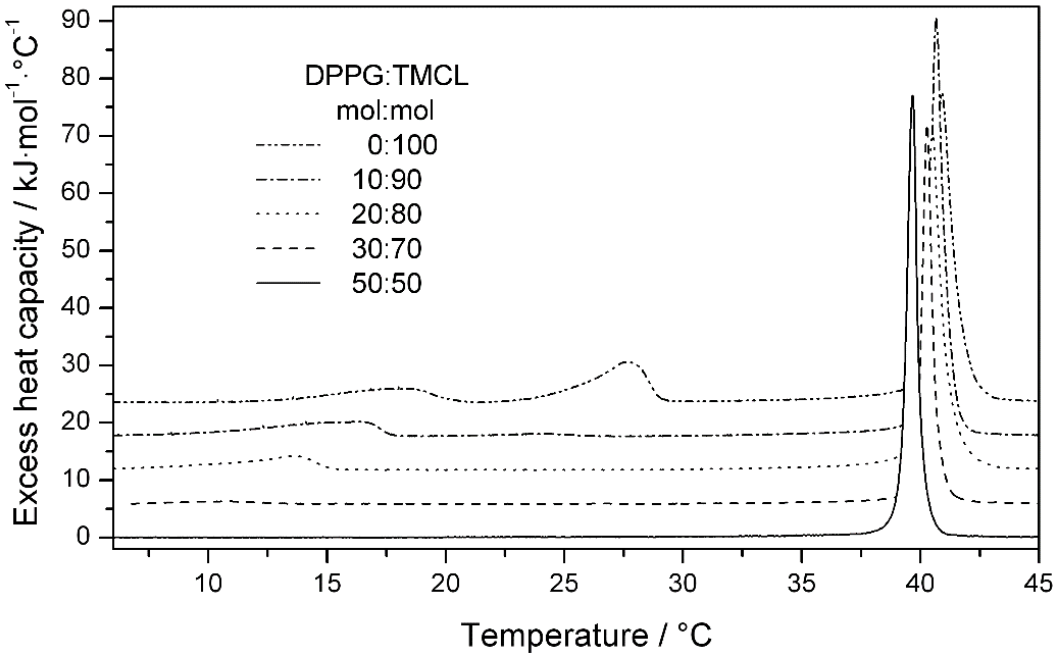

Figure 13: Selected thermograms of binary mixtures of DPPG/TMCL ($X_{DPPG} \leq 0.5$) at a scan-rate of 30°C/h. Molar ratios of DPPG/TMCL are indicated in the panel.

Table 5: Phase transition temperatures and enthalpies for binary mixtures of DPPG/TMCL*.

	low-temperature transitions				pre-transition		main transition	
	SGII/ L_{R1} → $L_{\beta'}$	ΔH	$L_{c'}$ → L_{β}	ΔH	$L_{\beta'}$ → $P_{\beta'}$	ΔH_{pre}	L_{β} /$P_{\beta'}$ → L_{α}	ΔH_m
X_{DPPG}	T [°C]	[kJ·mol^{-1}]	T [°C]	[kJ·mol^{-1}]	T_{pre} [°C]	[kJ·mol^{-1}]	Tm [°C]	[kJ·mol^{-1}]
1	9.2 / 14.4	2,3			33.2	5,8	40.7	38.6
0.95	7.5 / 13.1	~1.5			34.7	6,4	40.2	43.6
0.9	5.9 / 11.8	~0,5			36.5	5,9	39.9	42.8
0.8							39.4	48.2
0.7							39.4	51.7
0.6							39.8	47.9
0.5							39.9	51.1
0.4	7.7	1.1					40.1	53.5
0.3	10.8	4.8					40.3	54.4
0.2	13.4	8.6					40.6	54.6
0.1	15.3	13.0	24.1	1.3			40.6	55.8
0	17.9	10.4	27.7	23.8			40.9	55.5

* Phase designation see text.

A biphasic behaviour was observed for the main transition temperature of the binary mixtures (Table 5). Adding DPPG to TMCL resulted at first in a monotonic decrease of the main transition temperature until a molar ratio of DPPG/TMCL 80/20 and in a monotonic increase upon further addition of DPPG (39.4°C as compared to 40.9°C for TMCL and 40.7°C for DPPG). Similarly, the cooperativity of the main transition, which is a measure for the size of the average lipid domain undergoing the gel-fluid transition, showed also a biphasic behaviour with a breakpoint around X_{DPPG} = 0.8. An average cluster size of about

50 lipids was calculated within the composition range of $X_{DPPG} \leq 0.8$, which corresponds to the value calculated for pure TMCL, while at higher DPPG content the cooperativity increased with an average cluster size of 180 lipids calculated for DPPG. Unlike, these two parameters, the main transition enthalpy showed a non-monotonic decrease from 55.5 kJ/mol for pure TMCL to 38.6 kJ/mol for pure DPPG (Table 5). However, considering the different numbers of hydrocarbon chains linked to the glycerol moiety of the two lipids and their respective impact on the chain melting process suggests to plot the main transition enthalpy with respect to the ratio of number of acyl chains. This graph then shows that the main transition enthalpy follows a linear dependence (Figure 14).

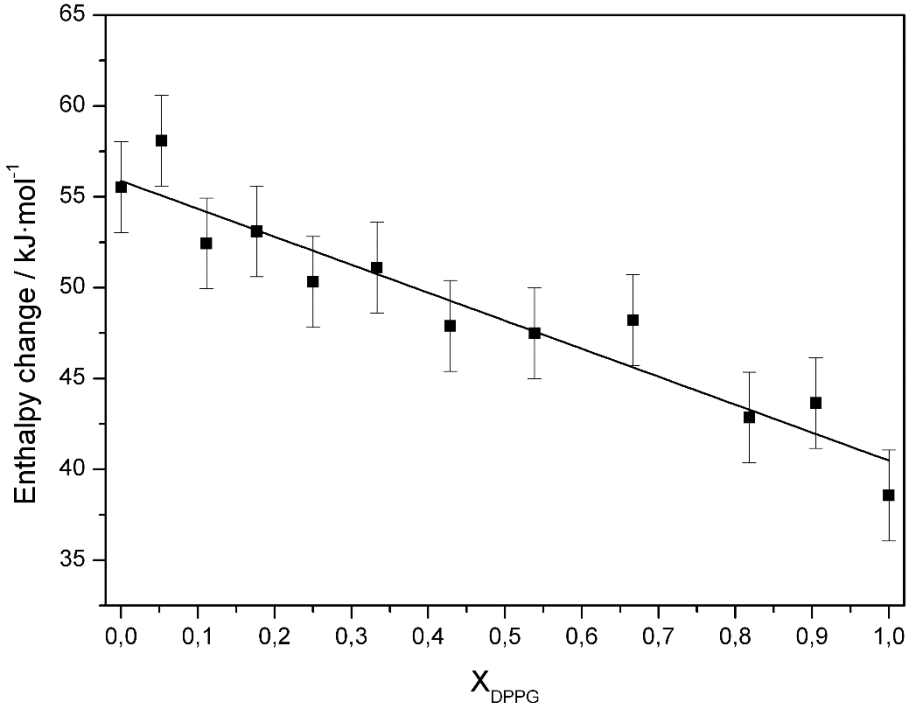

Figure 14: Main transition enthalpy of binary mixtures of DPPG/TMCL plotted with respect to the ratio of C16/C14 hydrocarbon chains.

A different behaviour was observed for the low temperature transitions of the individual lipids, which in general were rapidly abolished upon admixture of the other lipid component (Figure 12, Figure 13, Table 5). The low temperature transition of pure TMCL with corresponding values of 27.7°C and 23.8 kJ/mol, characteristic for the transformation of the

$L_{c`}$- into the L_{β}-phase, was hardly discernible from the baseline when 10 mol% of DPPG were added (24.1°C, 1.3 kJ/mol). On the other hand, the second low temperature transition observed for TMCL at 17.9°C persisted up to 40 mol% DPPG under the given experimental conditions, whereby the corresponding transition temperatures and enthalpies decreased monotonically with the admixture of DPPG from T = 17.9°C and ΔH = 10.4 kJ/mol (pure TMCL) to T = 7.7 °C and ΔH = 1.1 kJ/mol (X_{DPPG} = 0.4), respectively. Within the composition range of $0.5 \leq X_{DPPG} \leq 0.8$ no low temperature phase transitions were observed. For $X_{DPPG} \geq 0.9$ weak double peaks at 9.2 °C and 14.4 °C , similar to pure DPPG dispersions were observed, which we therefore ascribed analogously to the headgroup tilt and Y-transitions [27, 28]. In the same DPPG concentration range the pre-transition temperature increased from 33.2 °C for pure DPPG to 36.5 °C (X_{DPPG} = 0.9) without significant changes in the enthalpy (Figure 12, Table 5) reflecting a stabilization of the $L_{\beta'}$ phase by adding TMCL to DPPG.

The corresponding individual membrane structures were deduced from x-ray scattering experiments. Figure 15 shows the wide-angle pattern of pure TMCL below the main transition. The pattern at 5°C was characterized by a very broad peak with a maximum around d ~ 4.1 Å, and small peaks at lower (d ~ 4.59 Å) and higher angle (d ~ 3.66 Å), whereby $d = 2\pi/q$ The two sharp peaks are close to the positions reported for the $L_{c'}$ phase in TMCL [20]. On the other hand, based on the observations by Tenchov et al. [28] in phosphatidylethanolamines and the present experimental protocol, the two peaks could also originate from a L_{R1} phase.

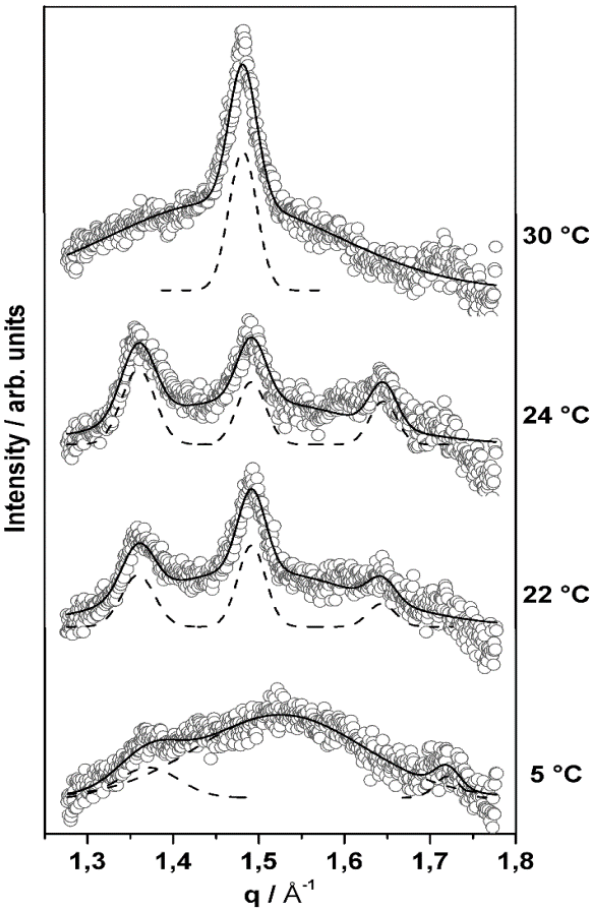

Figure 15: WAXS patterns of TMCL recorded at 5, 22, 24 and 30°C, respectively. Open circles show experimental data points, dashed lines represent Gaussian peak fit and solid line is the sum of the fit, showing that in the low temperature range the WAXS pattern can be described by a superposition of different phases (for details see text).

Similar to the SGII phase found in pure DPPG in the present study, the L_{R1} phase describes a highly compact gel phase, but with untilted hydrocarbon chains arranged on an orthorhombic lattice of four-nearest-neighbour type [28]. The broad peak indicates the presence of a domain with weak positional correlations of the acyl chains. Also Lewis et al. [20] described a metastable gel phase in TMCL of relatively small crystalline domains. This is in agreement with our observation, because the peak width scales inversely with the lateral domain size. Once the temperature was increased to 22°C, i.e. above the lowest phase transition, three clearly resolved Bragg peaks were detected. Thereby, the peaks at d = 4.62Å and d = 3.85Å, respectively, are characteristic for the 2D rectangular lipid arrangement of a well formed $L_{c`}$ phase, while the rather sharp symmetric peak at $d$ = 4.22Å is indicative for a lamellar $L_{\beta}$ gel phase. This shows that the $L_{c`}$ phase is now coexisting with a well ordered lamellar gel phase with untilted hydrocarbon chains. Increasing slightly the temperature up to 24°C,

shows relative increase of the peak intensities of subgel phase with respect to the L_β phase. Heating further to 30°C we observed a single symmetric peak in the WAXS pattern demonstrating the existence of a single L_β-gel phase. The L_β phase expanded laterally with increasing temperature as indicated from the change of the WAXS peak from d = 4.21Å at 30°C to d = 4.28Å at 37°C. The wide-angle data of pure DPPG were typical for an $L_{\beta'}$ phase at low temperatures (sharp d_{20} and broad d_{11} peak) and showed a single broad peak in the $P_{\beta'}$ phase in agreement with previous reports [27] (Figure 16)

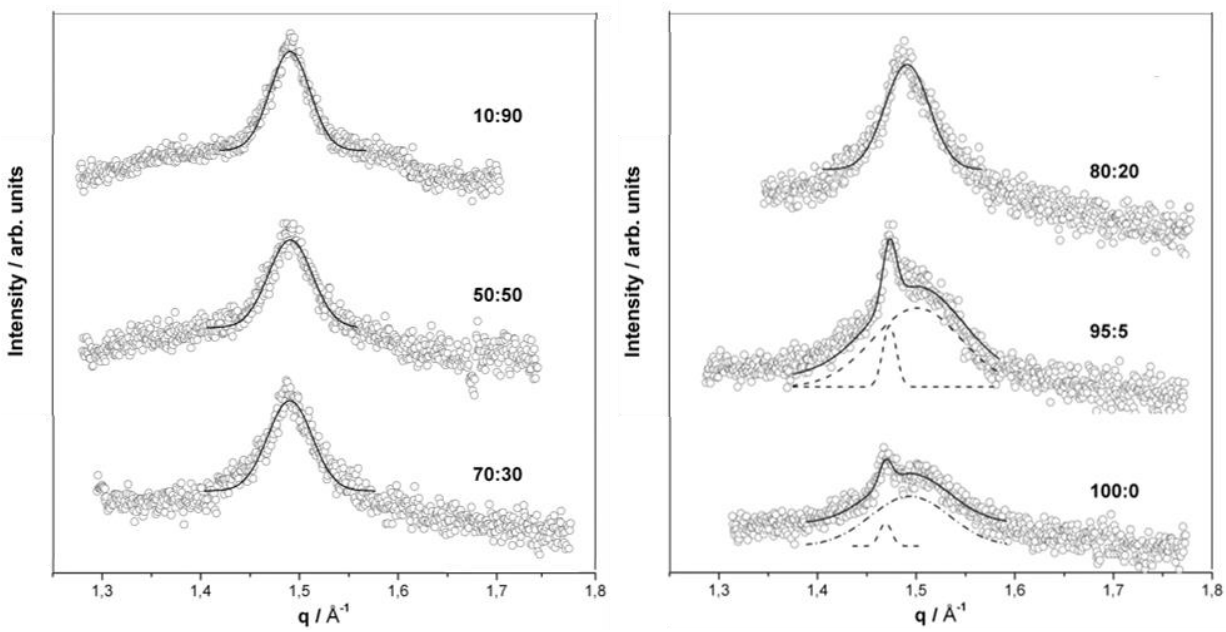

Figure 16: WAXS patterns of selected DPPG/TMCL mixtures recorded at 22°C (molar ratio indicated in the panel). Open circles show experimental data points, dashed lines represent Gaussian peak fit and solid line is the sum of the fit.

Mixtures of TMCL and DPPG have to accommodate the different packing properties of the individual lipid species. At 22°C, i.e. above the second phase transition of TMCL, already 10 mol% of DPPG suffices to practically abolish the subgel phase. The WAXS patterns shows a single peak centred at d = 4.21 Å, a situation which persists up to TMCL:DPPG molar ratios of 20:80 (Figure 16). The peak width is rather broad and compares to the one of the $P_{\beta'}$ phase of pure DPPG. SAXS data, however, show no indications for a ripple phase, but peaks

that index on a single lamellar lattice (Figure 17). Thus, for $0.01 \leq X_{DPPG} \leq 0.8$ the TMCL:DPPG form a lamellar L_β phase.

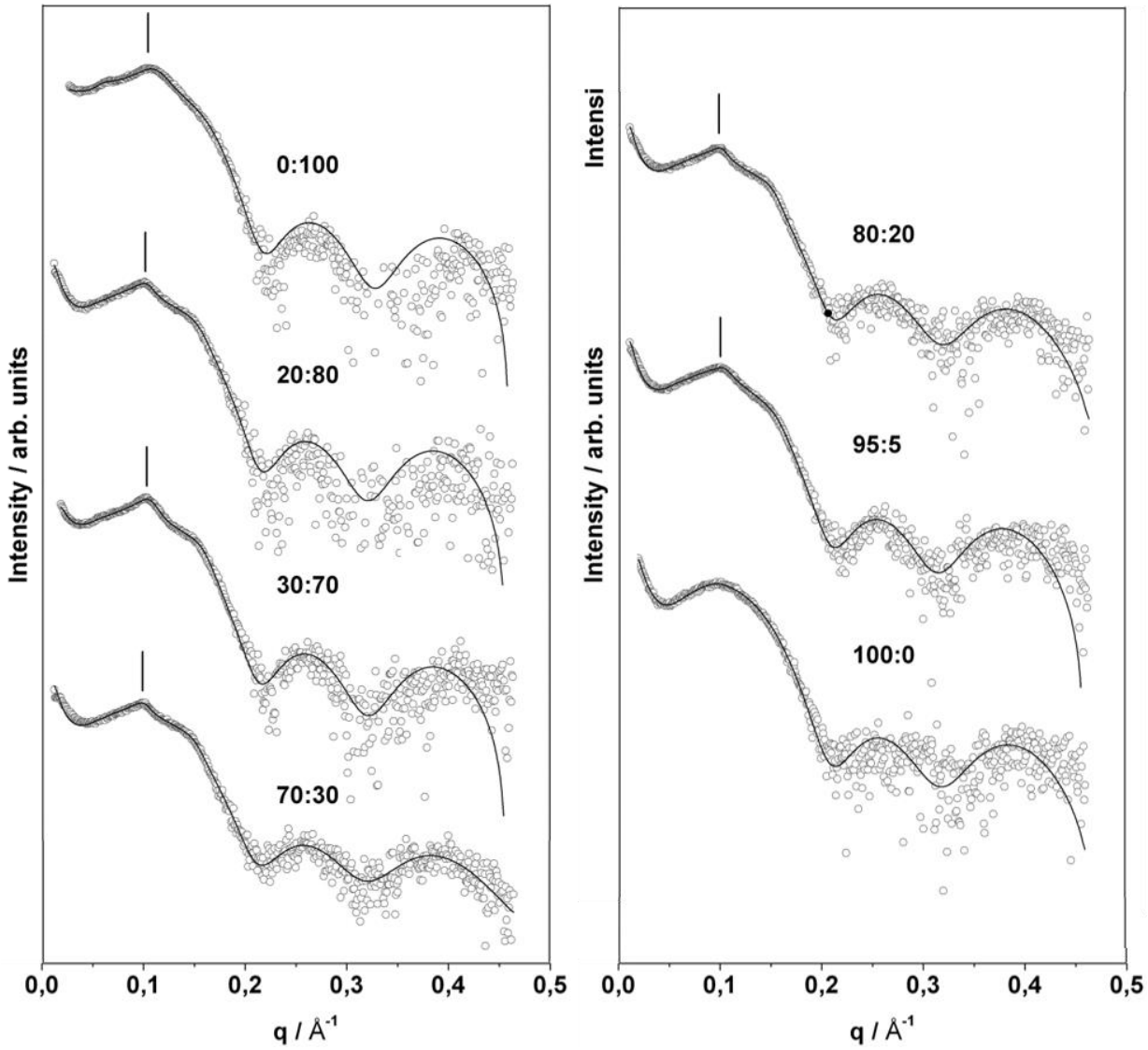

Figure 17: SAXS patterns in the lamellar gel phase at 30°C for the binary system DPPG/TMCL (molar ratio is indicated in the panel). Open circles represent experimental data points and solid lines give the best fit of the global analysis model to the scattered intensities. Position of the second order reflection of the pseudo Bragg peak for oligolamellar vesicles is indicated in the panel.

The extended peak width indicates packing inconsistencies of the TMCL/DPPG hydrocarbon chain lattices. A sharp d_{20} and a broad d_{11} reflection, characteristic for $L_{\beta'}$ phases, are observed for $X_{DPPG} \geq 0.95$ (Figure 16). Thus, the four hydrocarbons of TMCL quickly diminish the $L_{\beta'}$ phase upon its addition to DPPG. A very similar situation is also observed at 30°C, i.e. the WAXS pattern exhibited the same shape and width as compared to the

pattern recorded at 22°C. Thus, for $0 \leq X_{DPPG} \leq 0.8$ we found a loosely packed untilted lamellar L_β gel phase, while tilted hydrocarbon chains dominate the $L_{\beta'}$ gel phase at higher DPPG content. Figure 18 shows the corresponding peak positions. The transition from loosely packed L_β to well ordered $L_{\beta'}$ agrees with our DSC results on the cooperativity (see above). Hence, TMCL, over a large concentration range dominates the acyl chain packing in the gel phase.

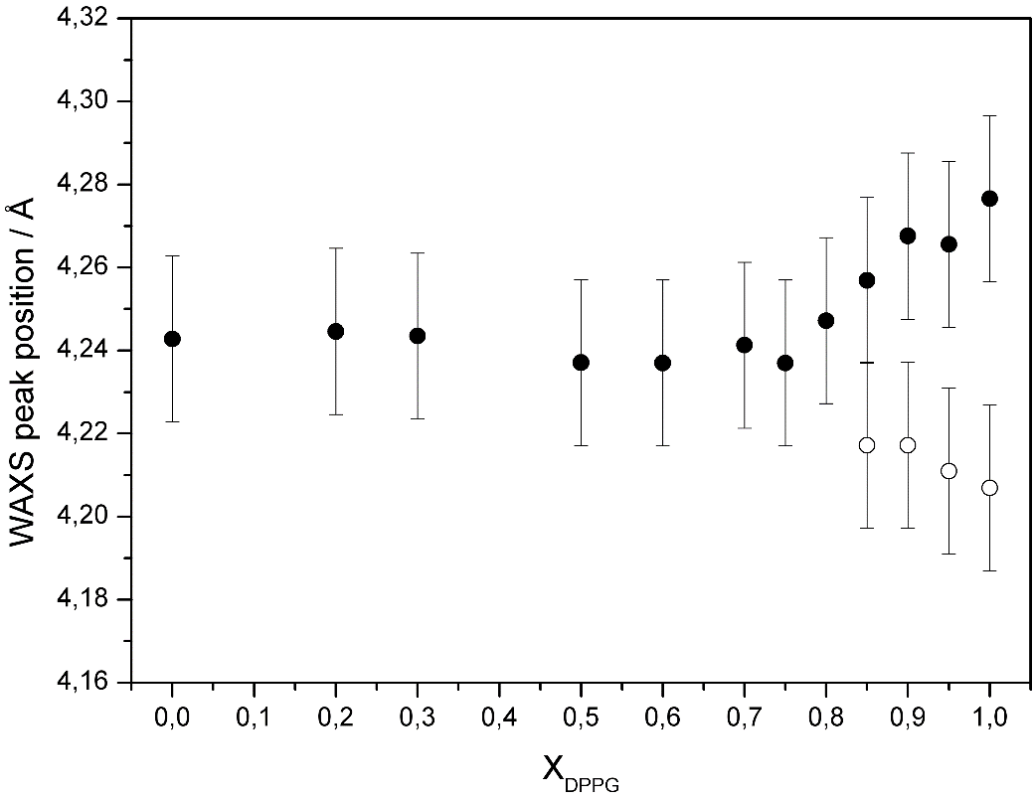

Figure 18: Position of the Bragg peaks of the wide-angle pattern of binary mixtures of DPPG/TMCL recorded at 30°C. Within the composition range of XDPPG ≤ 0.8 the samples adopt a L_β phase. At higher DPPG content a $L_{\beta'}$ phase was detected (full circles correspond to the sharp d20 peak and open circles to the broad d11 peak).

Interestingly, untilting of the hydrocarbon chains by addition of TMCL to DPPG does not lead to an increase of the membrane thickness, as derived from fits to the SAXS data (Figure 17). The bilayer thickness rather remains constant at dB = 57.9 ± 0.3 Å for XDPPG ≥ 0.8 and then decreases monotonically to dB = 56.0 ± 0.3 Å, the final value of pure TMCL (Figure 19).

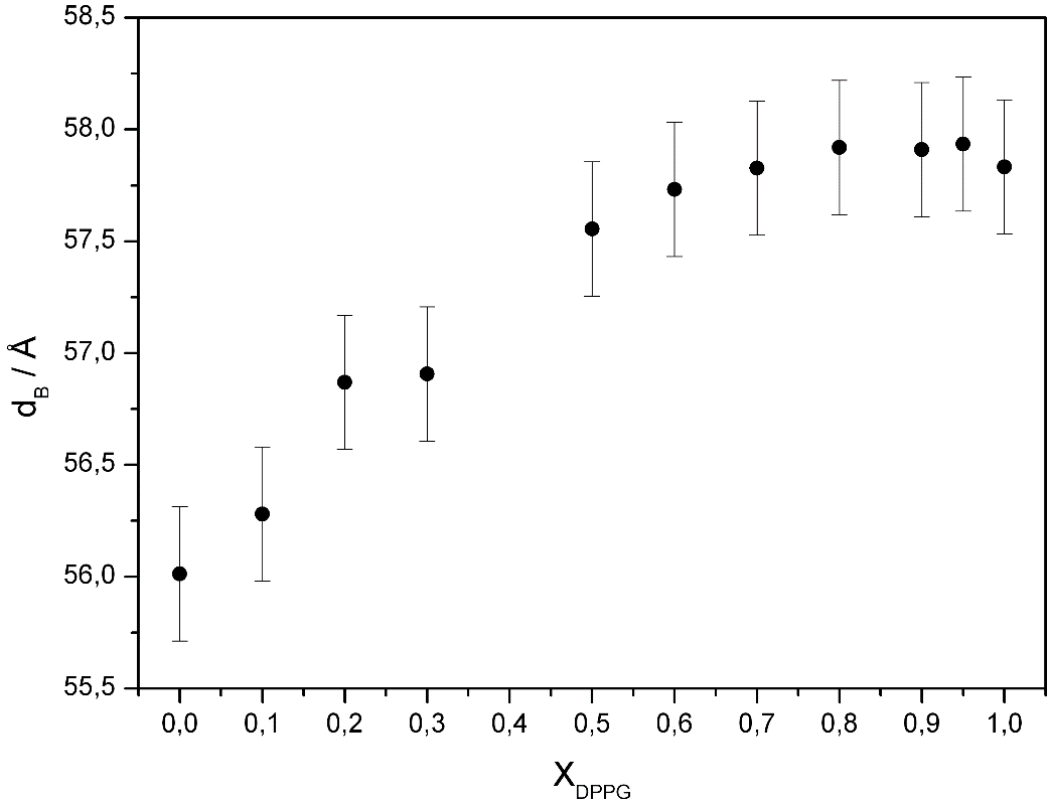

Figure 19: Bilayer thickness (dB) of the lamellar gel phase of binary mixtures of DPPG/TMCL at 30°C calculated from zH applying the global analysis model to the scattered intensities (for details see Materials and Methods).

The constant bilayer thickness above 80 mol% DPPG, correlates with the occurrence of the Lβ'-phase within this composition and temperature range and suggests that small amounts of TMCL can be incorporated within this phase without markedly affecting the tilt angle of the acyl chains. The decease of d_B, which is paralleled by the removal of the chain tilt by TMCL at lower DPPG concentration, may be explained by a partial interdigitation of the longer (C16) acyl chains of DPPG with the shorter (C14) acyl chains of TMCL to compensate for the difference of two methylene groups. This would also account for the packing problems and the correlated low melting cooperativity in this concentration regime.

The SAXS data also revealed that incorporation of TMCL affects the lamellarity of the liposomes formed (Figure 17). SAXS-patterns recorded for pure DPPG were typical for unilamellar vesicles or positionally uncorrelated bilayers (absence of Bragg peaks). However, after admixture of TMCL, pseudo-Bragg peaks were detected in the SAXS

patterns characteristic for oligolamellar vesicles (OLVs) as observed e.g. for anionic/zwitterionic PG/PE mixtures [29]. The formation of oligolamellar vesicles depends on the balance of attractive (van der Waals) and repulsive (hydration, steric, electrostatic) forces. Latter are strongly influenced by both the composition of the buffer and the charge of the lipid head groups. A decrease or a shielding of the surface net charge causes decreased repulsive forces and consequently the formation of OLVs [30]. This seems to be the case for samples containing TMCL considering that the phosphate residues form a tight bicyclic structure with H-bonds to the hydroxyl group on the centred glycerol [11]. As a consequence one of the acidic protons is trapped in this configuration forming an acid-anion and, in turn, reducing the net charge to –1 at neutral pH instead of –2 as expected from the presence of the two phosphate groups. Taking into account the increased cross sectional area of the TMCL molecule owing to the four hydrocarbon chains this property results in a reduced surface charge density and therefore enables formation of OLVs.

3.5 Schematic phase diagram

A schematic presentation of the phase diagram of the binary mixture of DPPG and TMCL based on their heat capacity functions is given in Figure 20. Phase assignment, as indicated in the figure, was deduced from the x-ray diffraction data. The phase sequence observed for pure DPPG is indicated in the figure and in agreement with earlier data [27].

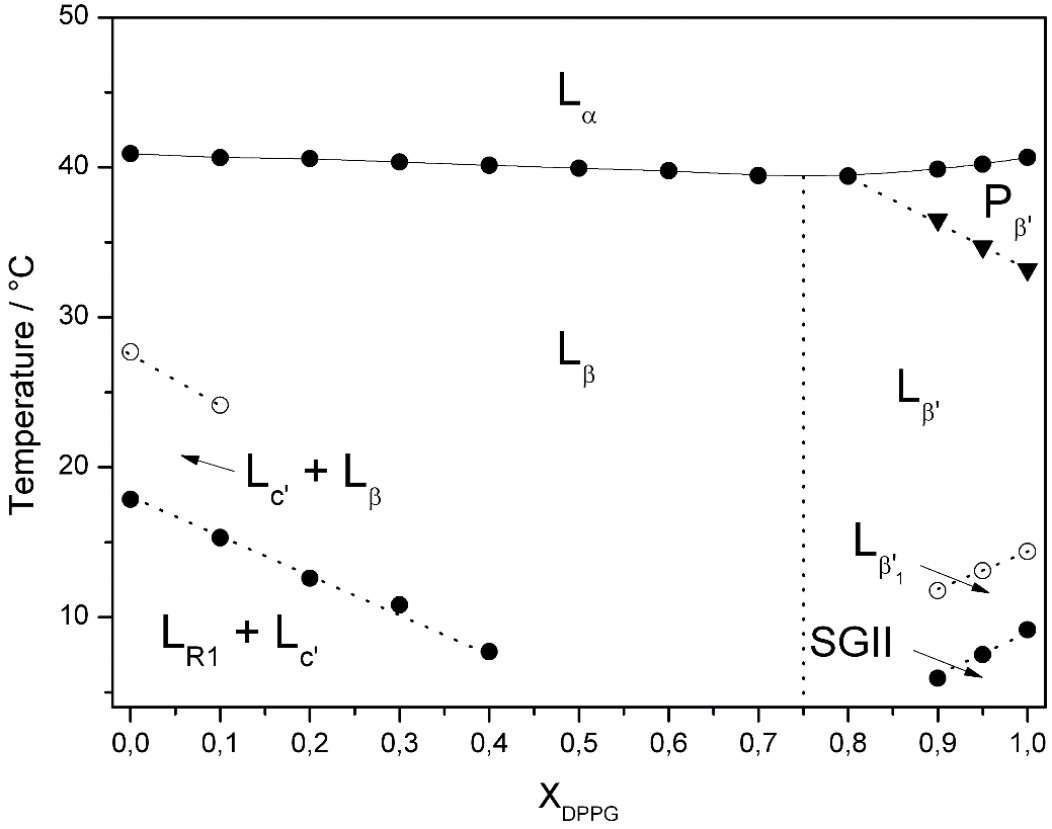

Figure 20: Schematic phase diagram of the binary system DPPG/TMCL under physiological buffer condition (130 mM NaCl, 20mM NaPi, pH 7.4) established from DSC experiments. Phase assignment was performed by SWAX experiments: metastable subgel phase, L_{R1}; subgel phase, $L_{c`}$; subsubgel phase, SGII; lamellar-gel phase with tilted, $L_{\beta`}$, and untilted hydrocarbon chains, L_{β}; ripple-gel phase, $P_{\beta`}$, and fluid phase with melted hydrocarbon chains, L_{α}.

Under the experimental protocol used, which did not apply overnight incubation of the samples at -20°C but only 15 min at 1°C, TMCL formed a metastable weakly ordered L_{R1} phase [28] that coexisted with the subgel $L_{c`}$ phase at low temperatures. At higher temperatures the $L_{c`}$ phase coexists with the lamellar L_{β} gel phase. As can be deduced from the phase diagram, incorporation of small amounts (≤ 10 mol%) of one lipid strongly affects

the low temperature phase behaviour of the other lipid component, whereby DPPG prevented the formation of the subgel $L_{c`}$ phase and TMCL abolished the subsubgel (SGII) phase. Thus, over a wide temperature and composition range a lamellar L_β gel phase is the predominant structure below the chain melting transition.

The width of the respective wide angle patterns, which showed no significant changes upon heating or amount of DPPG added, was comparable to the width of the wide angle pattern obtained for the $P_{\beta`}$ ripple-gel phase. This suggests that the lipid components do not mix ideally in the gel phase, which is supported by the small average lipid cluster size of about 50 lipids calculated for this composition range ($X_{DPPG} \leq 0.8$). Further, the composition dependence of the main transition temperature, showing lower transition temperatures for all binary mixtures with a minimum around $X_{DPPG} = 0.8$, suggests nonideal mixing of the binary components (eutectic mixture). In contrast to the hydrocarbon chain packing, the bilayer thickness was dependent on the molar ratio of the two lipids within this composition range. Adding DPPG to TMCL resulted in a concentration dependent increase of the bilayer thickness by about 2 Å in total, corresponding to the segment of about 2 methylene groups, and reached the value of pure DPPG at $X_{DPPG} = 0.8$. This behaviour may be explained by the need of different degrees of partial interdigitation in the methyl region of the bilayer core to compensate for the differences in the effective hydrocarbon lengths of DPPG and TMCL. Nonideal miscibility was also reported for another binary mixture being of relevance for bacterial membrane mimetic systems, namely phosphatidylglyerol and -ethanolamine [26, 29]. In these systems, phase separation of pure components was observed in the gel phase, which was attributed to be mainly due to differences in the headgroup interactions. In the present case, packing constrains due to different numbers of hydrocarbon chains per lipid have to be overcome and drive the system into a nonideal mixture. Our SAXS data show that pure TMCL membranes are less charged than pure DPPG membranes. Non-random mixing

of the two components therefore most likely leads to lateral inhomogeneities of the bilayer charge density. Therefore it will be of interest, to investigate if membrane-active molecules such as antimicrobial peptides can even discriminate between these two anionic lipids. So far, a particular preference of the binding to DPPG headgroups compared to cardiolipin was reported for a synthetic antimicrobial hexapeptide [31]. Different binding capabilities to various anionic phospholipids were also demonstrated for the beta-sheet peptide protegrin-1 [32]. Furthermore, lipid demixing has been shown in a number of studies of lipid mixtures being composed of neutral and anionic phospholipids giving rise to the formation of peptide poor and peptide-rich domains [31, 33-36]. Lateral phase separation induced by antimicrobial peptides was suggested to have implications on structure and integrity of membranes and may affect adversely the function of membrane proteins [2, 37].

Acknowledgement:

This work has been supported by the Austrian Science Funds FWF
(grant no. P18100-B10 to A.H.)

Reference list:

[1] K.Lohner, Development of novel antimicrobial agents: emerging strategies (Horizon Scientific Press, Wymondham, 2001).

[2] K.Lohner and S.E.Blondelle, Molecular mechanisms of membrane perturbation by antimicrobial peptides and the use of biophysical studies in the design of novel peptide antibiotics, Comb.Chem.High Throughput.Screen. 8 (2005) 241-256.

[3] K.Lohner, New strategies for novel antibiotics: peptides targeting bacterial cell membranes., Gen.Physiol.Biophys. 28 (2009) 105-116.

[4] E.Sevcsik, G.Pabst, W.Richter, S.Danner, H.Amenitsch, and K.Lohner, Interaction of LL-37 with model membrane systems of different complexity: influence of the lipid matrix, Biophys.J. 94 (2008) 4688-4699.

[5] H.U.Koch, R.Haas, and W.Fischer, Eur.J.Biochem. The role of lipoteichoic acid biosynthesis in membrane lipid metabolism of growing Staphylococcus aureus, 138 (1984) 357-363.

[6] F.L.Hoch, Cardiolipins and biomembrane function, Biochim.Biophys.Acta 1113 (1992) 71-133.

[7] Y.Kanemasa, T.Yoshioka, and H.Hayashi, Alteration of the phospholipid composition of Staphylococcus aureus cultured in medium containing NaCl, Biochim.Biophys.Acta 280 (1972) 444-450.

[8] A.Okabe, Y.Hirai, H.Hayashi, and Y.Kanemasa, Alteration in phospholipid composition of Staphylococcus aureus during formation of autoplast, Biochim.Biophys.Acta 617 (1980) 28-35.

[9] F.L.Hoch, Cardiolipins and mitochondrial proton-selective leakage, Bioenerg.Biomembr. 30 (1998) 511-532.

[10] K.Matsumoto, Dispensable nature of phosphatidylglycerol in Escherichia coli: dual roles of anionic phospholipids, Mol.Microbiol. 39 (2001) 1427-1433.

[11] T.H.Haines and N.A.Dencher, Cardiolipin: a proton trap for oxidative phosphorylation, FEBS Lett. 528 (2002) 35-39.

[12] H.Palsdottir and C.Hunte, Lipids in membrane protein structures, Biochim.Biophys.Acta 1666 (2004) 2-18.

[13] R.P.Huijbregts, A.I.de Kroon, and B.de Kruijff, Topology and transport of membrane lipids in bacteria, Biochim.Biophys.Acta 1469 (2000) 43-61.

[14] E.Mileykovskaya, Subcellular localization of Escherichia coli osmosensory transporter ProP: focus on cardiolipin membrane domains, Mol.Microbiol. 64 (2007) 1419-1422.

[15] M.Schlame, Cardiolipin synthesis for the assembly of bacterial and mitochondrial membranes, J.Lipid Res. (2007).

[16] K.Matsumoto, J.Kusaka, A.Nishibori, and H.Hara, Mol.Microbiol. 61 (2006) 1110-1117.

[17] A.Watts, K.Harlos, W.Maschke, and D.Marsh, Control of the structure and fluidity of phosphatidylglycerol bilayers by pH titration, Biochim.Biophys.Acta 510 (1978) 63-74.

[18] G.Cevc, Membrane electrostatics, Biochim.Biophys.Acta 1031 (1990) 311-382.

[19] G.Degovics, A.Latal, and K.Lohner, X-ray studies on aqueous dispersions of dipalmitoyl phosphatidylglycerol in the presence of salt., J.Appl.Cryst. 33 (2000) 544-547.

[20] R.N.Lewis, D.Zweytick, G.Pabst, K.Lohner, and R.N.McElhaney, Calorimetric, x-ray diffraction, and spectroscopic studies of the thermotropic phase behavior and organization of tetramyristoyl cardiolipin membranes, Biophys.J. 92 (2007) 3166-3177.

[21] P.Garidel, C.Johann, and A.Blume, Nonideal mixing and phase separation in phosphatidylcholine-phosphatidic acid mixtures as a function of acyl chain length and pH, Biophys.J. 72 (1997) 2196-2210.

[22] S.Mabrey and J.M.Sturtevant, Investigation of phase transitions of lipids and lipid mixtures by sensitivity differential scanning calorimetry, Proc.Natl.Acad.Sci.U.S.A 73 (1976) 3862-3866.

[23] G.Pabst, M.Rappolt, H.Amenitsch, and P.Laggner, Structural information from multilamellar liposomes at full hydration: full q-range fitting with high quality x-ray data, Phys.Rev.E.Stat.Phys.Plasmas.Fluids Relat Interdiscip.Topics. 62 (2000) 4000-4009.

[24] G.Pabst, J.Katsaras, V.A.Raghunathan, and M.Rappolt, Structure and interactions in the anomalous swelling regime of phospholipid bilayers, Langmuir 19 (2003) 1716-1722.

[25] G.Pabst, A.Hodzic, J.Strancar, S.Danner, M.Rappolt, and P.Laggner, Rigidification of neutral lipid bilayers in the presence of salts, Biophys.J. 93 (2007) 2688-2696.

[26] K.Lohner, A.Latal, G.Degovics, and P.Garidel, Packing characteristics of a model system mimicking cytoplasmic bacterial membranes, Chem.Phys.Lipids 111 (2001) 177-192.

[27] G.Pabst, S.Danner, S.Karmakar, G.Deutsch, and V.A.Raghunathan, On the propensity of phosphatidylglycerols to form interdigitated phases, Biophysical Journal 93 (2007) 513-525.

[28] B.Tenchov, R.Koynova, and G.Rapp, New ordered metastable phases between the gel and subgel phases in hydrated phospholipids, Biophys.J. 80 (2001) 1873-1890.

[29] B.Pozo-Navas, K.Lohner, G.Deutsch, E.Sevcsik, K.A.Riske, R.Dimova, P.Garidel, and G.Pabst, Composition dependence of vesicle morphology and mixing properties in a bacterial model membrane system, Biochim.Biophys.Acta 1716 (2005) 40-48.

[30] B.Pozo-Navas, V.A.Raghunathan, J.Katsaras, M.Rappolt, K.Lohner, and G.Pabst, Discontinuous unbinding of lipid multibilayers, Phys.Rev.Lett. 91 (2003) 028101-1 – 028101-4.

[31] A.Arouri, Dathe M., and Blume A., Peptide induced demixing in PG/PE lipid mixtures: A mechanism for the specificity of antimicrobial peptides towards bacterial membranes?, Biochim.Biophys Acta 1788 (2009) 650-659.

[32] W.Jing, E.J.Prenner, H.J.Vogel, A.J.Waring, R.I.Lehrer, and K.Lohner, Headgroup structure and fatty acid chain length of the acidic phospholipids modulate the interaction of membrane mimetic vesicles with the antimicrobial peptide protegrin-1, J.Pept.Sci. 11 (2005) 735-743.

[33] K.Lohner and E.J.Prenner, Differential scanning calorimetry and X-ray diffraction studies of the specificity of the interaction of antimicrobial peptides with membrane-mimetic systems, Biochim.Biophys.Acta 1462 (1999) 141-156.

[34] K.Lohner, A.Latal, R.I.Lehrer, and T.Ganz, Differential scanning microcalorimetry indicates that human defensin, HNP-2, interacts specifically with bBiomembrane mimetic systems, Biochemistry 36 (1997) 1525-1531.

[35] R.F.Epand, M.A.Schmitt, S.H.Gellman, and R.M.Epand, Role of membrane lipids in the mechanism of bacterial species selective toxicity by two alpha/beta-antimicrobial peptides,. Biochim.Biophys Acta 1758 (2006) 1343-1350.

[36] R.F.Epand, B.P.Mowery, S.E.Lee, S.S.Stahl, R.I.Lehrer, S.H.Gellman, and R.M.Epand, Dual mechanism of bacterial lethality for a cationic sequence-random copolymer that mimics host-defense antimicrobial peptides, J.Mol.Biol. 379 (2008) 38-50.

[37] R.F.Epand and R.M.Epand, Lipid domains in bacterial membranes and the action of antimicrobial agents, Biochim.Biophys Acta 1418 (2009) 97-105.

[38] K.Lohner, in: Development of novel antimicrobial agents: Emerging strategies, ed. K.Lohner, The role of membrane lipid composition in cell targeting of antimicrobial peptides. (Horizon Scientific Press, Wymondham, Norfolk, U.K., 2001, 149-156.

4 Biological activity and structural aspects of PGLa interaction with membrane mimetic systems

Karl Lohner* and Florian Prossnigg

Published in:

Biochimica et Biophysica Acta 1788 (2009) 1656–1666

Content from original publication and fit to the format of this thesis

4.1 Abstract

Peptidyl-glycine-leucine-carboxyamide (PGLa), isolated from granular skin glands of *Xenopus laevis*, is practically devoid of secondary structure in aqueous solution and in the presence of zwitterionic phospholipids, when added exogenously, but adopts an α-helix in the presence of anionic lipids. The peptide was shown to exhibit antifungal activity and to have antimicrobial activity towards both Gram-negative and Gram-positive bacteria. As a broad variety of peptides is found in the secretions of amphibian skin combinatorial treatment of PGLa and magainin 2 were studied showing enhanced activity by a heterodimer formation. Thus production of mutually recognizing peptides seems to be an effective way in nature to increase selective membrane activity.

Biophysical studies on membrane mimics demonstrated that PGLa can discriminate between different lipid species, preferentially interacting with negatively charged lipids, which are major components of bacterial but not mammalian cell membranes. This emphasizes the role of electrostatic interactions as a major determinant to trigger the affinity of antimicrobial peptides towards bacterial membranes. PGLa induced the formation of a quasi-interdigitated phase in phosphatidylglycerol bilayers below their chain melting transition, which is due to the creation of voids below the peptide being aligned parallel to the membrane surface. In the fluid phase of phosphatidylglycerol the peptide inserts perpendicularly into the bilayer above a threshold concentration, which results in a hydrophobic mismatch of the peptide length and bilayer core for lipids ≤ C16. This mismatch is compensated by stretching of the acyl chains and in turn thickening of the bilayer demonstrating that membrane thinning cannot be taken generally as the hallmark of pore formation by antimicrobial peptides. Furthermore, PGLa was shown to affect membrane curvature strain of phosphatidylethanolamine, another main lipid component of bacterial membranes, where a

cubic phase coexists with the fluid bilayer phase. Investigations on living *E. coli* showed distinct changes in cell envelope morphology, when treated with the peptide. In a first stage loss of surface stiffness and consequently of topographic features were observed, followed in a second stage by permeabilization of the outer membrane and rupture of the inner (cytoplasmic) membrane supposedly by the mechanism(s) derived from model studies.

Keywords:

amphibian skin, antimicrobial peptides, lipid discrimination, membrane thinning/thickening, non-bilayer structures

4.2 Introduction

Nowadays, we face a worldwide re-emergence of infectious diseases and a rapid increase in pathogenic bacteria that are multi-resistant to commercially available antibiotics. Hence the World Health Organization ranked antibiotic resistance as a priority disease and published a comprehensive document “Global Strategy for the Containment of Antimicrobial Resistance” suggesting some guidance on the implementation of interventions such as improving the use of antibiotics, enforcing regulations, strengthening health-care systems and encouraging the development of novel antibiotics. Latter is a pressing need, because the number of new antibiotics markedly decreased within the last decades. However, new drugs with similar structures relative to existing antibiotics will remain highly vulnerable to bacterial resistance mechanisms and will have only a limited life span. Therefore, alternative agents with novel mechanisms of action have to be developed. One emerging strategy is based on host defence peptides, which have evolved in nature to contend with invaders as an active system of defence (see also Zasloff this special issue).

This review focuses on one of the antimicrobial peptides found in skin secretions of frogs, namely PGLa (peptidyl-glycine-leucine-carboxyamide). In the first part of the review it will be reported about the discovery of this peptide and its biological activities. It will be described, how this peptide acts synergistically with magainin, another antimicrobial peptide component of frog, to combat pathogenic fungi, which are one cause of the world-wide decline of the population of this animal species. The potential of this peptide to be used for the development of a novel antimicrobial therapeutic will be also briefly addressed. As this peptide act on the cell membrane level a large extent of this review is devoted to studies using membrane mimetic systems, which have shed light on the mode of action of PGLa. It will be shown that the mechanism of membrane perturbation strongly depends on the

phospholipid matrix and that PGLa is able to discriminate between different lipid species. These biophysical studies suggest that the peptide is capable of forming pores in lipid bilayers. However, it was also shown that PGLa affects membrane properties such as curvature strain and induces lipid-peptide domain formation owing to the preferential interaction of the cationic peptide with the anionic membrane lipids. Both perturbations may alter the environment of membrane proteins leading to membrane dysfunction. The final part of the review deals with microscopy experiments on living *E. coli* cells showing that indeed membrane damage may be considered as the mode of killing by PGLa.

4.3 Discovery and characterization of PGLa

The skin of frog is a rich source of peptides [1], which are present in large quantities, in particular in the *Xenopus* species, as well as in *Bombina* as outlined by Simmaco and co-authors as well as by Zasloff within this special issue. A comprehensive analysis performed for the South African clawed frog, *Xenopus laevis* [2] showed that major components are peptidyl-glycine-leucine-carboxyamide or PGLa, consisting of 21 amino acid residues, magainins (23 residues) and a 25 residue peptide derived from the xenopsin precursor, which differ in their primary structure. The existence of PGLa was predicted through screening of a c-DNA library for clones encoding the precursor of caerulein by Kreil and co-workers [3], when searching in amphibian skin secretions for peptides closely related to mammalian hormones and neurotransmitters. The novel predicted peptide comprised 24 amino acids starting with tyrosine and ending with an amidated leucine and thus was designated PYL^a. In this study it was concluded that this peptide can form a membrane-active amphipathic helix similar to peptides with bacteriostatic, cytotoxic and/or lytic properties. The natural counterpart was isolated two years later from skin secretion of *Xenopus laevis* by the same group [4], which was very similar to PYL^a except for the absence of the first three N-terminal amino acids (Tyr-Val-Arg). This truncated peptide, corresponding to the amino acids 39 to 59 of the precursor protein, can be generated by additional processing at the single arginine residue, another proteolytic cleavage in addition to the predicted processing events. The peptide can undergo further fragmentations producing at least eight different peptides [5]. The most abundant fragments related to amino acids 1-11 and 12-21, obtained through cleavage at the Gly-Lys site of PGLa. The actual peptide was characterized by HPLC and mass spectroscopic analysis [4, 5] yielding the primary structure:

GMASKAGAIAGKIAKVALKAL-carboxyamide

now termed PGLa with a molecular weight of 1968.5. At neutral pH this peptide, ultimately

shown to be antimicrobial [6] has a positive net charge of 5 because of the four lysine residues and the amino group at the N-terminal glycine. Furthermore, the peptide possesses, as does melittin, an amidated C-terminus, which supposedly increases its resistance to proteases as shown for magainin [7]. PGLa has little homology to other peptides found in the skin secretions of *Xenopous laevis*, but owing to the general similarities, it is often included in the magainin family.

In aqueous solution, PGLa is less soluble than magainin 2a [8]. CD spectra of the peptide dissolved in physiological buffer indicated that the peptide is practically devoid of secondary structure at concentrations below 1 mg/ml [9]. At higher peptide concentrations, the percentage of random structure decreased and of β-structure increased. Additionally a small amount of α-helix was detected. Similarly, IR experiments with PGLa in D_2O solution showed at acidic and neutral pD a maximum at 1643 cm^{-1}, which is characteristic for peptides with little or no well-defined secondary structure [10]. Raman [8] and CD studies [11, 12] also showed little regular structure in aqueous solution at neutral pD for magainins. In contrast, Raman data [8] obtained at low temperatures in saline solution at pH 7.4 indicated that PGLa formed reversibly a precipitate containing β-sheet (63%) and reverse turn structure (21%). Jackson et al. [10] explained this observation by the different experimental conditions, which probably reflects aggregation of the peptide in the Raman study. As peptide aggregation is often accompanied by intermolecular H-bonds, the formed intermolecular β-sheets may be mistaken for intramolecular β-sheets.

4.4 Tissue distribution and biological activities of PGLa

The tissue distribution and cellular localization of PGLa and peptides of the magainin family in *Xenopus laevis* was early on studied. Two genes from this family, magainin and PGLa, are expressed at high level in the skin and throughout the gastrointestinal tract as well as in the small intestine [13-16]. Initial studies on the biosynthesis of PGLa demonstrated that it is located in the granular skin glands of *Xenopus laevis* and proceeds through a pathway that involves discrete morphological rearrangements of the entire secretory compartment [13]. However, the peptide was found not only being stored at high concentration in the skin but being also abundant in the gastrointestinal system of the frog [14]. The antimicrobial activity detected in extracts of stomach tissue led to the purification of nine antimicrobial peptides, shown to undergo the same processing as their dermal counterparts. In the gastric mucosa, the peptides are stored in granular cells, which have a spherical, syncytial multinucleated structure containing a cytoplasmic space filled with dense rice-shaped granules [15]. This enteric peptide-producing cell is strikingly similar both morphologically and biochemically to the granular gland of the amphibian skin. Finally, PGLa and magainin gene expression was also found in large, eosinophilic granular cells of the *Xenopus laevis* small intestine, which share some common feature with the mammalian Paneth cell, a site of expression of antimicrobial peptides [16]. Thus, the biological activity of PGLa was tested on a number of bacteria and fungi, but also on viruses and human cells in order to gain information on the potential of the peptide for therapeutic development and to understand first line defence mechanism.

In this respect, the capability of amphibians to defend themselves against pathogens gained some major interest because of the world-wide decline of the population of these animals. Pathogens associated with the mass mortality of amphibians are the fungi, *Batrachochytrium*

dendrobatidis and *Basidiobolus ranarum*, respectively, as well as the bacterium *Aeromonas hydrophila* [17 and references therein]. *A. hydrophila* is an opportunistic bacterium found on the skin and in the digestive tracts of healthy amphibians, but capable to induce diseases as shown for the South African clawed frog *Xenopus laevis* and American toad *Bufo Americanus*. All these pathogens can infect the skin of the animals and thus it was of interest to study the protective effect of antimicrobial peptides isolated from the granular glands of skin. Six peptides originating from three different frogs were tested: PGLa, caerulein precursor fragment (CPF), magainin 1 and 2 from *X. laevis*, ranalexin from the bullfrog *Rana catesbeiana* and dermaseptin from *Phyllomedusa sauvagii* [17]. All peptides were able to kill or inhibit the growth of both fungi but showed different efficacy. At least one peptide of each species was effective against both fungi at a concentration of about 10-20 μM. PGLa was highly active against *Basidiobolus ranarum* inhibiting growth at a concentration of 3.1 μM. However, higher peptide concentrations were necessary to prevent significant growth at later time points (after 48 h) and to completely eliminate growth during 4 days of culture, a pattern also observed with other peptides. All six peptides, however, were ineffective against the bacterium *Aeromonas hydrophilia*. Because these peptides are released in the skin together, an equimolar mixture of PGLa and magainin 2 was tested at concentration as high as 50 μM each, but failed to inhibit growth of the bacterium. In contrast, a synergistic effect was observed on the fungi, e.g. complete growth inhibition of *B. ranarum* at a concentration of 0.4 μM of each peptide was achieved. This suggests that antimicrobial peptides in the skin of amphibians can act as a first line of defence against fungi.

Antifungal activity of cationic amphiphilic peptides is also of interest because of the rise in number of immunocompromised patients, which has led to an increase in mucosal and systemic fungal infections, and concomitantly to the development of antifungal drug resistance owing to the prophylactic use of antifungal agents [18]. A number of pathogenic

Candida strains as well as *C. neoformans* were shown to be highly susceptible to PGLa with IC_{50}-values lower than amphotericin B [17] (Table 6).

Table 6: Killing activities of PGLa and amphotericin B against pathogenic yeasts.

Strain	IC_{50} [µM]*	
	PGLa	**amphotericin B**
Candida pseudotropicalis 311	1.3 ± 0.7	7.2 ± 1.9
Candida albicans 315	1.0 ± 0.3	2.2 ± 0.18
Candida krusei 355	0.8 ± 0.3	>70
Candida parapsilonis 356	0.8 ± 0.4	6.0 ± 1.0
Candida glabrata 359	8.5 ± 1.0	1.9 ± 0.2
Cryptococcus neoformans 316	0.4 ± 0.2	1.0 ± 0.1

* Data are taken from Helmerhorst et al. [44] and represent means ± standard deviations from two independent experiments.

Only *Candida glabrata* was less sensitive to cationic antifungal agents like PGLa most likely due to the regulation of the expression of drug efflux pumps, which affects negatively the efficacy and intracellular accumulation of cationic molecules [19]. In some pilot experiments, PGLa was added to dilution series of amphotericin B, fluconazole, and 5-flucytosine to assess the effects of the peptide on the minimal inhibitory concentration of these agents [20]. Addition of PGLa to amphotericin B showed a synergistic effect against several *Aspergillus, Candida* and *Cryptococcus* strains, while no enhanced activity was found in combination with fluconazole or 5-flucytosine. *Aspergillus fumigatus* being resistant to amphotericin B was shown to be also sensitive to sole PGLa [17]. Nevertheless, Helmerhorst et al. [21] pointed out that the candicidal activity of cationic peptides may strongly depend on the ionic strength of the test media. Therefore, the authors compared growth inhibition of *Candida albicans* and lysis of human erythrocytes at low and high ionic strength for several peptides including peptides of the magainin family. Subtle differences of

biological activities between these peptides were only detectable at low ionic strength, while all peptides showed weak haemolytic and antifungal activity at physiological buffer conditions. PGLa, when tested under low salt concentration (buffer supplemented with 297 mM glucose to prevent osmotic lysis of erythrocytes) was highly active against both human erythrocytes (HC_{50} = 0.6 µM) and *C. albicans* (IC_{50} = 1.1 µM) and thus is poorly selective. In contrast, magainin 2 exhibited a reasonable selectivity also at low ionic strength.

Antimicrobial peptides have also been strongly considered for the development of novel antibiotics owing to their strong growth inhibitory and microbicidial activity against bacteria in *in vitro* assays. Table 7 summarizes the antimicrobial activity of PGLa and magainin 2 on some representative bacterial species of Gram-negative and Gram-positive bacteria demonstrating that both peptides exhibit a similar spectrum and range of minimal inhibitory concentration (MIC). In a more recent study a lower MIC-value of 8 µg/ml was reported for *E. coli* and growth inhibition of the Gram-positive bacteria *B. subtilis* and *M. luteus* was observed in the same concentration range (MIC = 4 µg/ml) [22]. Therefore, PGLa has served as a template for synthetic peptides, which exhibited improved antimicrobial activity, but also increased potential towards hemolytic activity [e.g. 23, 24].

Table 7: Spectrum of antimicrobial activity of the Xenopus granular gland peptides PGLa and magainin 2 (Mag2).

		Minimal inhibitory concentration [µg/ml]	
Bacteria	**Species**	**PGLa**	**Mag2**
Gram-negative	*Escherichia coli*	32* 10-50**	64* 10-50**
	Pseudomonas aeruginosa	128* 200-500**	128* 50-100**
Gram-positive	*Staphylococcus aureus*	64* 50-100**	256* >500**
	Streptococcus pyogenes	10-50**	10-50**

* Data taken from Blazyk et al. [23]
** Data taken from Soravia et al. [6]

A development towards a therapeutic agents requires however that these peptides have low cytotoxicity towards the host cell. Comparing the haemolytic and antimicrobial activity of a peptide yields an estimate for the cell selectivity of the investigated peptides as described above. Sometimes it is difficult to compare the reported haemolytic activity of a given peptide owing to different experimental protocols, which often differ regarding cell density. For PGLa e.g. 7 % hemolysis at 1000 µg/ml peptide [6] and 18 % hemolysis at 500 µg/ml peptide were reported [24].

As mentioned earlier the broad variety of peptides found in the secretions of amphibian skin has suggested to investigate whether combinatorial treatment can also enhance antimicrobial activity. In fact, the equimolar mixture of PGLa and magainin 2 showed a significant improvement of antimicrobial activity in comparison to the sole peptides [25], but also a marked functional synergism in tumor cells [26] and model membranes [8, 26, 27, 28]. Cross-linking experiments suggested the formation of a heterodimer composed of parallel helices [29]. This was confirmed by a chemically fixed heterodimer by adding a Gly-Gly-Cys group to each peptide linked via a disulfide bond [25]. This hybrid peptide showed membrane permeabilizing activity against negatively charged liposomes and antimicrobial activity similar to the physical mixture of PGLa and magainin 2 (Table 8).

Table 8: Comparison of antimicrobial activities and hemolysis of PGLa and magainin 2 (Mag2) with their equimolar mixture and hybrid peptide, respectively.

	Minimal inhibitory concentration [µM]*			
Species	**L18W-PGLa**	**Mag2**	**mixture**	**hybrid****
Escherichia coli	20	20	2.5	1.25
Staphylococcus epidermidis	5	20	2.5	5
	% hemolysis***			
human erythrocytes	2.0	1.2	13.4	77.9

* Data taken from Nishida et al. [25], the Try-analog (L18W-PGLa) showing the same activity as PGLa
** concentrations are expressed as concentrations reduced to monomers,
*** after 3 h incubation of erythrocytes (1% v/v) with 15.6 µM (L18W-PGLa or Mag2) or 31.2 µM (mixture and hybrid) peptides.

In addition, this synthetic heterodimer showed enhanced activity against zwitterionic liposomes and human erythrocytes as compared to the physical mixture and the individual peptides (Table 8). These observations suggest that the production of mutually recognizing peptides seems to be an effective way in nature to increase selective membrane activity [25].

4.5 Interaction of PGLa with membrane-mimetic systems

4.5.1 Lipid discrimination and membrane selectivity of PGLa

As addressed briefly in the previous chapter antimicrobial peptides can exhibit selective activity towards bacterial and mammalian cells, which is thought to be strongly related to the different membrane architecture and lipid composition of eukaryotic and bacterial cell membranes [30,31 and references therein]. The general differences in the lipid composition between these cell membranes relates to the increased amount of negatively charged lipids in the outer membrane leaflet of bacterial cell membranes, which serves as a primary target of the cationic peptides. Thus, zwitterionic lipids such as PC and sphingomyelin (SM) are characteristic for mammalian cell membranes, while the negatively charged lipids PG and diPG or cardiolipin are main components that comprise - together with PE - bacterial cytoplasmic membranes. Moreover, the cell envelope of Gram-negative bacteria is a complex structure consisting of the cytoplasmic or inner membrane and a unique outer membrane with an intervening layer of peptidoglycan (Figure 21).

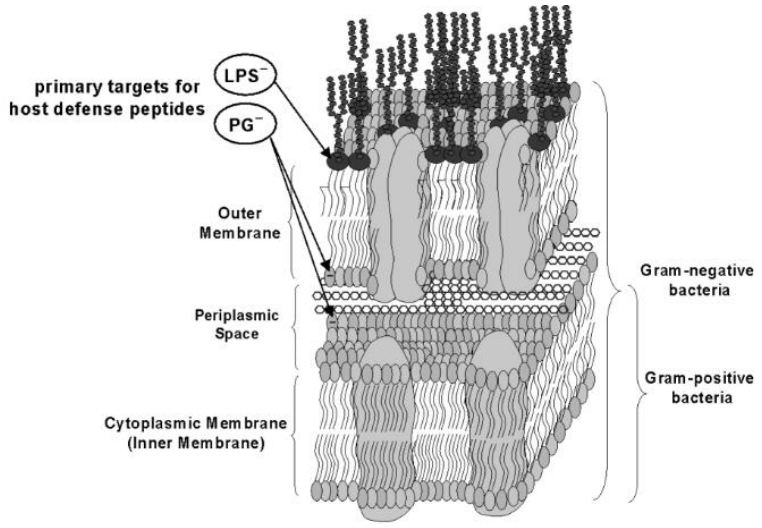

Figure 21: Schematic representation of the membrane architecture of Gram-negative bacteria consisting of an outer membrane with an asymmetric distribution of lipolpolysaccharides (LPS) and phospholipids, and a cytoplasmic or inner membrane. Phosphatidylglycerol is the most abundant negatively charged phospholipid species found in both Gram-negative and Gram-positive bacteria. Latter has only a cytoplasmic membrane. Predominant lipid targets of antimicrobial peptides are indicated.

The outer membrane has a distinctive, highly asymmetric composition with anionic lipopolysaccharides (LPS or endotoxin) located exclusively in its outer leaflet, which is of particular interest in respect of interaction of cationic antimicrobial peptides with these bacteria (see Mangoni and Shai [89]). In contrast, Gram-positive bacteria have a simple lipid bilayer membrane protected by a lipoteichoic acid layer, which confers the bacterial surface a negative charge too. Although recent studies showed that the lipid net charge is not the decisive factor determining the activity and membrane-perturbing mechanism(s) of antimicrobial peptides [32], electrostatic interaction will govern adsorption of these peptides on the membrane surface [31]. In addition, upon interaction with the negatively charged lipid headgroup conformational changes can be induced, which transform antimicrobial peptides that are unstructured in aqueous solution into a membrane-active, mostly α-helical conformation (see below). Thereby, induction of the active conformation upon interaction with the target membrane represents one possibility to control membrane selectivity.

Early biophysical studies on membrane model systems clearly demonstrated that indeed a number of antimicrobial peptides can distinguish between different lipid species, which led to the concept of lipid discrimination [9, 30, 33, 34]. For example, preferential interaction with negatively charged phospholipids was reported for the β-sheet peptides such as tachyplesin from horseshoe crab [35], human neutrophil peptide [34, 36] or protegrin-1 from porcine leukocytes [37]. Furthermore, magainin killed more effectively Gram-negative bacteria containing an inner membrane with higher amounts of phosphatidylglycerol [38], which emphasizes the role of electrostatic interactions as a major determinant to trigger the affinity of antimicrobial peptides towards bacterial membranes.

The same general observation was made for PGLa. Biophysical studies on the interaction of PGLa with liposomes consisting of dipalmitoylphosphatidylcholine (DPPC) and egg

sphingomyelin, a simple mimic for mammalian cell membranes, and of the acidic dipalmitoylphosphatidylglycerol (DPPG), representative of bacterial membranes, demonstrated that PGLa also discriminates between these lipids [9]. Microcalorimetric experiments showed that PGLa had no effects on the thermotropic phase behavior of liposomes composed of the choline phosphatides, while separation of a distinct peptide-rich domain was observed for phosphatidylglycerol liposomes (Figure 22). In addition to the main transition of pure DPPG at 40°C a second narrow transition owing to the peptide perturbed lipid domains was found at 41°C, which enthalpy increased upon increasing concentrations of PGLa. The assumption of a peptide-enriched domain was supported by X-ray diffraction experiments, which indicated that PGLa penetrates into the hydrophobic core of the bilayer inducing an untilting of the hydrocarbon chains as observed in the gel phase of the pure lipid. The nature of the peptide induced lipid domains was revealed only recently [39] and will be described in the following chapter.

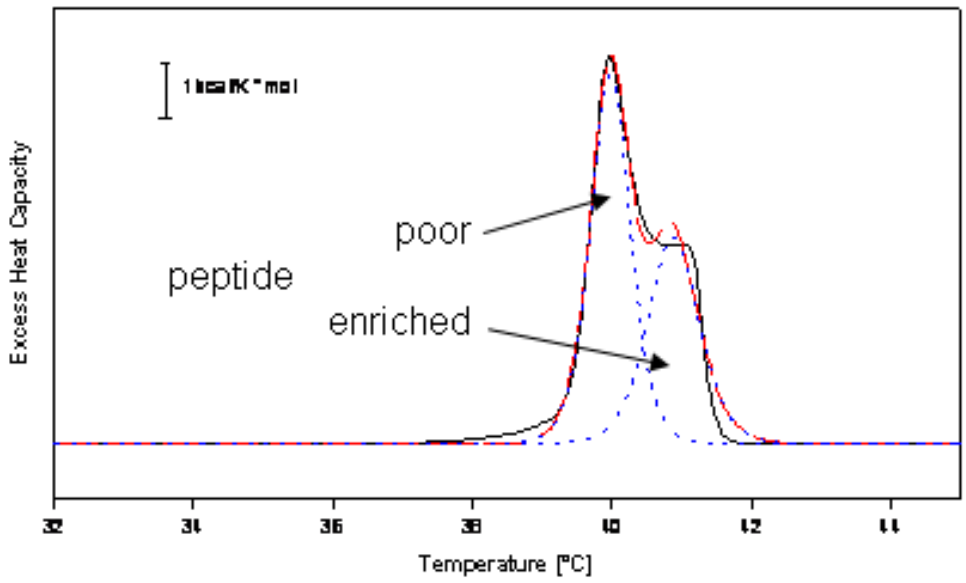

Figure 22: Thermogram of DPPG in the presence of PGLa at a lipid/peptide molar ratio of 50. Lipid and peptide were co-dispersed in 10 mM NaPi, pH 7.4. Experimental data (solid line), fitted data (broken line), individual components of peptide poor and enriched domains (dotted line).

Discrimination between neutral and negatively charged lipid species is further supported by monolayer studies, where PGLa was found to mix with PG at a molecular level, but to form separate islands in zwitterionic PC monolayers [40, 41]. Structural details of the phospholipid monolayers in the presence and absence of PGLa were obtained from Synchrotron experiments (Figure 23) showing that the peptide strongly perturbed the lipid acyl chain order of distearoylphosphatidylglycerol (DSPG) [40].

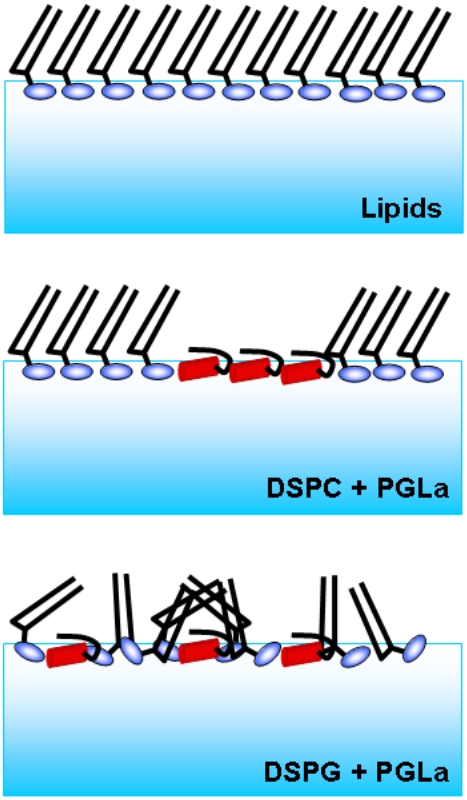

Figure 23: Models of lipid organization in a monolayer with and without PGLa based on X-ray reflectivity and grazing incidence diffraction data. Molecular mixing of PGLa and DSPG with perturbed hydrocarbon chain order as well as formation of separate domains of PGLa and DSPC is shown.

An increase of bending rigidity of the DSPG monolayer was observed, while adding PGLa to a DSPC monolayer resulted in a reduction of the overall bending rigidity [41]. One can envisage that changes of membrane bending rigidity owing to peptide insertion into the lipid bilayer may result in domain and/or defect structures, which will affect membrane integrity.

Surface pressure/potential-area isotherms showed that the antimicrobial frog skin peptide, PGLa, formed a very stable monolayer with 2 PGLa molecules per kinetic unit and a

collapse pressure of ~22mN/m, which is below the lateral pressure of biological membranes [40]. X-ray grazing incidence diffraction indicated that the peptide-dimer formation did not lead to self-aggreagation with subsequent crystallite formation. The scattering length density profile derived from X-ray reflectivity measurements yield information on the PGLa monolayer that protrudes into the air phase by about 0.8 nm suggesting that the peptide is aligned parallel to the air/water interface [40]. In bilayers different orientations of PGLa were reported depending on peptide concentration, phase state and synergistic interactions with magainin-2, ranging from a surface aligned monomeric state, via tilted dimers, to an upright inserted state [e.g. 28, 39, 42, 45, 48], which are described in detail by Ulrich and coworkers within this special issue. The process of PGLa binding and insertion was studied thermodynamically using PC/PG mixtures (3/1 mol/mol) showing an exothermic binding of the peptide to the membrane surface, followed by a slower endothermic process above a treshold concentration [43]. Latter was related to pore formation, which was also deduced from other biophysical approaches [27, 39].

Information on the secondary structure of PGLa upon interaction with lipids was obtained by various spectroscopic techniques. CD-spectra of PGLa in the presence of the zwitterionic phosphatidylcholine and sphingomyelin, closely resembled the features of the spectrum gained for the peptide in buffer solution indicating that the peptide adopts a random structure [9]. A different behavior was observed in the presence of DPPG, where two defined minima at 210 and 222 nm were detected [9], characteristic for an α-helical structure in agreement with IR-data [10]. A helical structure to about 60% was calculated, which suggests an α-helical C-terminal and a more or less unstructured N-terminal part. This would be consistent with the primary structure of PGLa, from where it can be inferred that several Gly residues, known as helix breakers, are located in the more hydrophobic N-terminal part of the sequence, while the remainder consists predominantly of helix stabilizing amino acids,

namely Ala, Leu and Lys. This was confirmed by calculating a helix probability profile, which shows a marked increase in helicity for the C-terminal half in the presence of anionic lipids [9] and is in agreement with multidimensional solution NMR spectroscopy data showing that PGLa is helical between residues 6 and 21, when associated with detergent micelles [46]. This study also revealed that the amino-terminal residues are highly mobile and that the fluctuations of backbone sites decrease from Ala at position 6 towards the C-terminus with Ala at position 20 being essentially rigid. If PGLa, however, is not added exogenously but co-dispersed from a dry lipid/peptide film, and if there is no excess of water present in the sample into which the cationic peptide can escape, it will form an α-helix even in neutral phosphatidylcholine [47] and phosphatidylethanolamine bilayers [68]. A helical wheel projection of PGLa indicates the lateral amphipathic character of the peptide clustering the positively charged Lys residues on one side of the helix (Figure 24).

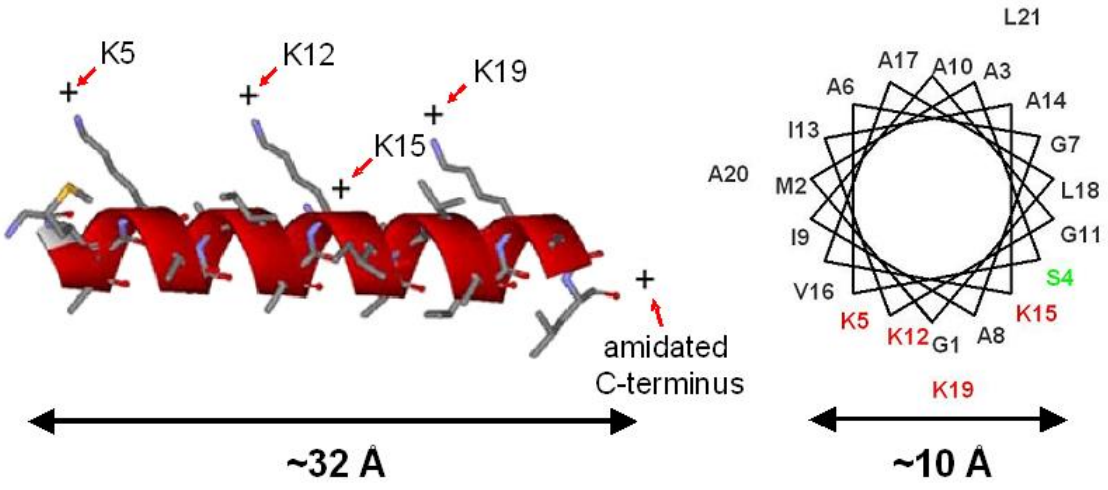

Figure 24: α-helical structure of PGLa assuming a full helix (coordinates kindly provided by A. Ulrich, Forschungszentrum Karlsruhe, Germany) and helical wheel presentation. Position of lysine residues and amidated C-terminal (amide is not shown) as well as length and diameter of the helix are indicated in the panel.

It should be noted however that induction of an α-helix is not necessarily sufficient to induce antimicrobial activity. For example, an alanine substitution analog of PGLa, where the bulky Ile residues, supposed to act as membrane anchor, were replaced by Ala, exhibited even a

slightly higher content of α-helix in the presence of bacteria mimetic vesicles, but did not show any appreciable antimicrobial activity against *E. coli* and *S. aureus* [49]. This observation can be attributed to the lower hydrophobic moment per residue and total hydrophobicity of the alanine substitution analog as compared to PGLa affecting membrane partitioning.

4.5.2 PGLa has distinct effects on the bilayer thickness of PG

Recently it was demonstrated, how profoundly the mechanism of membrane disruption depends on the nature of the membrane lipid composition, varying not only with lipid headgroup charge but also with hydrocarbon chain length [32, 50]. Based on systematic studies on LL-37 a phase diagram for PG and PC showing different lipid/peptide arrangements as a function of hydrocarbon chain length and peptide concentration was established. Further, it had been suggested that this phase diagram is generally applicable to membrane-active peptides localized parallel to the membrane surface, as similar effects were observed for PGLa and melittin [50].

A follow-up study using X-ray diffraction, solid-state 2H-NMR, differential scanning calorimetry, and dilatometry, investigated in detail the structural changes occurring in PG bilayers by addition of PGLa as a function of the acyl chain length (C14 to C18) [39]. The effects of the peptide varied strongly with the phase state of the lipid in a concentration dependent manner. In the gel phase, PGLa induced a quasi-interdigitated phase (Figure 25), which co-exists in various proportions with the original lamellar gel phase, manifested as two separate phase transition, as had been observed in initial DSC studies [9].

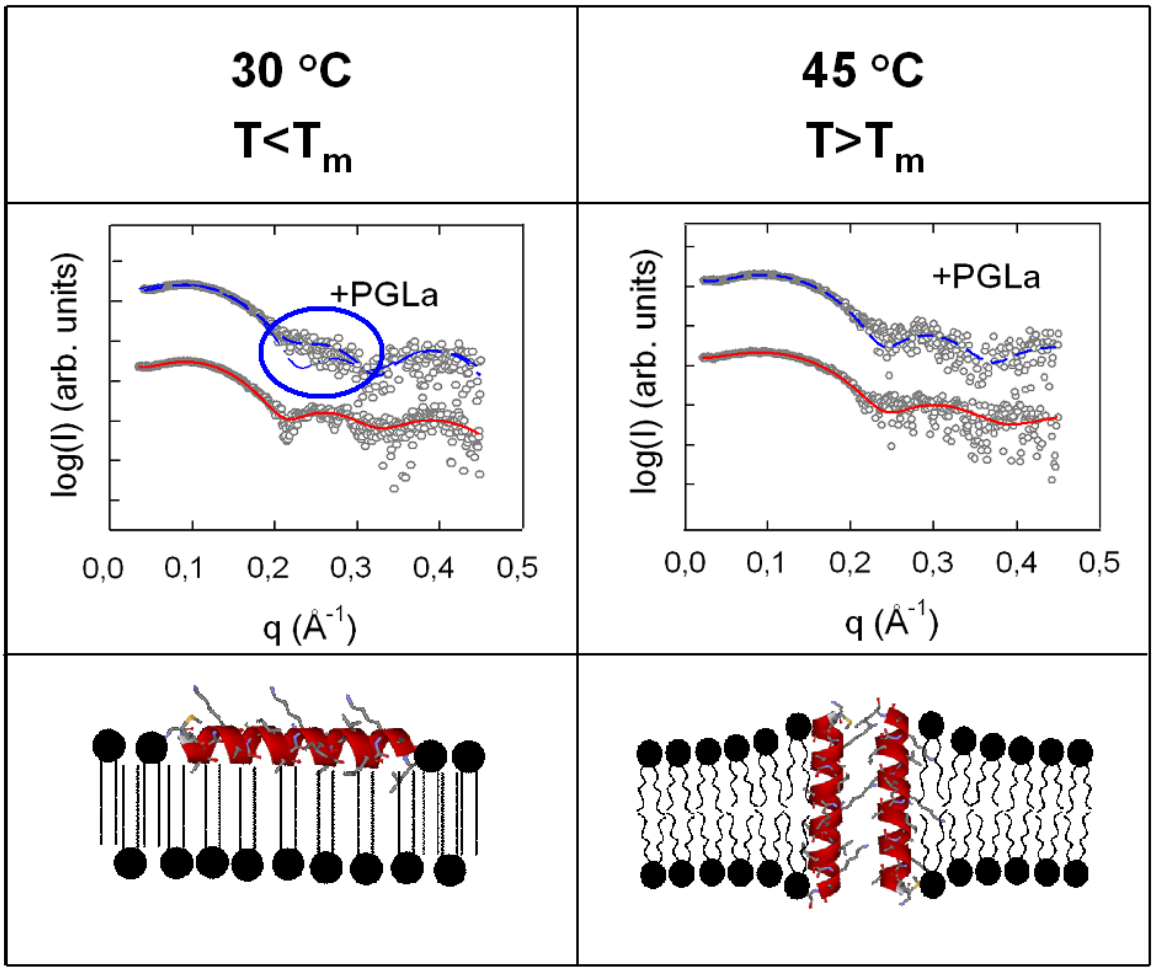

Figure 25: Schematic representation of structural changes induced by PGLa, when incorporated in DPPG bilayers. In the lamellar gel phase (T < T_m) PGLa aligns parallel to the membrane surface inducing an averaged thinning of the bilayer, while in the fluid phase (T > Tm) it inserts perpendicular to the membrane plane inducing a thickening of the bilayer. Typical small angle scattering curves of DPPG in the gel and fluid phase in the absence and presence of PGLa are presented. Solid lines show the model fits to the data (red line: pure DPPG, blue line: DPPG/PGLa). The circle indicates the deviation of model fits assuming no and the presence of a quasi-interdigitated phase. Lipid/peptide molar ratio is 25.

Thereby the higher melting transition is due to the conversion of the quasi-interdigitated phase into the fluid L_α phase. The presence of this structure was most prominent for the longest chain PG studied, i.e. DSPG. The occurrence of a quasi-interdigitated structure was also reported for LL-37 for these PGs [50]. While PGLa had no profound effect on DPPC, LL-37 led to a disintegration of the lamellar organization of this zwitterionic lipid into disk-like micelles. However, interdigitation was observed for the longer-chain C18 and C20 PC. This dual behavior of LL-37 was attributed to a balance between electrostatic interactions

reflected in different penetration depths of the peptide and hydrocarbon chain length as outlined below [50]. These observations clearly indicate that there is a tight coupling between the peptide properties and those of the lipid bilayer.

Induction of interdigitation of hydrocarbon chains in the gel-phase can be understood in terms of the "free volume" (void) model, as described earlier for small amphiphilic molecules such as e.g. alcohols, anesthetics or surfactants [51, 52]. It has been suggested that the lateral expansion of a phospholipid bilayer caused by the intercalation of amphiphilic molecules between phospholipid molecules and the mismatch between their hydrocarbon chain lengths results in the creation of voids in the hydrophobic region of the bilayer. In analogy, when peptides get embedded into the gel phase bilayer at the water/lipid interface aligned parallel to the membrane surface, it will create a void below the peptide. The extent of void formation will depend on the size and penetration depth of the peptide. It was shown that cationic peptides penetrate less deeply into the hydrophobic core of anionic as compared to neutral bilayers [53]. Formation of free volume within the hydrophobic core of the bilayer is energetically unfavourable and hence the system will rearrange in a way to maximize the hydrophobic interactions. Elimination of the free volume can be achieved via increased *trans-gauche* isomerisation of the hydrocarbon chains of the neighboring lipids or by moving the methyl ends of the opposing lipid monolayer close to the peptide, thereby generating the interdigitated lipid structure. Both will result in a decrease of the bilayer thickness though to various degree. A compensation of the free volume by an elastic monolayer deformation is not possible due to the high bending rigidity in the gel phase [54]. An increased acyl chain disorder was observed in DPPG/PGLa mixtures both from wide-angle X-ray diffraction and NMR data arising from phospholipids at the borderlines of the defect zones between the co-existing gel phases. This phenomenon was not observed for DSPG indicating that PGLa very effectively transforms the bilayer into an interdigitated

phase, which is consistent with the larger void induced in the hydrophobic core of the bilayer and the propensity of DSPG to form an interdigitated phase even in the absence of the peptide [55].

In the biologically more relevant fluid phase PGLa forms pores in PG membranes above a critical threshold concentration [39]. Thus the authors addressed the question, how this translates into structural changes of the fluid phase, as previous experiments had shown that LL-37 leads to a thinning of PC and PG bilayers [32]. Membrane thinning has been also observed in several other lipid/peptide interaction studies [56 and references therein]. In the fluid phase the bilayer may respond elastically to a peptide embedded in the water/lipid interface, because the bending rigidity is about one order of magnitude lower than in the gel phase, which can lead to a local membrane deformation and thinning on the global average over the membrane upon insertion of the peptides [56-58]. In contrast to these findings PGLa induced a membrane thickening of DMPG and DPPG bilayers, while no changes in the overall bilayer structure was detected for DSPG [39]. Latter observation was explained by considering the length of the α-helix of PGLa and the thickness of the lipid bilayer core showing that PGLa remarkably fits into the hydrophobic core of DSPG, when inserted perpendicular to the bilayer plane. However, in case of DPPG the peptide cannot be accommodated with its full length and thus the lipid responds to the insertion of the peptide by stretching of the hydrocarbon chains leading to an increase of membrane thickness by about 2 Å (Figure 25). Such a behavior was reported earlier for PC bilayers in the presence of hydrophobic model peptides of various length with N- and C-terminal interface anchors [59]. In the case of DMPG, the increase in bilayer thickness was less pronounced than for DPPG due to tilting of the peptide with respect to the bilayer normal, which has been observed in DMPC/DMPG [47]. These results demonstrate that membrane thinning cannot be taken generally as the hallmark of pore formation by antimicrobial peptides.

4.5.3 Cubic phase formation – effect on membrane curvature

Microorganisms such as e.g. *Escherichia coli* or *Acholeplasma laidlawii* have been shown to precisely regulate their lipid composition in a narrow window close to a bilayer to non-bilayer phase boundary, thereby conferring upon these membranes a degree of non-lamellar structure forming propensity [60-62]. The presence of non-lamellar phase forming lipids such as PE, cardiolipin or monoglucosyldiacylglycerol lead to an increase in the lateral pressure in the center of the bilayer because of their cone-shaped molecular geometry (smaller headgroup area as compared to the cross sectional area at the methyl region of the acyl chains). This in turn results in a bilayer state, where the desire for monolayer curvature is physically frustrated, which is in contrast to lamellar phase forming lipids such as PG or choline phospholipids exhibiting a cylindrical molecular shape and therefore a uniform lateral pressure throughout the hydrocarbon chain region of the bilayer. Thus, it was proposed that antimicrobial peptides may lower the bilayer to non-bilayer phase boundary leading to membrane rupture in case of bacteria with high content of non-lamellar phase forming lipids [31].

Formation of non-bilayer structures may be understood qualitatively in terms of this lateral pressure profile [63] balancing the repulsive and attractive interactions between the individual lipid molecules within the compound of the lipid bilayer. Insertion of a membrane active compound affects this balance and may lead to a long-range effect in form of a globally curved membrane [64]. Such effects are particularly pronounced, if lipids exhibit a propensity to negative curvature such as phosphatidylethanolamines, which make up more than 80 percent of the total phospholipids of *E. coli* [30]. This amino phospholipid can adopt non-bilayer structures, such as the inverted hexagonal (H_{II}) and cubic (Q_{II}) phases [65, 66], whereby the L_{α}- H_{II} phase transition temperature depends on the acyl chain composition

being around 75°C for palmitoyloleoyl-PE (POPE) [65, 67]. A recent differential scanning calorimetry and small-angle X-ray diffraction study showed that pure POPE partially converts into cubic phases upon cooling from the H_{II} phase [68]. Thereby, two Q_{II} phases of space group Pn3m and Im3m, respectively, coexist with the L_α phase and vanish upon the transition into the L_β gel phase (Figure 26).

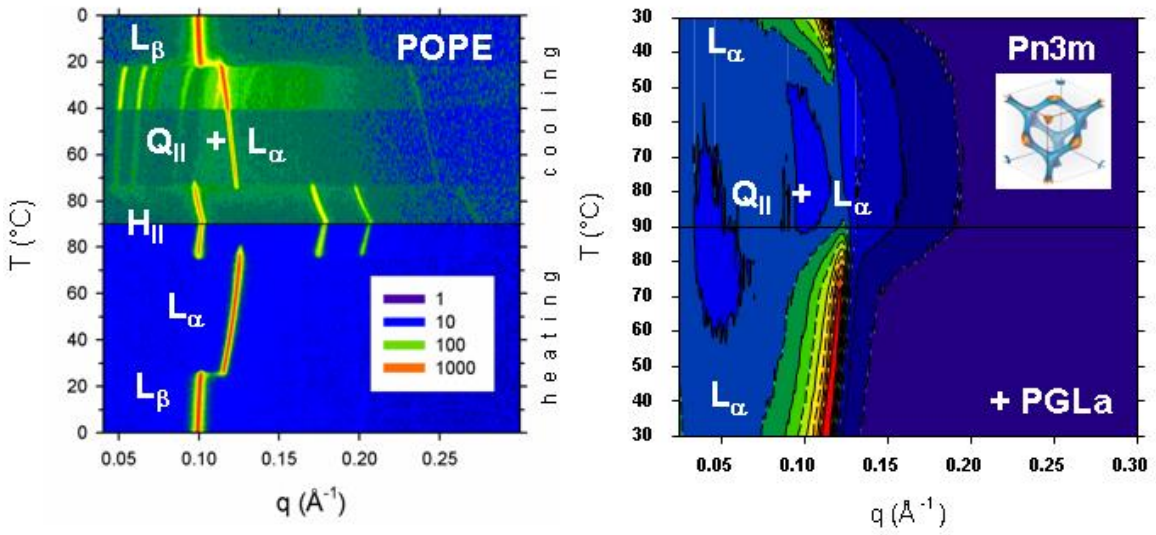

Figure 26: Structural phase transitions of pure POPE (left) and in the presence of PGLa (right) as a function of temperature. A contour plot of the small-angle X-ray diffraction data obtained upon heating and cooling is shown. Phase assignment is indicated in the panel (lamellar gel phase, L_β, fluid lamellar phase, L_α, inverted hexagonal phase, H_{II} and cubic phases, Q_{II}). The insert shows the water channels within the unit cell of Pn3m (adapted from http://www.msri.org/about/sgp/jim/geom/surface/global/skeletal/index.html).

Adding PGLa (4 mol%) to POPE caused an increase of the bilayer to non-bilayer phase transition temperature by about 9°C and a significant broadening of the transition range [68]. Small angle X-ray diffraction showed that a pure L_α phase exists up to 70°C. Upon further heating the intensity of the Bragg peak being characteristic for the lamellar phase continuously decreased on account of peaks that can be ascribed to a cubic phase belonging to the space group Pn3m with a lattice spacing of 131 Å at 90°C, which coexists with the fluid L_α phase. Upon cooling the Q_{II} phases vanished and at 30°C only the fluid L_α phase was observed (Figure 26).

In the presence of melittin (4 mol%) the L_α–H_{II} transition was abolished and only a bilayer structure was observed in the temperature range studied, which was explained by electrostatic repulsion due to the charged peptide [68]. Seemingly this does not play a role for PGLa, which has the same net charge as melittin, but exhibited a strongly reduced bilayer separation as compared to melittin. This is most likely due to shielding of the positive charges of PGLa by insertion into the lipid bilayer supported by the observation that PGLa significantly affected the chain melting transition of POPE. In conjunction with NMR data that indicated that PGLa inserts into PC membranes above a critical threshold concentration [47] and permeability experiments that suggested pore formation [27] it was proposed that PGLa is present in the PE bilayer as lipid/peptide pores as well as inserted as monomers [68]. It was suggested that the monomeric fraction of PGLa is responsible for the increase of transition temperature by stabilization of a negative Gaussian curvature modulus but facilitates at higher temperature the formation of the Q_{II} phases similar to fusion peptides by creating local defects. The complete stabilization of the L_α phase, i.e. the fraction which did not convert into a cubic phase, was attributed to be due to lipid/PGLa pores, as the formation of a fusion pore in such a case would require that the lipid/peptide pores first come into registry and then promote trans-membrane contact. In the absence of any driving force for this mechanism the authors concluded that such a scenario remains highly unlikely.

A different behavior was observed for gramicidin S, which led to a complete transformation of the fluid L_α phase into Q_{II} phases [68]. The capability of gramicidin S to strongly promote cubic phase formation was shown earlier using lipid extracts from *E. coli* and *A. laidlawii* [69]. It was proposed that the formation of the bicontinous cubic lipid phases is due to the limited flexibility of the β-turn of gramicidin S as well as to the clustered location of the ornithine side chains that strongly promotes negative curvature. A significant increase in monolayer curvature stress is likely to be of major importance for the formation of non-

lamellar structures [33]. Promotion of such structures in PE model systems has been also shown for other antimicrobial peptides [31 references therein]. Huang and coworkers [56 and references therein] proposed that membrane thinning, related to the elastic response of the lipid bilayer, is compensated by an increase of the hydrophobic cross sectional area of the lipid acyl chains. In case of PE this lateral expansion would further enhance the existing mismatch between the cross-sectional areas of the headgroup and hydrocarbon side chains, inducing the lipid monolayer to curl.

Finally, it should be mentioned that some antimicrobial peptides such as nisin [70] or a 17 β-amino acid oligomer [71] can stabilize the inverse hexagonal phase. In case of nisin this was explained in analogy to hydrophobic molecules such as squalene [72] being due to insertion of the large hydrophobic section of nisin (segment 1-19), which will lead to an increase of the hydrophobic volume in the bilayer interior. This in turn will promote negative curvature and hence formation of inverted non-lamellar structures. Similarly it was argued that owing to the penetration depth of a 17 β-amino acid oligomer H_{II}-structures were facilitated by expanding the regions of the bilayer below the pivotal plane more than regions close to the interface. Again this will result in an increase of negative curvature strain [71].

The different packing properties may have also implications for membrane function. For example, as mentioned earlier it has been suggested that the high lateral hydrocarbon chain pressure, exhibited by such lipids, controls the conformation of integral membrane proteins. In accordance with this assumption are observations that non-lamellar lipids are often required for functional reconstitution of membrane proteins [73] and that PE is found in protein rich membrane domains [74]. Therefore, one may speculate that antimicrobial peptides that affect the lateral hydrocarbon chain pressure upon insertion may lead to

conformational changes of integral membrane proteins and hence to impairment of membrane function.

4.5.4 Images on the impact of PGLa on living E. coli cells

The influence of PGLa on living *E. coli* was investigated by imaging the cells with atomic force microscopy [75, 76] showing distinct changes in cell envelope morphology, when treated with the peptide. AFM images obtained under physiological aqueous conditions [75], where the mica was pre-treated with polylysine for better immobilization of the bacteria, revealed that PGLa induces formation of micelles within 5 minutes of treatment accompanied by a morphological change of the bacteria from a rod-shape to a fluid flattened structure. After 30 min only the lower parts of cellular membrane was left attached to the substrate, which had lengths and widths that correspond to the size of the fixed bacterial cell. Another important observation relates to the complete removal of the pilar structure attached to the bacteria indicating that the peptide leads to disruption of the outer membrane. However, under these conditions the resolution of the images were low most likely due to the deformation of the bacteria during scanning and therefore observation of bacteria in air was also performed giving a better resolution than in water.

These experiments demonstrated that interaction of PGLa with *E. coli* strongly reduced the cell stiffness and increased the surface roughness [75, 76], which was also observed in the presence of magainin 2a and the cytolytic peptide melittin [76]. In general the roughness of the outer membrane increased with the increase in peptide concentration, with melittin having the most pronounced effect. This morphological change may be caused by exposure of the peptidoglycan layer and/or peptide incorporation into the LPS-containing outer membrane causing a “crumbling” effect due to an increase of the lateral monolayer area. Incorporation of cationic antimicrobial peptides into the LPS layer was also suggested in

earlier studies [e.g. 77, 78]. Such a damage to the outer membrane may in turn enhance the penetration of peptides to the highly sensitive inner membrane. Peptide transfer across the outer membrane to the periplasmic space, which involves the direct binding of the cationic peptides to LPS, was proposed by Hancock and termed the so-called self-promoted uptake system [79]. The packing of LPS molecules, which is essential for the permeability control and membrane integrity, strongly depends on divalent cations [80]. Interaction of the cationic peptides may displace Mg^{2+} ions from the LPS layer of the cell surface leading to insertion of the peptide into the outer membrane cross binding the negative charges of LPS as has been shown for example for the antimicrobial peptide polymyxin B [81, 82]. In fact, addition of 10 mM Mg^{2+} ions prior to PGLa treatment partially inhibited the effects of the peptide [75]. Under these experimental conditions PGLa showed less damage to *E. coli* cells owing to the competition for the negative charges present in LPS molecules. Interestingly, bacteria treated with the chelating agent EDTA did neither show substantial damage of the membrane nor measurable differences in stiffness as compared to the untreated bacteria. Furthermore, the treated bacteria retained their overall morphology. The effect simply seems to be restricted to a roughening of the outer membrane. This observation is in agreement with the suggestion that EDTA removes Mg^{2+} ions from the LPS layer of *E. coli* increasing the electrostatic repulsion within the LPS molecules [84]. The observed roughness can then be explained by an increase in the area of the LPS monolayer and partial loss of LPS without formation of holes or discontinuities. Although EDTA increases the permeability of the outer membrane, treatment of *E. coli* cells with this chelating agent during short periods is not lethal, but can be used to introduce macromolecules through the outer membrane without significant loss in viability [81, 83]. The fact that *E. coli* retained its rigidity and morphology during the EDTA treatment suggested that it obviously does not affect the peptidoglycan layer, which serves as a strong mechanical structure as well as diffusion barrier.

AFM-images obtained in the presence of magainin 2a and melittin showed similar but in some aspects different effects on *E. coli* cells as compared to PGLa [76]. These experiments, performed below and above their LC_{50}-value, gave additional interesting details upon the action of membrane-active peptides on bacterial cells. Images obtained below LC_{50} demonstrated that all three peptides tested induced the most damage at the apical ends of the cell. This is of interest, because results from experiments with a cardiolipin sensitive dye demonstrated that cardiolipin domains were located at the apical ends of *E. coli* inner membrane [73]. Therefore it is tempting to speculate that these peptides may preferentially interact with the negatively charged cardiolipin.

In fact, it has been shown that the antimicrobial peptide protegrin-1 can distinguish between different negatively charged lipids [85]. This is further supported by recent observation on a synthetic antimicrobial peptide, which induced demixing of a cardiolipin and phosphatidylglycerol mixture [86]. In this respect it is also interesting to note that leakage experiments showed that in the case of rabbit defensin, cardiolipin seems to be essential for creating lesions as no leakage was observed for liposomes composed of phosphatidylglycerol and -ethanolamine [36]. On the other hand, phase segregation in this model system, which is a mimic of the bacterial cytoplasmic membrane, was reported for PGLa [33] and also observed for other antimicrobial peptides such as HNP-2 [32, 34] or alpha/beta antimicrobial peptides [87] emphasizing the preferential interaction of the cationic peptides with negatively charged lipids. Formation and segregation of lipid domains may influence membrane properties and in turn membrane function by creating defect zones of increased permemabilty and membrane domains of changed fluidity.

Melittin was most effective in cell rupture, as can be expected from its low MIC and non-selective membranolytic activity. Already below LC_{50} melittin induced the formation of

grooves and pore-like lesions as well as the collapse of the cell structure at the apical ends, with one end being more elastic [76]. In addition, a large amount of released vesicles or peptide aggregates, which may include LPS and membrane-associated compounds, were clearly visible. Above LC_{50} in addition to a collapse of the apical ends, the outer membrane showed severe damage with large lesions. Furthermore, a very pronounced leakage of cytosolic fluid was observed clearly indicating the damage of the inner membrane. Below LC_{50} magainin 2a induced blebbing (surface-bound vesiculation) of the LPS-rich outer membrane as well as some lesions in agreement with an earlier electron microscopy study [88]. Above LC_{50} it almost completely destructed the bacterial cell, where vesiculation, deep lesions as well as a collapse of the apical and the septal region of the cell were observed. A possible exposure of parts of the more rigid peptidoglycan layer was also suggested. The effects observed for PGLa below LC_{50} were intermediate between the changes induced by melittin and magainin 2a, while above LC_{50} PGLa had similar but less visiual effects as compared to magainin 2a.

In summary, the first stage of action can be characterized by the loss of surface stiffness and consequent loss of bacteria topographic features owing to the incorporation of the peptides into the LPS layer. In a second stage after permeabilization of the outer membrane the peptides also interact with the inner (cytoplasmic) membrane finally leading to total cell rupture as suggested by the loss of cytoplasmic material. Biophysical studies have shown that a number of relevant parameters have to be considered to understand the effect of antimicrobial peptides on membranes and thus caution has to be taken to derive the molecular mechanism(s) from model studies. Nevertheless, the studies described within this review suggest that disruption of the inner membrane by PGLa will most likely occur by pore formation but changes in membrane fluidity due to lipid segregation and membrane curvature strain may be considered as well.

Acknowledgement:

The authors would like to thank Georg Pabst and Andrea Hickel for stimulating discussions and providing material for the manuscript. Part of the work was supported by the Austrian Science Funds P18100-B10.

Reference list:

[1] V. Erspamer, Half a century of comparative research on biogenic-amines and active peptides in amphibian skin and mollus can tissues, Comp. Biochem. & Biophysiol. C-Comp. Pharmacol. & Toxicol. 79 (1984) 1-7.

[2] G. Giovannini, L. Poulter, B.W. Gibson, D.H. Williams, Biosynthesis and degradation of peptides derived from Xenopus laevis prohormones, Biochem. J. 234 (1987) 113-120.

[3] W. Hoffmann, K. Richter, G. Kreil, A novel peptide designated PYLa and its precursor as predicted from cloned mRNA of Xenopus laevis skin, EMBO J., 2 (1983) 711-714.

[4] D. Andreu, H. Aschauer, G. Kreil, R.B. Merrifield, Solid-phase synthesis of PYLa and isolation of its natural counterpart, PGLa [PYLa-(4-24)] from skin secretion of Xenopus laevis, Eur.J.Biochem.149 (1985) 531-535.

[5] B.W. Gibson, L. Poulter, D.H. Williams, J.E. Maggio, Novel peptide fragments originating from PGLa and the caerulein and xenopsin precursors from Xenopus laevis, J.Biol.Chem.261 (1986) 5341-5349.

[6] E. Soravia, G. Martini, M. Zasloff,. Antimicrobial properties of peptides from Xenopus granular gland secretions, FEBS Lett. 228 (1988) 337-340.

[7] D. Juretic, H.C. Chen, J.H. Brown, L. Morell, R.W. Hendler, H. Westerhoff, Magainin 2 amide and analogues. Antimicrobial activity, membrane depolarization and susceptibility to proteolysis, FEBS Lett. 249(1989) 219-223.

[8] R.W. Williams, R. Starman, K.M. Taylor, K. Gable, T. Beeler, M. Zasloff, D. Covel, Raman spectroscopy of synthetic antimicrobial frog peptides magainin 2a and PGLa, Biochemistry 29 (1990) 4490-4496.

[9] A. Latal, G. Degovics, R.F. Epand, R.M. Epand, K Lohner, Structural aspects of the interaction of peptidyl-glycylleucine-carboxyamide, a highly potent antimicrobial peptide from frog skin, with lipids, Eur.J.Biochem. 248 (1997) 938-946.

[10] M. Jackson, H.H. Mantsch, J.H. Spencer, Conformation of magainin-2 and related peptides in aqueous solution and membrane environments probed by Fourier transform infrared spectroscopy, Biochemistry 31 (1992) 7289-7293.

[11] H.C. Chen, J.H. Brown, J.L. Morell, C. Huang, Synthetic magainin analogues with improved antimicrobial activity, FEBS Lett. 236 (1988) 462-466.

[12] K. Matsuzaki, M. Harada, T. Handa, S. Funakoshi, N. Fujii, H. Yajima, Magainin 1-induced leakage of entrapped calcein out of negatively-charged lipid vesicles, Biochim.Biophys.Acta 981 (1989) 130-134.

[13] B.E. Flucher, C. Lenglachner-Bachinger, K. Pohlhammer, H. Adam, C.J. Mollay, Skin peptides in Xenopus laevis: morphological requirements for precursor processing in developing and regenerating granular skin glands, C.J.Cell Biol .103 (1986) 2299-2309.

[14] K.S. Moore, C.L. Bevins, M. Brasseur, N. Tomassini, K. Turner, H. Eck, M. Zasloff, Antimicrobial peptides in the stomach of Xenopus laevis, J.Biol.Chem. 266 (1991) 19851-19857.

[15] K.S. Moore, C.L. Bevins, N. Tomassini, K.M. Huttner, K. Sadler, J.E. Moreira, J. Reynolds, M. Zasloff, A novel peptide-producing cell in Xenopus: multinucleated gastric mucosal cell strikingly similar to the granular gland of the skin, J.Histochem.Cytochem. 40 (1992) 367-378.

[16] D.S. Reilly, N. Tomassini, C.L. Bevins, M. Zasloff, A Paneth cell analogue in Xenopus small intestine expresses antimicrobial peptide genes: conservation of an intestinal host-defense system, J.Histochem.Cytochem. 42 (1994) 697-704.

[17] L.A. Rollins-Smith, J.K. Doersam, J.E. Longcore, S.K. Taylor, J.C. Shamblin, C. Carey, M. Zasloff, Antimicrobial peptide defenses against pathogens associated with global amphibian declines, A.Dev.Comp.Immunol. 26 (2002) 63-72.

[18] T. White, K.A. Marr, R.A. Bowden, Clinical, cellular, and molecular factors that contribute to antifungal drug resistance, Clin.Microbiol.Rev. 11 (1998) 382-402.

[19] E.J. Helmerhorst, C. Venuleo, A. Beri, F.G. Oppenheim, Candida glabrata is unusual with respect to its resistance to cationic antifungal proteins, Yeast 22 (2005) 705-714.

[20] W. van't Hof, I.M. Reijnders, E.J. Helmerhorst, E. Walgreen-Weterings, I.M. Simoons-Smit, E.C. Veerman, A.V. Amerongen, Synergistic effects of low doses of histatin 5 and its analogues on amphotericin B anti-mycotic activity, AntonieVanLeeuwenhoek 78 (2000) 163-169.

[21] E.J. Helmerhorst, I.M. Reijnders, W van 't Hof, E.C. Veerman, A.V. Nieuw, A. Amerongen, A critical comparison of the hemolytic and fungicidal activities of cationic antimicrobial peptides, FEBSLett. 449 (1999) 105-110.

[22] E. Strandberg, D. Tiltak, M. Ieronimo, N. Kanithasen, P. Wadhwani, A.S. Ulrich, Influence of C-terminal amidation on the antimicrobial and hemolytic activities of cationic α-helical peptides, PureAppl.Chem. 79 (2007) 717-728.

[23] J. Blazyk, R. Wiegand, J. Klein, J. Hammer, R.M. Epand, R.F. Epand, W.L. Maloy, U.P. Kari, A novel linear amphipathic beta-sheet cationic antimicrobial peptide with enhanced selectivity for bacterial lipids, J.Biol.Chem. 276 (2001) 27899-27906.

[24] E.N. Kanithasen, D. Tiltak, J. Burck, P. Wadhwani, O. Zwernemann, A.S. Ulrich, Solid-state NMR analysis comparing the designer-made antibiotic MSI-103 with its parent peptide PGLa in lipid bilayers, Biochemistry 47 (2008) 2601-2616.

[25] M. Nishida, Y. Imura, M. Yamamoto, S. Kobayashi, Y. Yano, K. Matsuzaki, Interaction of a magainin-PGLa hybrid peptide with membranes: insight into the mechanism of synergism, Biochemistry 46 (2007) 14284-14290.

[26] H.V. Westerhoff, M. Zasloff, J.L. Rosner, R.W. Hendler, A. De Waal, A. Vaz, A. Gomes, P.M. Jongsma, A. Riethorst, D. Juretic, Functional synergism of the magainins PGLa and magainin-2 in Escherichia coli, tumor cells and liposomes, Eur.J.Biochem. 228 (1995) 257-264.

[27] K. Matsuzaki, Y. Mitani, K.Y. Akada, O. Murase, S. Yoneyama, M. Zasloff, K. Miyajima, Mechanism of synergism between antimicrobial peptides magainin 2 and PGLa, Biochemistry 37 (1998) 15144-15153.

[28] P. Tremouilhac, E. Strandberg, P. Wadhwani, A.S. Ulrich, Synergistic transmembrane alignment of the antimicrobial heterodimer PGLa/magainin, J.Biol.Chem. 281 (2006) 32089-32094.

[29] T. Hara, Y. Mitani, K. Tanaka, N. Uematsu, A. Takakura, T. Tachi, H. Kodama, M. Kondo, H. Mori, A. Otaka, F. Nobutaka, K. Matsuzaki, Heterodimer formation between the antimicrobial peptides magainin 2 and PGLa in lipid bilayers: a cross-linking study, Biochemistry 40 (2001) 12395-12399.

[30] K. Lohner, The Role of Membrane Lipid Composition in Cell Targeting of Antimicrobial Peptides. in: "Development of Novel Antimicrobial Agents: Emerging Strategies", (Ed. K. Lohner), Horizon Scientific Press, Wymondham, Norfolk, U.K. (2001) 149-165.

[31] K. Lohner, S.E. Blondelle. Molecular mechanisms of membrane perturbation by antimicrobial peptides and the use of biophysical studies in the design of novel peptide antibiotics. Comb.Chem.HighThroughputScreen 8 (2005) 239-255.

[32] E. Sevcsik, G. Pabst, W. Richter, S. Danner, H. Amenitsch, K. Lohner. Interaction of LL-37 with model membrane systems of different complexity – Influence of the lipid matrix, Biophys.J. 94 (2008) 4688-4699.

[33] K. Lohner, E.J. Prenner. Differential scanning calorimetry and X-ray diffraction studies of the specificity of the interaction of antimicrobial peptides with membrane-mimetic systems, Biochim.Biophys.Acta 1462 (1999) 141-156.

[34] K. Lohner, A. Latal, R.I. Lehrer, T. Ganz. Differential scanning microcalorimetry indicates that human defensin, HNP-2, interacts specifically with biomembrane mimetic systems, Biochemistry 36 (1997) 1525-1531.

[35] T. Nakamura, H. Furunaka, T. Miyata, F. Tokunaga, T. Muta, S. Iwanaga, M. Niwa, T. Takao, Y. Shimonishi, Tachyplesin, a class of antimicrobial peptide from the hemocytes of the horseshoe crab (Tachypleus tridentatus). Isolation and chemical structure. J.Biol.Chem. 263 (1988) 16709-16713.

[36] S.H. White, W.C. Wimley, M.E. Selsted, Structure, function, and membrane integration of defensins, Curr.Opin.Struct.Biol. 5 (1995) 521-527.

[37] A. Latal, R.I. Lehrer, S.S.L. Harwig, K. Lohner, Interaction of enantiomeric protegrins with liposomes. Prog.Biophys.Mol.Biol. 65 (1996) 121.

[38] K. Matsuzaki, K. Sugishita, M. Harada, N. Fujii, K. Miyajima, Interactions of an antimicrobial peptide, magainin 2, with outer and inner membranes of Gram-negative bacteria. Biochim.Biophys.Acta. 1327 (1997) 119-130.

[39] G. Pabst, S. Grage, S. Danner-Pongratz, W. Jing, A.S. Ulrich, A. Watts, K. Lohner, A. Hickel. Membrane thickening by the antimicrobial peptide PGLa. Biophys.J. 95 (2008) 5779-5788.

[40] O. Konovalov, I. Myagkov, B. Struth, K. Lohner, Lipid discrimination in phospholipid monolayers by the antimicrobial frog skin peptide PGLa. A synchrotron X-ray grazing incidence and reflectivity study, Eur.Biophys.J. 31 (2002) 428-437.

[41] O. Konovalov, S.M. O'Flaherty, E. Saint-Martin, G. Deutsch, E. Sevcsik, K. Lohner, The bending rigidity of phospholipid monolayers in presence of an antimicrobial frog peptide studied by X-ray grazing incidence diffraction. PhysicaB 357 (2005) 185-189.

[42] P. Tremouilhac, E. Strandberg, P. Wadhwani, A.S. Ulrich, Conditions affecting the re-alignment of the antimicrobial peptide PGLa in membranes as monitored by solid state 2H-NMR, Biochim.Biophys.Acta 1758 (2006) 1330-1342.

[43] T. Wieprecht, O. Apostolov, M. Beyermann, J. Seelig, Membrane binding and pore formation of the antibacterial peptide PGLa: thermodynamic and mechanistic aspects, Biochemistry 39 (2000) 442-452.

[44] E.J. Helmerhorst, I.M. Reijnders, W. van't Hof, I. Simoons-Smit, E.C. Veerman, A.V. Amerongen, Amphotericin B- and fluconazole-resistant Candida spp., Aspergillus fumigatus, and other newly emerging pathogenic fungi are susceptible to basic antifungal peptides, Antimicrob.AgentsChemother. 43 (1999) 702-704.

[45] R.W. Glaser, C. Sachse, U.H. Durr, P. Wadhwani, A.S. Ulrich, Orientation of the antimicrobial peptide PGLa in lipid membranes determined from 19F-NMR dipolar couplings of 4-CF3-phenylglycine labels, J.Magn.Reson. 168 (2004) 153-163.

[46] B. Bechinger, M. Zasloff, S.J. Opella, Structure and dynamics of the antibiotic peptide PGLa in membranes by solution and solid-state nuclear magnetic resonance spectroscopy, Biophys.J. (1998) 74, 981-987.

[47] E.P. Strandberg, P. Wadhwani, U.H. Tremouilhac, A. Durr, A.S. Ulrich., Solid-state NMR analysis of the PGLa peptide orientation in DMPC bilayers: structural fidelity of 2H-labels versus high sensitivity of 19F-NMR, Biophys. J. 90 (2006) 1676-1686.

[48] R.W. Glaser, C. Sachse, U.H. Durr, P. Wadhwani, S. Afonin, E. Strandberg, A.S. Ulrich, Concentration-dependent realignment of the antimicrobial peptide PGLa in lipid, Biophys.J. 88 (2005) 3392-3397.

[49] S.E. Blondelle, K. Lohner, Combinatorial libraries: a tool to design antimicrobial and antifungal peptide analogues having lytic specificities for structure-activity relationship studies, Biopolymers 55 (2000) 74-87.

[50] E. Sevcsik, G. Pabst, A. Jilek, K. Lohner, How lipids influence the mode of action of membrane-active peptides, Biochim.Biophys.Acta 1768 (2007) 2586-2595.

[51] K. Lohner, Effects of small organic molecules on phospholipid phase transitions, Chem.Phys.Lipids 57 (1991) 341-362.

[52] P. Balgavý, F. Devínsky, Cut-off effects in biological activities of surfactants. Adv.ColloidInterfaceSci. 66 (1996) 23-63.

[53] M. Dathe, J. Meyer, M. Beyermann, B. Maul, C. Hoischen, M. Bienert, General aspects of peptide selectivity towards lipid bilayers and cell membranes studied by variation of the structural parameters of amphipathic helical model peptides, Biochim.Biophys.Acta 1558 (2002) 171-186.

[54] R. Dimova, B. Pouligny, C. Dietrich, Pretransitional effects in dimyristoylphosphatidylcholine vesicle membranes: optical dynamometry study. Biophys.J. 79 (2000) 340-356.

[55] G. Pabst, S. Danner, S. Karmakar, G. Deutsch, V.A. Raghunathan, On the propensity of phosphatidylglycerols to form interdigitated phases, Biophys.J. 93 (2007) 513-525.

[56] H.W. Huang, Molecular mechanism of antimicrobial peptides: the origin of cooperativity, Biochim.Biophys.Acta 1758 (2006)1292-1302.

[57] C. Li, T. Salditt, Structure of magainin and alamethicin in model membranes studied by x-ray reflectivity, Biophys.J. 91 (2006) 3285-3300.

[58] G. Pabst, S. Danner, R. Podgornik, J. Katsaras, Entropy-driven softening of fluid lipid bilayers by alamethicin, Langmuir 23 (2007) 11705-11711.

[59] M.R. de Planque, D.V. Greathouse, R.E. Koeppe, H. Schafer, D. Marsh, J.A. Killian, Influence of lipid/peptide hydrophobic mismatch on the thickness of diacylphosphatidylcholine bilayers. A 2H NMR and ESR study using designed transmembrane alpha-helical peptides and gramicidin A, Biochemistry 37 (1998) 9333-9345.

[60] S. Morein, A. Andersson, L. Rilfors, G. Lindblom, Wild-type Escherichia coli cells regulate the membrane lipid composition in a „window“ between gel and non-lamellar structures, J.Biol.Chem. 271 (1996) 6801-6809.

[61] L. Rilfors, A. Wieslander, G. Lindblom, Mycoplasma Cell Membranes, in: S. Rottem, I. Kahane (Eds.), Subcellular Biochemistry, Plenum Press, New York, Vol. 20, 1993, 109-166.

[62] R.N. McElhaney, Membrane structure, in: J. Maniloff, R.N. McElhaney, L.R. Finch, J.B. Baseman (Eds.), Mycoplasmas: Molecular Biology and Pathogenesis, American Society for Microbiology, Washington DC, 1992, 113-155.

[63] J.M. Seddon, R.H. Templer, Polymorphism of lipid water systems, in: R. Lipowsky, E. Sackmann (Eds.), Structure and dynamics of membranes, North-Holland, Amsterdam, 1995, 97-160.

[64] P. Laggner, K. Lohner, Liposome phase systems as membrane activity sensors for peptides, in: J. Katsaras, T. Gutberlet (Eds.), Lipid bilayers. Structure and interactions, Springer, Berlin, 2000, 233-264.

[65] M. Rappolt, A. Hickel, F. Bringezu, K. Lohner, Mechanism of the lamellar/inverse hexagonal phase transition examined by high resolution x-ray diffraction, Biophys.J. 84 (2003) 3111-3122.

[66] D.P. Siegel, J.L. Banschbach, Lamellar/inverted cubic (Lalpha/QII) phase transition in N-methylated dioleoylphosphatidylethanolamine, Biochemistry 29 (1990) 5975-5981.

[67] K. Lohner, Is the high propensity of ethanolamine plasmalogens to form non-lamellar lipid structures manifested in the properties of biomembranes? Chem.Phys.Lipids 81 (1996) 167-184.

[68] A. Hickel, S. Danner, H. Amenitsch, G. Degovics, M. Rappolt, K. Lohner, G. Pabst, Influence of antimicrobial peptides on the formation of nonlamellar lipid mesophases, Biochim Biophys Acta. 1778 (2008) 2325-2333.

[69] E. Staudegger, E.J. Prenner, M. Kriechbaum, G. Degovics, R.N.A.H. Lewis, R.N. McElhaney, K. Lohner, X-ray Studies on the interaction of Gramicidin S with microbial lipid extracts: Evidence for cubic phase formation, Biochim.Biophys.Acta 1468 (2000) 213-230.

[70] R. El Jastimi, M. Lafleur, Nisin promotes the formation of non-lamellar inverted phases in unsaturated phosphatidylethanolamine, Biochim.Biophys.Acta. 1418 (1999) 97-105.

[71] R.F. Epand, N. Umezawa, E.A. Porter, S.H. Gellman, R.M. Epand, Interactions of the antimicrobial beta-peptide beta-17 with phospholipid vesicles differ from membrane interactions of magainins, Eur.J.Biochem. 270 (2003) 1240-1248.

[72] K. Lohner, G. Degovics, P. Laggner, E. Gnamusch, F. Paltauf, Squalene promotes the formation of non-bilayer structures in phospholipid model membranes. Biochim.Biophys.Acta 1152 (1993) 69-77.

[73] E. Mileykovskaya, W. Dowhan, Visualization of phospholipid domains in Escherichia coli by using cadiolipin specific fluorescent dye 10-nonyl acridine orange, J.Bacteriol. 128 (2000) 1172-1175.

[74] S. Vanounou, A.H. Parola, I. Fishov, Phosphatidylethanolamine and phosphatidylglycerol are segregated into different domains in bacterial membrane. A study with pyrene-labelled phospholipids, Mol.Microbiol. 49 (2003) 1067-1079.

[75] A. da Silva Jr., O. Teschke, Effects of the antimicrobial peptide PGLa on live Escherichia coli, Biochim.Biophys.Acta 1643 (2003) 95-103.

[76] M. Meincken, D.L. Holroyd, M. Rautenbach, Atomic force microscopy study of the effect of antimicrobial peptides on the cell envelope of Escherichia coli, Antimicrob.AgentsChemother. 49 (2005) 4085-4092.

[77] L. Ding, L. Yang, A.J. Waring, R.I. Lehrer, H.W. Huang, Interaction of antimicrobial peptides with lipopolysaccharides, Biochemistry 42 (2003) 12251-12259.

[78] K. Matsuzaki, K. Sugishita, K. Miyajima, Interactions of an antimicrobial peptide, magainin 2, with lipopolysaccharide-containing liposomes as a model for outer membranes of gram-negative bacteria, FEBSLett. 449 (1999) 221-224.

[79] R.E.W. Hancock, The bacterial outer membrane as a drug barrier, TrendsMicrobiol. 5 (1997) 37-42.

[80] S. Snyder, D. Kim, T.J. McIntosh, Lipopolysaccharide bilayer structure: effect of chemotype, core mutations, divalent cations, and temperature, Biochemistry 38 (1999) 10758-10767.

[81] M. Vara, Agents that increase the permeability of the outer membrane. Microbiol.Rev. 56 (1992) 395-411.

[82] R.E.W. Hancock. Alterations in outer membrane permeability. Annu.Rev.Microbiol. 38 (1984) 237-264.

[83] H. Nikaido, Prevention of drug access to bacterial targets: permeability barriers and active efflux, Science 264 (1994) 382-388.

[84] A. Aspedon, E.A. Groisman, Antimicrobial peptide resistance mechanism in bacteria, in: K. Lohner (Ed.), Development of Novel Antimicrobial Agents: Emerging Strategies, Horizon Scientific Press, Wymondham, Norfolk, U.K., 2001, 31-44.

[85] W. Jing, E.J. Prenner, H.J. Vogel, A. Waring, R.I. Lehrer, K. Lohner, Headgroup structure and fatty acid chain length of the acidic phospholipids modulate the interaction of membrane mimetic vesicles with the antimicrobial peptide protegrin-1, J.Pept.Sci. 11 (2005) 735-743.

[86] A. Arouri, M. Dathe, A. Blume, Peptide induced demixing in PG/PE lipid mixtures: A mechanism for the specificity of antimicrobial peptides towards bacterial membranes? Biochim.Biophys.Acta. 1788 (2009) 650-659.

[87] R.F. Epand, M.A. Schmitt, S.H. Gellman, R.M. Epand, Role of membrane lipids in the mechanism of bacterial species selective toxicity by two alpha/beta-antimicrobial peptides, Biochim.Biophys.Acta 1758 (2006) 1343-1350.

[88] K. Matsuzaki, K. Sugishita, M. Harada, N. Fujii, K. Miyajima, Interactions of an antimicrobial peptide, magainin 2, with outer and inner membranes of Gram-negative bacteria, Biochim.Biophys.Acta 1327 (1997) 119-30.

[89] M.L. Mangoni, Y. Shai, Temporins and their synergism against Gram-negative bacteria and in lipopolysaccharide detoxification, In Biochimica et Biophysica Acta (BBA) - Biomembranes, 1788 (2009) 1610-1619

5 Summary and outlook

To summarize this thesis, we presented the phase diagram of the binary lipid model system consisting of DPPG and TMCL, two predominant lipids of the cytoplasmic membrane of Gram-positive bacteria. Both pure lipids show a similar main transition temperature of ~41°C, but exhibit different phase behaviour in the low temperature regime. TMCL adopts L_{R1} and L*c'* structures, while DPPG forms a SGII phase, which can be explained by the molecular differences, in particular molecular shape of those lipids. Addition of only small amounts of one lipid to the other leads to loss of these low temperature phases.

Looking at the lipidome of Gram-positive bacteria demonstrates that the content of cardiolipin strongly varies between different species. For example, cytoplasmic membranes of *Bacillus subtilis* and *Micrococcus luteus* are characterized by CL content of more than 50%, while *Staphylococcus aureus* (or also *Bacillus megaterium*) have a rather small CL content. Thus, it was important to establish a phase diagram over the whole range of binary mixtures in order to be able to describe the characteristics of the biologically relevant lipid compositions. As mentioned in chapter 2, this thesis was part of a research project dedicated to investigate the effect of the lipid matrix of *Staphylococcus aureus* on the activity of antimicrobial peptides. The established binary lipid model system for PG/CL is the basis for further investigations to include lysyl-PG as third lipid for a ternary lipid model system. This more complex model system will serve then as a reference system for the different lipid mixtures of susceptible and resistant *S. aureus* strains, respectively.

Beside the phase behaviour of the membrane mimetic system, the properties of the antimicrobial peptide PGLa is presented within this thesis, being a promising candidate for the development of a new antimicrobial compound. As mentioned in chapter 4, PGLa with

its 5 positive charges targets preferentially negatively charged lipids, predominant components of Gram-positive bacterial membranes. Hence, one of the next steps will be to investigate the interaction of PGLa with the binary model system described in this work. In this respect, first screening assays using DSC were performed at relevant PG/CL mixtures for *S. aureus* (DPPG/TMCL 90/10 mol/mol) and *B. subtilis* (DPPG/TMCL 50/50 mol/mol) as well as with both pure lipids (Figure 27). All lipid samples were prepared by adding PGLa stock solution to yield a lipid-to-peptide molar ratio of 25/1 mol/mol.

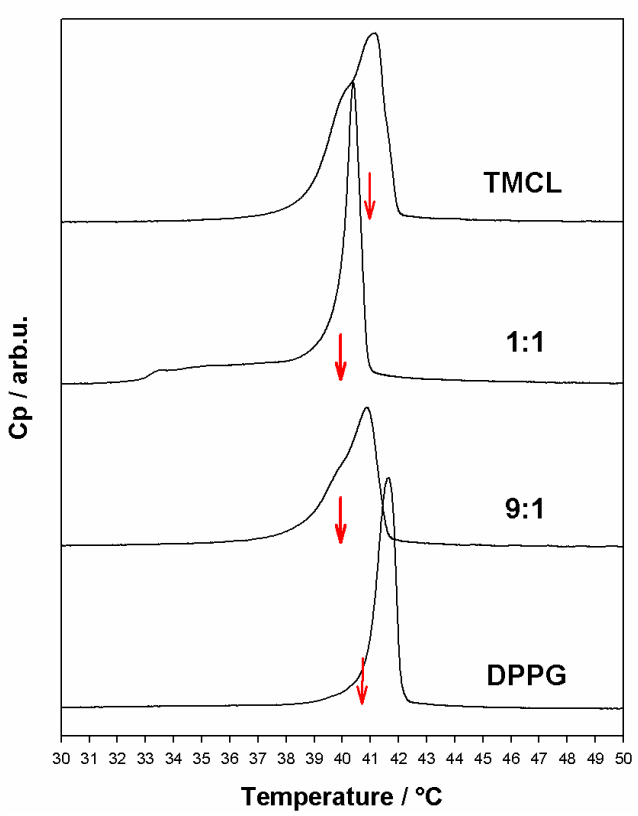

Figure 27: DSC thermograms of lipid-PGLa mixtures. Red arrows indicate the main transition temperatures of the pure lipids and lipid mixtures, respectively, in the absence of PGLa.

DSC thermograms of TMCL-PGLa samples show an asymmetric main transition with a maximum at 41.1°C, which corresponds to a lipid-enriched TMCL domain (Figure 28 and Table 5). The shoulder at low temperature can be as attributed to a peptide-enriched domain with a fitted peak maximum at ~40.2°C. The calculated enthalpies are 36.3 kJ/mol and 18.4 kJ/mol for the peptide-enriched and the lipid-enriched domain, respectively. These data are

indicative for a lipid segregation within the bilayer, where about two third of the lipids are affected by the presence of the peptide.

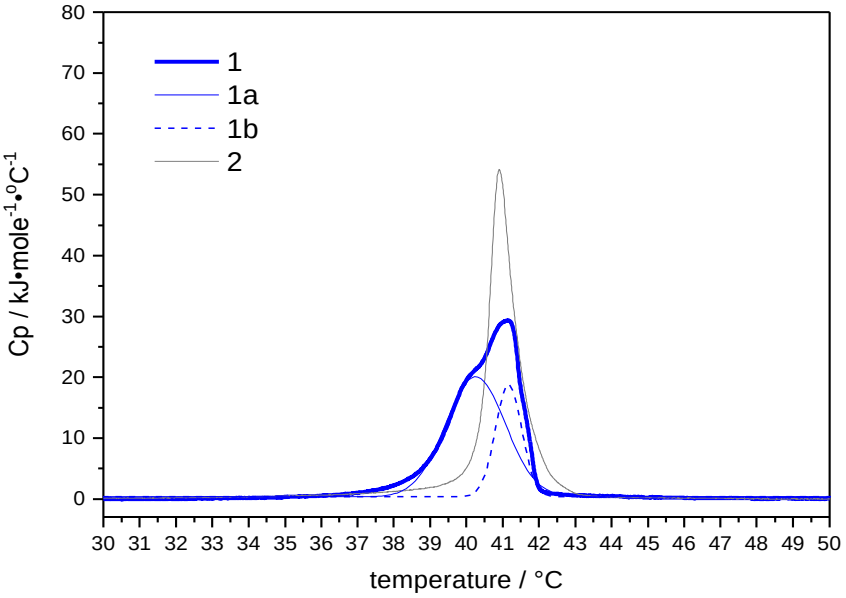

Figure 28: DSC thermogram of pure TMCL in presence of PGLa; 1 blue bold: recorded 3rd heating scan of lipid-peptide mixture; blue solid and dashed: Gaussian fits for 1a: peptide-enriched and 1b: lipid enriched phase; 2 gray: thermogram of pure TMCL

DSC measurements of DPPG samples show a sole peak around 41.5 °C (Figure 27 and Figure 29), which is a shift of ~1,4 °C to higher temperatures compared to peptide-free DPPG which is in agreement with Latal et al. [1] and Pabst et al. [2]. Latter clearly demonstrated that this thermotropic behaviour is due to the formation of a quasi-interdigitated gel phase. The earlier described sub-gel transition (SGII→$L_{\beta'}$) and the pre transition ($L_{\beta'} \rightarrow P_{\beta'}$) characteristic for pure DPPG vanished upon addition of the peptide being in agreement with the formation of the quasi-interdigitated phase in the presence of PGLa. We detected no distinct differences between the first and third heating scan, which suggests that the interaction of PGLa with DPPG reaches equilibrium within the time course of the preparation of the sample.

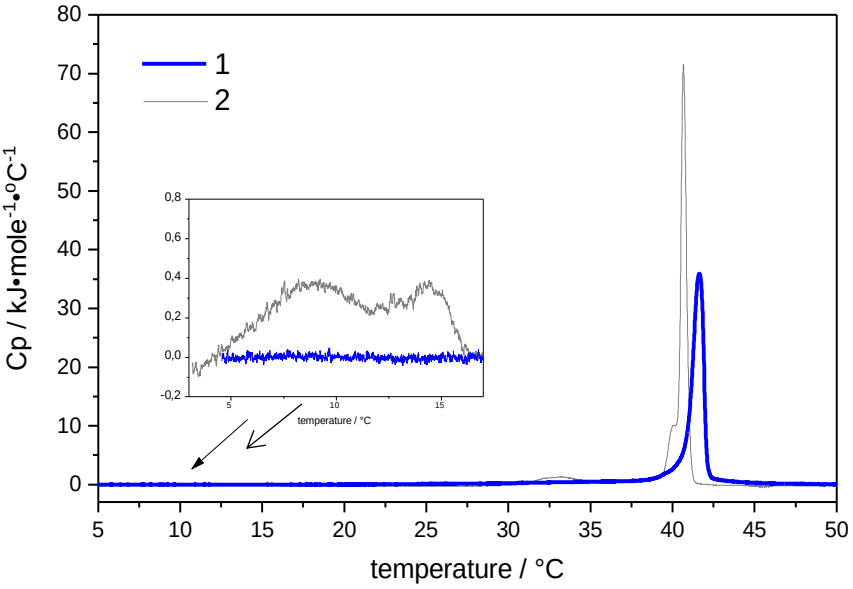

Figure 29: DSC thermogram of pure DPPG in presence of PGLa; 1 blue bold: recorded 3rd heating scan of lipid-peptide mixture; 2: thermogram of pure lipid; Insert shows the magnified low temperature transition range of the pure lipid.

Similar to TMCL samples, DSC recordings of lipid mixtures with a DPPG/TMCL ratio of 90/10 show an asymmetric peak with a maximum at 40.9 °C (Figure 27) and a shoulder shifted to lower temperatures.

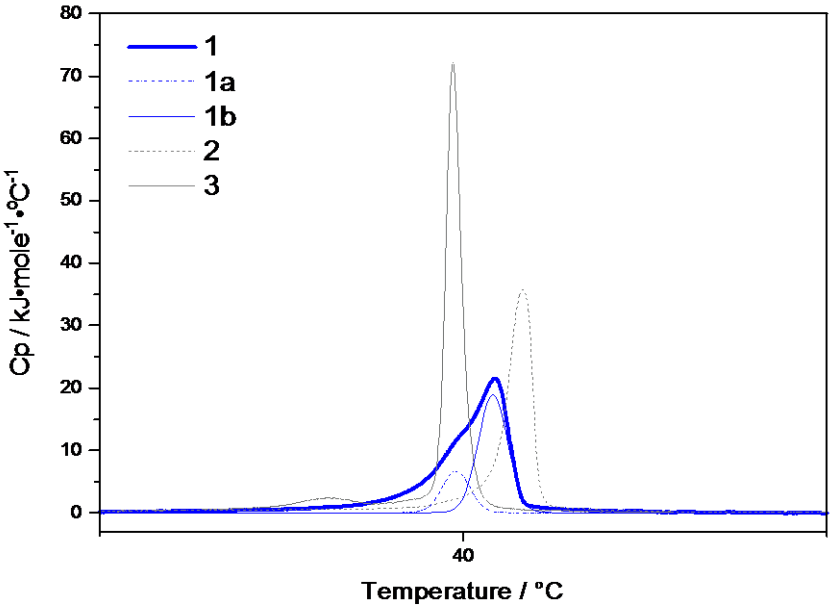

Figure 30: DSC thermogram of lipid mixture DPPG/TMCL = 90/10 mol/mol in presence of PGLa; 1 blue bold: recorded 3rd heating scan of the lipid-peptide mixture; blue solid and dashed: Gaussian fits for 1a: lipid-enriched and 1b: peptide enriched phase; reference data: 2: thermogram of pure lipid mixture DPPG/TMCL = 90/10; 3: thermogram of pure DPPG in presence of PGLa

Two overlapping Gaussians, with a maximum at 39.8°C and 40.8°C, respectively, can fit this transition (Figure 30). Here, the lower temperature transition can be attributed to a TMCL-enriched domain, while the other corresponds to a DPPG-peptide enriched domain. Note that upon reheating the TMCL-enriched peak decreases to the favour of the peptide-enriched.

For lipid mixture with DPPG/TMCL = 50/50 mol/mol, a broad endotherm ranges from 33°C to42 °C (Figure 31) finishing with a sharp peak with a peak temperature of 40.4°C. This behaviour suggests that lipid-peptide domains with enriched DPPG content exist, while the very broad shoulder starting at 32 °C may be due to a mix of lipid-peptide domains of varying composition. Again, reproducible thermograms were only observed after the third heating scan demonstrating that the system is not *per se* in equilibrium.

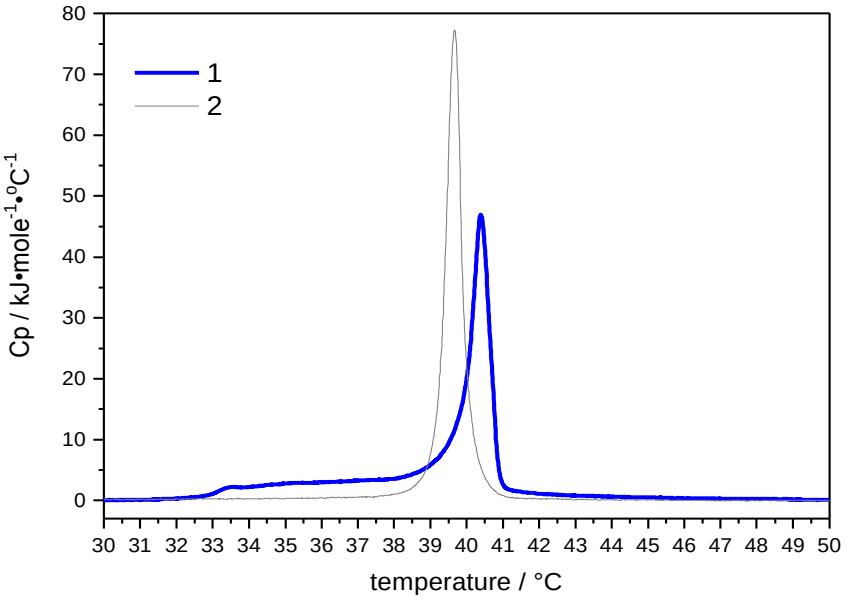

Figure 31: DSC thermogram of lipid mixture DPPG/TMCL = 50/50 mol/mol in presence of PGLa; 1 blue: recorded 3rd heating scan of lipid-peptide mixture; 2 gray: thermogram of pure lipid mixture.

In summary, the preliminary DSC experiments present already first indications how PGLa interacts with the binary system of DPPG and TMCL. For high DPPG content, the formation of an interdigitated phase leads to a stabilisation of the bilayer and therefore a higher temperature shift of the chain melting transition [2]. With the admixture of TMCL,

separation of the two lipids, i.e. clustering, is observed resulting in lipid and lipid-peptide domains of different physico-chemical properties. Such domains give rise to defects being regions of enhanced membrane permeability, which can lead to loss of membrane integrity. In further investigations, X-ray scattering and leakage experiments – as indicator of membrane permeabilization – will be used to elucidate the details of structural changes of lipid bilayers in presence of PGLa, which will allow a more-in-depth description of the molecular mode of action of this antimicrobial peptide. The next consecutive step is to investigate PGLa and the ternary lipid model system DPPG/lysyl-PG/TMCL to elucidate the effect of the cationic lysyl-PG on the peptide`s activity. Based on this work, amino acid modifications should lead to new PGLa derivatives with tailored antimicrobial activity.

Reference list:

[1] A. Latal,, G. Degovics, R. F. Epand, R. M. Epand, and K. Lohner. 1997. Structural aspects of the interaction of peptidyl-glycylleucine-carboxyamide, a highly potent antimicrobial peptide from frog skin, with lipids. Eur. J. Biochem. 248:938–946.

[2] G. Pabst; S. Grage; S. Danner-Pongratz; W. Jing; A.S. Ulrich; A. Watts; K. Lohner and A. Hickel 2008, Membrane thickening by the antimicrobial peptide PGLa., Biophys J.; 95(12):5779-88